Dissertation zur Erlangung des Doktorgrades
der Fakultät für Chemie und Pharmazie
der Ludwig-Maximilians-Universität München

Transcription-coupled repair of DNA-protein crosslinks

Aleida Acampora
aus
Neapel, Italien

2023

Erklärung

Diese Dissertation wurde im Sinne von § 7 der Promotionsordnung vom 28. November 2011 von Herrn Prof. Dr. Julian Stingele betreut.

Eidesstattliche Versicherung

Diese Dissertation wurde eigenständig und ohne unerlaubte Hilfe erarbeitet.

München, 13.10.2023

……

Aleida Acampora

Dissertation eingereicht am 18.10.2023

1. Gutachter: Prof. Dr. Julian Stingele
2. Gutachter: Prof. Dr. Boris Pfander

Mündliche Prüfung am 13.12.2023

LIST OF CONTENTS

ABSTRACT

DNA is a naturally fragile molecule that is intrinsically susceptible to damage. A huge variety of endogenous and exogenous insults can challenge DNA integrity; therefore, specialized DNA repair pathways operate in cells to ensure genome stability. DNA-protein crosslinks (DPCs) are particularly toxic DNA lesions that, due to their bulky nature, can interfere with every chromatin process such as replication and transcription. In the last decade, a multitude of general and dedicated mechanisms have been identified to be involved in DPC resolution. It has been shown that when a DPC blocks replication, proteolytic degradation of the crosslinked protein is required to allow fork resumption. DPCs can also hamper RNAPII progression, however how cells respond to DPCs-dependent transcription blockage is unknown.

In this study we uncovered that DPCs induced by formaldehyde (FA) shut down transcription and induce degradation of RNA polymerase II (RNAPII). DPC induction by FA treatment triggers the recruitment of the upstream transcription-coupled NER (TC-NER) factors CSB and CSA to stalled RNAPII. Accordingly, CSB and CSA provide resistance towards DPCs-inducing agents and their loss impairs efficient transcription recovery after FA treatment. Conversely, TC-NER factors acting downstream of CSB and CSA are not required for transcription resumption upon FA treatment. In addition, genetic data suggest that CSB promotes DPC tolerance in parallel to and independently of already known DPC repair factors.

Lastly, using our newly established DPC-sequencing (DPC-seq) assay for the genome-wide mapping of DPCs, we discovered that CSB specifically promotes DPC repair in actively transcribed genes. Therefore, this study provides the first evidence for the existence of a CSB-dependent specialized transcription-coupled DPC repair pathway.

1 INTRODUCTION

1.1 DNA damage and repair

Uncovering the nature of the genetic information has been object of interest for many years. In 1944 Avery, MacLeod and McCarty demonstrated that our hereditary material is deoxyribonucleic acid (DNA); in 1953 Watson and Crick published the DNA structure, finally revealing “the secret of life” (Avery et al., 1944; Watson and Crick, 1953). The backbone of a DNA molecule is an alternance of repetitive units (nucleotides) made up of sugar (deoxyribose), phosphate groups and one of four possible nitrogenous bases: adenine (A), thymine (T), cytosine (C) and guanine (G). Two complementary strands of DNA are coiled and connected by hydrogen bonds among bases to form a double helix (Watson and Crick, 1953).

DNA is constantly exposed to endogenous and exogenous insults that can modify its structure and generate mutations. A low amount of DNA alterations sustains evolution, however, infidelity in transmitting the genetic information during cell division can dramatically impact human health (Chatterjee and Walker, 2017). To protect DNA from damages and ensure genomic stability, cells have evolved a plethora of sensing and repair mechanisms that are object of current investigations (Jackson and Bartek, 2009).

1.1.1 Endogenous sources of DNA damage

DNA is an intrinsically fragile molecule, and, therefore, it is susceptible to damage. In first instance, DNA molecule can undergo a spontaneous decomposition process (Lindahl, 1993). Alternatively, sequence changes can originate from errors and misincorporations during replication. Lastly, a multitude of endogenous agents can attack the DNA structure (Chatterjee and Walker, 2017).

Base modification is a significant source of endogenous mutagenesis. Adenine, guanine, cytosine and 5-methylcytosine can lose their amino group by deamination that generates hypoxanthine, xanthine, uracil and thymine, respectively (Lindahl, 1993). These events can arise spontaneously and occur more frequently in single-stranded (ss) than double-stranded (ds) DNA; therefore they usually happen during active replication or transcription (Yonekura et al., 2009). The enzyme uracil DNA glycosylase (UDG) immediately excises the uracil derived from cytosine deamination, but it does not recognize the thymine produced by 5-methylcytosine deamination that is, in turn, slowly removed by the thymine DNA glycosylase (TDG) (Lindahl, 1979). As a consequence, CG→TA transitions are quite frequent mutations, despite the relative low abundance of 5-methylcytosine (Breiling and Lyko, 2015). Abasic sites, also referred to as apurinic/apyrimidinic (AP) sites, are caused by breaks of the N-

glycosidic bonds of DNA (Lindahl, 1993). Both depurination (adenine/guanine removal) and depyrimidination (thymine/cytosine removal) can be generated by spontaneous hydrolysis or by DNA glycosylase-dependent base excision (Chen et al., 2019). AP sites are instable and therefore they can spontaneously convert into strand breaks, that are highly toxic for the cell (Loeb and Preston, 1986).

Cellular metabolism generates a multitude of reactive products (Lindahl, 1993). Reactive oxygen species (ROS) such as hydroxyl radical (•OH), hydrogen peroxide (H_2O_2), and superoxide radical ($O_2^{\bullet -}$) are significant sources of endogenous DNA damage, even though their limited production appears to be beneficial for cell homeostasis and immune response (Schieber and Chandel, 2014). Therefore, ROS radicals can attack both the DNA backbone and bases, generating single or double strand breaks (SSBs or DSBs) and base modifications, respectively (Dizdaroglu et al., 2002; Sharma et al., 2016). The reaction of hydroxyl radicals (•OH) with a guanine generates 8-oxoguanine (8-oxoG), which is the most frequent oxidative DNA lesion. 8-oxoG preferentially pairs with an adenine, instead of a cytosine, thus, the presence of this modified base, if not repaired, can introduce a point mutation (GC→TA). Inefficient repair of oxidated bases can further predispose to SSBs and DSBs (Cooke et al., 2003).

Endogenously produced aldehydes can also react with DNA and generate a variety of adducts (Vijayraghavan and Saini, 2023). Formaldehyde (FA) is produced through several physiological enzymatic processes, such as demethylation reactions or methanol metabolism (Shi et al., 2004; Walport et al., 2012). FA can react with guanine, adenine and cytosine to form hydroxymethyl adducts, causing the introduction of a point mutation during replication (Kawanishi et al., 2014). Additionally, FA can react with the amino groups of two adjacent DNA bases to form inter-strand crosslinks (ICLs), or it can covalently trap proteins on DNA, generating DNA-protein crosslinks (DPCs) (Heck et al., 1990; Huang and Hopkins, 1993). Analogously to FA, also acetaldehyde, that is mainly produced through ethanol oxidation by alcohol dehydrogenase (ADH) reaction, can introduce ICLs and DPCs (Brooks and Zakhari, 2014). In order to prevent toxicity, aldehydes are processed by specialized clearance machineries (Dingler et al., 2020). For instance, FA is continuously detoxified from the body by the highly conserved ADH5, a cytosolic enzyme that oxidizes the spontaneously formed glutathione (GSH) conjugate of FA (S-(hydroxymethyl)glutathione) to formate (Pontel et al., 2015). Similarly, acetaldehyde is converted to acetate by the mitochondrial aldehyde dehydrogenase (ALDH) 2, before it is activated to Acetyl-CoA and enters the Krebs cycle (Jacobson and Bernofsky, 1974). Deficiency of ALDH2 enzyme caused by a dominant-negative mutation in the ALDH2 gene (ALDH2*2) results in

acetaldehyde accumulation and it is responsible for a red flushing reaction upon alcohol consumption (Harada et al., 1981).

Endogenous alkylating agents, that can transfer alkyl groups on the DNA, give raise to a variety of lesions. A typical methyl donor is S-adenosylmethionine (SAM), that can react with DNA to generate several N- or O-adducts, such as N7-methylguanine, N3-methyladenine and O^6-methylguanine (Soll et al., 2017). N7-methylguanine can spontaneously depurinate, thereby generating a toxic AP site (Gentil et al., 1992). By contrast, N3-methyladenine can block replication, requiring the intervention of error-prone translesion synthesis (TLS) polymerases, thus increasing the risk of base substitutions (Johnson et al., 2007). The presence of O^6-methylguanine predisposes to point mutations, since the DNA polymerase can insert on the complementary strand either a cytosine and thymine with similar efficiency (Warren et al., 2006).

Lastly, DNA replication is itself an important source of DNA alterations (Ide et al., 1993). To ensure the correct propagation of genetic information, high-fidelity replicative DNA polymerases bear proof-reading activity, that allows the immediate detection and removal of misincorporated nucleotides (Derbyshire et al., 1995; Bebenek and Kunkel, 2004; Reha-Krantz, 2010). Despite this, a few nucleotide substitutions can escape this quality control and be retained in the newly synthesized DNA molecule. If not accurately detected and repaired, these changes can generate deleterious point mutations throughout the genome (Hsieh and Yamane, 2008).

1.1.2 Exogenous sources of DNA damage

Together with endogenously produced metabolites, several exogenous physical and chemical agents can attack DNA. The most significant sources of damage are ionizing radiation (IR) and ultraviolet (UV) radiation, but also chemicals, environmental pollutants, toxins and chemotherapeutic agents.

The definition of IR comprises α, β, γ, neutrons and X-rays that are present in our environment and that originate from diverse sources (Chatterjee and Walker, 2017). IR can attack one or both DNA strands to generate SSBs or DSBs, which are extremely toxic for the cells (Hutchinson, 1985; Lliakis, 1991). Alternatively, in the presence of water, IR produces •OH radicals, that can react with DNA to generate mutagenic 8-oxoG modified bases (Ward, 1988; Desouky et al., 2015). Furthermore, IR can induce DPC formation, through a mechanism that has not been fully elucidated yet (Fornace and Little, 1977; Ward, 1994; Nakano et al., 2017).

According to its wavelength, UV radiation is categorized in three groups: UVA (320-400 nm), UVB (290-320 nm) and UVC (190-290 nm). Sunlight, to which most of the living beings are constantly exposed, contains UVA and UVB, while most of UVC is filtered by the ozone layer. UVC is widely used in laboratory investigations because it has a higher absorption power, compared to UVA and UVB; however UVA and UVB can also attack and damage DNA (Kiefer, 2007). The energy of UV radiation can be absorbed by DNA, that, once excited, undergoes photochemical alterations (Davies, 1995). The two main DNA lesions induced by exposure to UV are cyclobutane pyrimidine dimers (CPDs) and 6-4 pyrimidine-pyrimidone photoproducts (6-4PPs). In CPDs, a cyclobutane ring covalently links the two adjacent pyrimidines, whereas in 6-4PPs, the C6 position of one pyrimidine is covalently linked to the C4 position of the adjacent pyrimidine; as a result, photolesions interfere with hydrogen bonding and disrupt normal base-paring (Mitchell et al., 1991; Rochette et al., 2003; Kiefer, 2007). UV radiation can also indirectly damage DNA. Therefore, UV radiation can be absorbed by excitable molecules in the vicinity of DNA, thus increasing ROS radicals generation and subsequent 8-oxoG formation (Brem et al., 2017). Additionally, UV radiation has been shown to produce other DNA lesions, such as ICLs, DPCs, SSBs and DSBs, revealing the complexity of its interaction with biological molecules (Peak and Peak, 1986; Kiefer, 2007; Gueranger et al., 2011; Yu and Lee, 2017).

Chemical agents present in the environment can damage DNA through very diverse mechanisms. Alkylating agents are toxic compounds present in water, food, tobacco smoke, in fuel and industrial emissions. Among others, the compound diepoxybutane (DEB), a chemical pollutant present in cigarette smoke, has been shown to generate DPCs (Gherezghiher et al., 2013). In addition, thanks to their significant cytotoxicity, some alkylating compounds, such as nitrogen mustards or platinum-derived compounds (cisplatin), are used as chemotherapeutic agents (Eastman, 1987; Cohen and Lippard, 2001; Emadi, 2009; Fu et al., 2012; Dasari and Tchounwou, 2014).

The ones presented above are only few examples, since the variety of exogenous compounds that can alter the structure of DNA is huge (Chatterjee and Walker, 2017). In conclusion, it is important to mention that some endogenous metabolic products, such as aldehydes, are also present in substantial amount in the environment. For example, FA is released as combustion by-product in industrial processes, but it is also present in cigarette smoke and cosmetic products, representing a significant risk for human health (Swenberg et al., 2013).

1.1.3 DNA repair pathways

In order to preserve our genomic material, cells possess specialized mechanisms to detect and repair DNA lesions. The DNA damage response (DDR) involves a network of surveillance-signalling pathways that maintain genome integrity (Jackson and Bartek, 2009). DNA repair pathways are briefly described in this section (Figure 1).

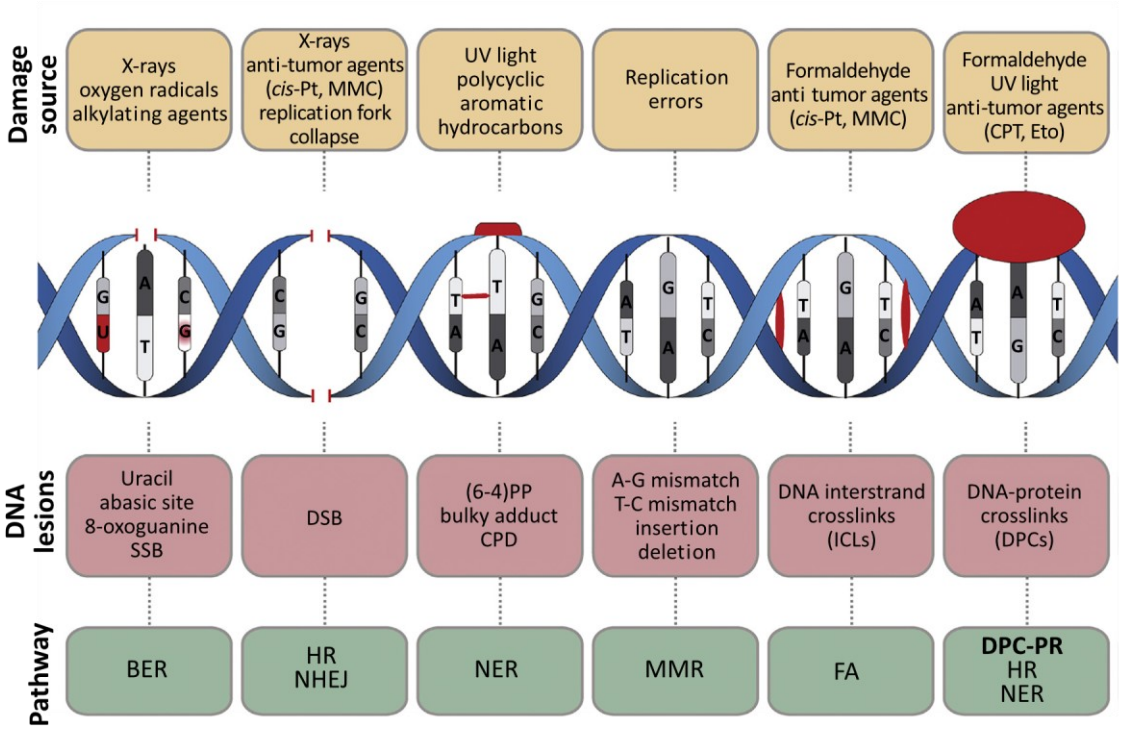

Figure 1. Schematic of DNA damage and repair pathways. Several agents can alter DNA sequence and structure, causing deleterious damages whose removal requires the intervention of specialized DNA repair systems. Replication inaccuracies can cause erroneous misincorporations and subsequent base mismatches. Resolution of these lesions requires the intervention of mismatch repair (MMR). Base modifications can occur either spontaneously, such as deamination, depurination, depyrimidination, either due to the attack of endogenous or exogenous agents. ROS and alkylating agents can introduce a variety of base modifications that are removed by specific enzymes (direct reversal repair) or by base excision repair (BER). Aldehydes, such as FA, can also react with DNA and give rise to complex lesions, such as ICLs, that are mainly repaired by Fanconi anemia pathway. FA, together with the anti-tumour agents camptothecin (CPT) and etoposide, also cause DPCs, whose resolution can involve several specialized and general mechanisms, comprising hydrolysis, proteolysis (DPC-PR), and nuclease-dependent removal, such as nucleotide excision repair (NER) and homologous recombination (HR). IR and UV radiations usually introduce SSBs or DSBs in the DNA helix, requiring the intervention of the error-free HR or the error-prone non-homologous end joining (NHEJ) repair pathways. Lastly, UV irradiation and a broad variety of chemical compounds generate bulky adducts, resolved by NER. Figure adapted from Vaz et al., 2017.

1.1.3.1 Direct reversal repair

DNA damage caused by oxidation, alkylation or UV radiation can be immediately resolved by the intervention of specific enzymes that directly reverse the lesion (Yi and He, 2013). Repair of O-alkylated DNA bases requires alkyltransferases and dioxygenases, while

removal of N-alkylated adducts is operated by AlkB family dioxygenases (Fu et al., 2012). O^6-methylguanine-DNA methyltransferase (MGMT) repairs O^6-methylguanine via transfer of the methyl group to a cysteine of its active site (Sedgwick et al., 2007). The demethylase AlkB homolog (ALKBH) catalyses direct reversal of certain N1-methyladenine and N3-methylcytosine through an oxidative dealkylation reaction (Duncan et al., 2002). Alkylated bases that cannot be directly reversed require the intervention of excision repair pathways. UV-induced DNA lesions can also be reversed by photolyases, specialized proteins that are able to revert CPDs and 6-4PPs (Okafuji et al., 2010). However, this system in not present in humans, where the removal of these bulky lesion particularly relies of nucleotide excision repair (NER).

1.1.3.2 Mismatch repair (MMR)

Mismatch repair (MMR) is a post-replicative DNA repair pathway involved in the detection and correction of base mismatches, rather than DNA lesions. Indeed, as described above, nucleotide misincorporation or small insertions and deletions can accidentally occur during replication and, if not immediately corrected, they can introduce point mutations (Pećina-Šlaus et al., 2020). This pathway contributes significantly to preserve genome stability. Indeed, mutations in MMR genes are causative for an hereditary cancer predisposition syndrome, known as Lynch syndrome or hereditary nonpolyposis colorectal cancer (HNPCC) (Fishel and Kolodner, 1995). In humans, mismatches, insertion and deletions are recognized by the MutSα heterodimer (MSH2/MSH6) or by MutSβ heterodimer (MSH2/MSH3). How these complexes are able to sense mismatches and initiate MMR has not been fully clarified yet, even though recent studies suggest that chromatin modifications might play a role (Li et al., 2013). Next, MutLα (MLH1/PMS2) is recruited together with proliferating cell nuclear antigen (PCNA) and replication factor C (RFC) to form a tetrameric slide clamp structure with MutSα/β. This activates the endonuclease activity of PMS2, that is able to generate a SSB near the mismatch (Kadyrova and Kadyrov, 2016). The presence of a cut in the DNA strand allows the exonuclease 1 (EXO1) to digest DNA in 5'-3' direction and remove the mismatched nucleotide (Genschel and Modrich, 2003). To terminate the reaction, DNA polymerase δ (Pol δ) resynthesizes the DNA and DNA ligase 1 (LIG1) closes the nick (Figure 2) (Prindle and Loeb, 2012; Pećina-Šlaus et al., 2020).

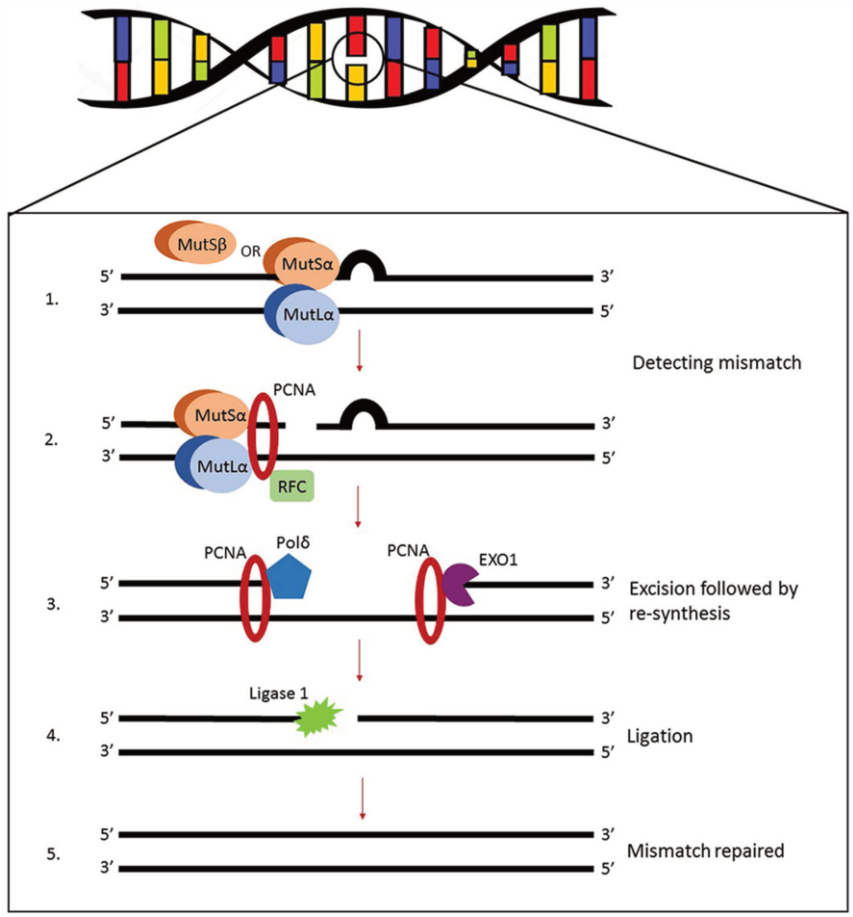

Figure 2. DNA mismatch repair. DNA mismatches are detected by MutSα (heterodimer MSH2/MSH6) or MutSβ (heterodimer MSH2/MSH3). Next, MutLα (heterodimer MLH1/PMS2), PCNA and RFC are recruited to the lesion site. The correct positioning of these factors activates the endonuclease activity of PMS2 that, generating a SSB near the mismatch, allows EXO1-dependent removal of the wrong nucleotide. Finally, Pol δ resynthesizes the DNA and LIG1 closes the nick, allowing the restoration of DNA sequence. Figure from Pećina-Šlaus et al., 2020.

1.1.3.3 Base excision repair (BER)

Base excision repair (BER) is a versatile repair mechanism involved in the removal of bases modified by deamination, hydrolysis, oxidation and alkylation. These lesions do not dramatically impact the structure of the DNA helix, therefore, their detection and elimination require the intervention of specific DNA glycosylases (Huffman et al., 2005). These enzymes cleave the N-glycosidic bond, removing the modified base and thus generating an AP site. In humans, 8 monofunctional and 3 bifunctional glycosylases have been identified and they operate through a short and long-patch repair pathway, respectively (Ide and Kotera, 2004; Svilar et al., 2011). Monofunctional glycosylases only possess glycosylase activity, while bifunctional glycosylases have glycosylase and β-lyase activity. The generation of an AP site by a monofunctional glycosylase requires the subsequent intervention of an AP endonuclease (APE1 in humans) that cleaves the phosphodiester

bond 5' to the AP site, generating a gap in the DNA strand (Wallace, 1998). This is followed by removal of 5'-deoxyribose phosphate, filling of the single nucleotide gap by Pol β and ligation, operated by either LIG1 or by LIG3/X-ray repair cross-complementing protein 1 (XRCC1) complex (Almeida and Sobol, 2007; Svilar et al., 2011). By contrast, the long patch path requires the phosphodiesterase activity of APE1 to process the DNA gap at 3'. This is followed by DNA displacing synthesis mediated by Pol β (in non-proliferating cells) or Pol δ/ε (in proliferating cells), followed by flap structure-specific endonuclease 1 (FEN1) and LIG1 flap/ligation (Almeida and Sobol, 2007; Svilar et al., 2011; Krokan and Bjoras, 2013). In specific conditions, poly (ADP-ribose) polymerase 1 (PARP1), due to its affinity for AP sites, can initiate repair (Dantzer et al., 1999). PARP1 belongs to the PARP enzyme family, that transfers ADP-ribose residues from nicotinamide adenine dinucleotide (NAD^+) to target proteins (Thomas and Tulin, 2013). Once recruited to the AP site, PARP1 initiates a poly (ADP-ribosyl)ation (PARylation) reaction on itself and on the proteins in close proximity, orchestrating, together with the scaffold protein XRCC1, the correct progression of repair (Pleschke et al., 2000; Svilar et al., 2011).

BER function is extremely relevant to ensure genomic stability, thus disfunctions in its factors predispose to diseases. Among the others, deficiencies in 8-oxoguanine DNA glycosylase 1 (OGG1), involved in the repair of 8-oxoG, are associated with cancer, neurodegeneration and metabolic diseases (Sampath et al., 2012; Jacob et al., 2013; Ali et al., 2015; Zhao et al., 2022).

1.1.3.4 Single-strand break (SSB) repair

Single-strand breaks (SSBs) can be induced by oxidative damage, trapping of DNA topoisomerase 1 (TOP1) or AP sites decomposition. SSB repair (SSBR) can be considered a branch of BER, since these two repair pathways share several factors, such as PARP1 and XRCC1 (Caldecott, 2008; Abbotts and Wilson, 2017). PARP1 has a strong affinity for SSBs, as a consequence, in the presence of such a lesion, it immediately binds DNA and initiates a PARylation reaction (Fisher et al., 2007). This triggers the recruitment of XRCC1, together with APE1, the processing enzyme aprataxin (APTX) and polynucleotide kinase/phosphatase (PNKP).

In the long patch path, APE1, PNKP and APTX process the DNA ends together with FEN1, thus allowing Pol β and Pol δ/ε to insert a few nucleotides and LIG1 to close the gap. In the short patch path (where the SSBs are generated during BER), the end processing is followed by Pol β-mediated gap filling and ligation by LIG3 (Caldecott, 2008; Abbotts and Wilson, 2017).

SSBR factors are additionally involved in the final steps of the TOP1 release reaction, where they allow the repair of the SSB generated during the process (this aspect will be further discussed in section 1.3.2.1) (Caldecott, 2008).

1.1.3.5 Double-strand break (DSB) repair

Double-strand breaks (DSBs) are breaks in both DNA strands that can be introduced either by exogenous sources, such as IR, ROS, chemotherapeutic agents or by endogenous mechanisms, such as immunoglobulin class switching and meiotic crossovers (Khan and Ali, 2017). DSBs are extremely toxic for the cell, because they can generate mutations and chromosomal rearrangements. Therefore, to ensure genome integrity, two major repair pathways exist: homologous recombination (HR) and non-homologous end joining (NHEJ) (Chapman et al., 2012). Immediate chromatin modifications orchestrate pathway choice, by recruitment and regulation of a multitude of downstream factors (Scully et al., 2019).

1.1.3.5.1 Homologous recombination (HR)

Homologous recombination (HR) pathway is mainly error-free and based on the invasion of the duplex DNA by a homologous single-stranded molecule, which then primes repair DNA synthesis. HR is active in S/G2 phases, since it requires the presence of the sister chromatid as a template (San Filippo et al., 2008; Wright et al., 2018). The first step is the recognition of the damage by the MRN (MRE11-RAD50-NBS1) complex, followed by DNA-end resection operated by MRE11 in concert with CtBP-interacting protein (CtIP). This results in the generation of a 3'-overhang that is extended by other exonucleases (such as EXO1), assisted by the helicase activity of Bloom syndrome protein (BLM) (Sung and Klein, 2006). During this process, the ssDNA-binding replication protein A (RPA) is first recruited to protect the exposed DNA and then displaced by BRCA2-mediated binding of the recombinase RAD51. RAD51 mediates the most relevant step of HR, which is the genome homology search for a complementary DNA sequence. The homology search is operated through a progressive invasion/displacement of dsDNA, that allows it to "probe" base pairing (Renkawitz et al., 2014). When RAD51 finds the complementary ssDNA, this is used as a template for the subsequent DNA extension at 3' of the DSB operated by Pol δ. The double Holliday junction that is formed during this repair process is dissolved by BTRR complex (BLM-TopIIIa-RMI1-RMI2) or alternatively resolved by either SLX-MUS complex (MUS81-EME1-SLX1-SLX4) either GEN1 resolvase (Nimonkar et al., 2011; Ho and West, 2022).

1.1.3.5.2 Non-homologous end joining (NHEJ)

In non-homologous end joining (NHEJ) repair pathway the two DSB ends are directly ligated together through an error-prone mechanism. Since NHEJ does not require a template sequence, its interventions frequently introduce insertions, deletions, substitutions and translocations (Lieber, 2010). NHEJ is potentially active in every cell cycle phase, however it mainly operates in G1, to compensate for HR unproficiency (Heyer et al., 2010).

The canonical NHEJ pathway is initiated by binding of the heterodimer Ku70 and Ku80 at the broken DNA ends, followed by recruitment and activation of DNA-dependent protein kinase catalytic subunit (DNA-PKcs). DNA-PKcs promotes repair by bringing together the DNA ends and recruiting downstream factors, such as Artemis, PNKP, APE1 and tyrosyl-DNA phosphodiesterase 1 (TDP1). The processing steps and factors depend on the DNA ends features, that can indeed originate from different sources. In any case, these reactions prepare the DNA ends for the subsequent religation, that is performed by a complex made up of XRCC4, XRCC4-like factor (XLF) and LIG4 (Graham et al., 2016).

1.1.3.6 Translesion synthesis (TLS)

Translesion synthesis (TLS) polymerases are specialized DNA polymerases that can replicate DNA even in the presence of aberrant or bulky lesions (Waters et al., 2009). TLS polymerases are low fidelity enzymes, that can ensure DNA synthesis progression inserting nucleotides, independently of the complementarity with the template. Although sequence context and type of lesions influence the accuracy degree of TLS polymerases, their low precision can cause nucleotide misincorporations and generate mutations (Lange et al., 2011; Sale, 2013). Furthermore, TLS polymerases are structurally different to replicative DNA polymerases, indeed they lack the 3’-5’ proofreading domain and possess an open active site, able to accommodate modified bases (Rothwell and Waksman, 2005). TLS repair is regulated by several factors, including PCNA ubiquitylation. Replication arrest stimulates PCNA monoubiquitylation operated by E3 ubiquitin ligase RAD18 and E2 ubiquitin conjugating enzyme RAD6. This induces a transient polymerase switch that allows TLS polymerases to continue DNA synthesis and bypass the lesion (Moldovan et al., 2007; Sale, 2013; Ma et al., 2020). This strategy allows DNA synthesis resumption and replication progression.

1.1.3.7 Inter-strand crosslink (ICL) repair

Inter-strand crosslinks (ICLs) are covalent linkages between complementary strands of double-stranded DNA. They are produced by reaction of endogenous or exogenous

reactive compounds, such as crosslinking and alkylating agents, but also aldehydes and ROS (Zhao et al., 2022). ICLs can interfere with every physiological chromatin process, thereby the detection and removal of these lesions is particularly complex and it results in an interplay of several DNA repair pathways (Ceccaldi et al., 2016). In general, the proteins involved in ICL repair belong to Fanconi anemia family, since mutations in their genes are causative for Fanconi anemia, a heterogeneous autosomal recessive disorder, characterized by cancer predisposition and various haematological disfunctions (Kee and D'Andrea, 2012).

The most toxic property of ICLs is to inhibit replication progression, thereby the Fanconi anemia proteins are involved in a replication-coupled mechanism that allows ICL resolution and fork progression (Akkari et al., 2000; Räschle et al., 2008). Currently, 22 Fanconi anemia proteins have been identified and classified in three groups (Ceccaldi et al., 2016; Milletti et al., 2020; Semlow and Walter, 2021). FANCA, B, C, E, F, G, L and M belong to group I, also known as Fanconi anemia core complex. DNA ICL is immediately detected by the UHRF1 sensor and/or by the FANCM-FAAP24-MHF1-MHF2 complex (Liang et al., 2015; Milletti et al., 2020). Next, Fanconi anemia core complex and associated proteins FAAP20, FAAP100 can be recruited to the lesion site. The group II heterodimeric complex FANCI-FANCD2 (ID2), in the presence of the ubiquitin-conjugating enzyme E2 T (UBE2T, also known as FANCT), is monoubiquitylated by the E3 ubiquitin ligase FANCL and directed to the ICL region (Meetei et al., 2003; Smogorzewska et al., 2007). Consequently, proteins of the group III are recruited to promote ICL repair. This group includes proteins involved in the incision of DNA, such as the nuclease FANCQ (also known as XPF or ERCC4), the scaffolding protein FANCP (SLX4), and proteins involved in HR repair, such as FANCD1 (BRCA2), FANCJ (BRIP1), FANCN (PALB2), FANCO (RAD51C), FANCR (RAD51), FANCS (BRCA1), FANCU (XRCC2), FANCV (REV7) and FANCW (RFWD3). ERCC1, XPF and SLX4, together with other factors, such as the nucleases sensitive to nitrogen mustard-(SNM)1A, SNM1B, Fanconi-associated nuclease 1 (FAN1), and MUS81 coordinate nucleotide excision to allow the unhooking of the ICL (Wang et al., 2011). Then, one strand is further processed by CtIP, MRN complex (MRE11-RAD50-NBS1), EXO1 or BLM-DNA2, while the second strand is fixed by TLS polymerase lesion bypass operated by REV1 or Pol ζ (REV3-REV7) and subsequent ligation. In turn, the ssDNA becomes substrate of HR Fanconi anemia proteins, that mediate RAD51 strand invasion and HR. The process is terminated by deubiquitylation of ID2 complex that is mediated by the deubiquitylating enzyme (DUB) ubiquitin specific peptidase 1 (USP1) (Figure 3) (Ceccaldi et al., 2016; Milletti et al., 2020).

Although so far most research has focused on replication-couped ICL repair mechanisms, these lesions can also interfere with other DNA processes, such as transcription (Williams et al., 2013). A few studies showed that TC-NER proteins (such as CSA, CSB and XPA) are required to repair ICLs and that, indeed, ICLs are resolved faster in actively transcribed genes (Islas et al., 1991; Larminat et al., 1993; Furuta et al., 2002; Smeaton et al., 2008; Enoiu et al., 2012). These studies suggested the existence of a transcription-coupled ICL repair pathway, however, the exact molecular mechanisms have not been elucidated yet. Lastly, it has also been shown that in absence of both replication and transcription progression, ICLs can be detected by the MMR complex MutSα and processed by MutLα and EXO1 (Kato et al., 2017).

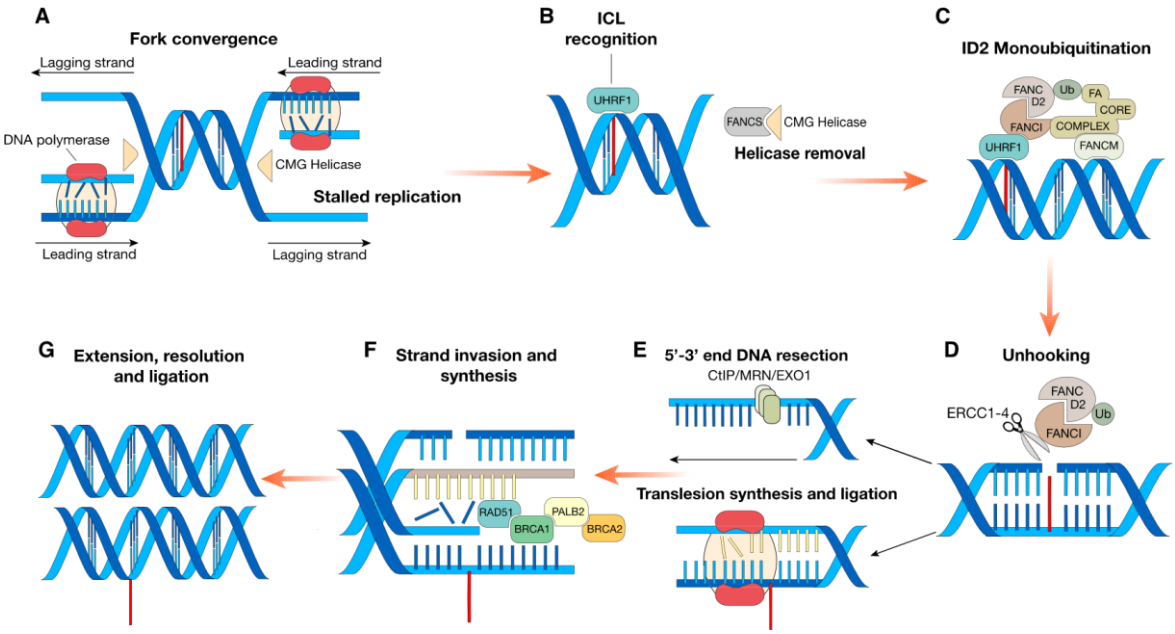

Figure 3. Repair of ICLs. A) Stalling of replication fork progression caused by an ICL activates Fanconi anemia pathway. **B-C)** Identification of ICL by the UHRF1 sensor and by FANCM-FAAP24-MHF1-MHF2 complex is followed by recruitment of Fanconi anemia core complex (group I). FANCI-FANCD2 heterodimer (group II) in the presence of UBE2T is monoubiquitylated by the E3 ubiquitin ligase FANCL and directed to the ICL region. **D)** Next, proteins of group III (nucleases and HR proteins) are recruited to promote ICL repair. ERCC1, ERCC4 and SLX4 operate the nucleotide excision and permit the DNA unhooking. **E)** At this point, the strand previously incised undergoes a further processing mediated by CtIP, MRN complex (MRE11-RAD50-NBS1), EXO1 or BLM-DNA2. Conversely, the complementary strand is fixed by TLS polymerases lesion bypass operated by REV1 or Pol ζ (REV3-REV7) and ligation. **F)** Finally, the ssDNA overhang becomes substrate of HR Fanconi anemia proteins (RAD51/BRCA2/PALB2/BRCA1), that mediate strand invasion and HR. **G)** USP1-mediated deubiquitylation of ID2 complex terminates the process, finalizing the DNA repair. Figure from Milletti et al., 2020.

1.2 Nucleotide excision repair (NER)

Nucleotide excision repair (NER) is a DNA repair pathway involved in the repair of a variety of DNA lesions, including CPDs and 6-4PPs induced by UV light. This pathway is also involved in the resolution of bulky DNA adducts generated by chemical compounds that locally disrupt base-pairing, distorting the DNA helix (Gillet and Schärer, 2006). NER operates through distinct subpathways: global genome NER (GG-NER) and transcription-coupled NER (TC-NER) (Kusakabe et al., 2019). GG-NER is activated when a DNA helix distortion is detected throughout the genome, whereas TC-NER operates when the elongating RNA polymerase II (RNAPII) is stalled by an obstacle encountered in the transcribed strand (Scharer, 2013). These two branches differ in the initial steps, however, once the lesion is detected, they converge on a unified mechanism of dual incision and repair (Figure 4).

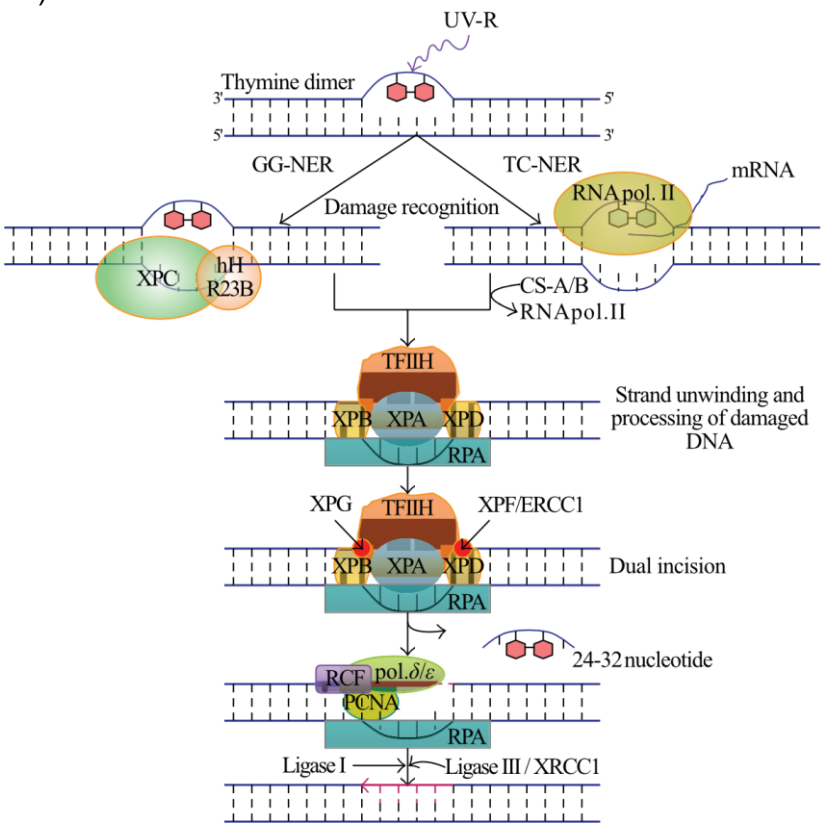

Figure 4. Nucleotide excision repair pathway(s). NER is involved in the repair of bulky DNA lesions and it operates through two distinct subpathways: GG-NER and TC-NER. In GG-NER the recognition of a DNA lesion throughout the genome is operated by XPC, which operates in a heterotrimeric complex with RAD23B (HR23B) and CETN2. Conversely, TC-NER is initiated by stalling of elongating RNAPII in the presence of a transcription-blocking lesion. RNAPII stall triggers the recruitment of CSB that, in turn, recruits CSA to activate NER. Following the lesion recognition step, where the two NER branches differ, GG-NER and TC-NER proceed through a unified pathway. Binding of TFIIH complex, XPA and RPA allows the verification of the lesion and subsequent local DNA unwinding. Next, the nucleases XPF-ERCC1 and XPG incise the DNA at 5' and 3' respectively to release a ~30 nucleotides stretch containing the lesion. Finally, Pol δ, Pol ε or Pol κ, in the presence of PCNA and RCF, operate the DNA gap filling synthesis to terminate repair. Figure adapted from Rastogi et al., 2010.

1.2.1 Global genome NER (GG-NER)

In humans, GG-NER is initiated by the protein Xeroderma pigmentosum (XP) C, that plays a crucial role in recognizing the DNA lesion. XPC is part of a heterotrimeric complex with RAD23B (HR23B) and CETN2 (Masutani et al., 1994; Araki et al., 2001). RAD23B stabilizes XPC, protecting it from polyubiquitylation and proteasomal degradation, whereas CETN2 enhances XPC DNA-binding affinity (Ng et al., 2003; Nishi et al., 2005, Nishi et al., 2013).
The huge amount of genomic DNA and its complex three-dimensional organization, raise the question of how XPC can scan and discriminate between physiological DNA openings and damaged sites. Structural and energetic studies on the XPC yeast homolog Rad4, revealed that the initiation complex searches for disruption on the DNA through a repetitive binding/twisting interrogation process. In the presence of a disruption in DNA hydrogen bonding, XPC undergoes a conformational change, allowing a β-hairpin domain to contact the undamaged nucleotides and open the helix (Min and Pavletich, 2007; Velmurugu et al., 2016). This unspecific scanning strategy adopted by XPC allows the detection of a broad range of base-unpairing lesions, however, it does not explain how CPDs, that only mildly disturb the DNA helix, are also repaired through NER. This observation suggests the existence of additional specialized mechanisms, that improve XPC proficiency in detecting DNA lesions (Sugasawa et al., 2001).
UV-damaged DNA-binding protein (UV-DDB) is a heterodimeric complex made up of DDB1 and DDB2/XPE that exhibits a significant higher affinity for CPDs, compared to XPC (Fujiwara et al., 1999; Fei et al., 2011). UV-DDB binding to damaged DNA occurs via the C-terminal region of DDB2 and it is required to recruit XPC to CPDs sites to activate canonical NER (Payne and Chu, 1994; Tang et al., 2000). In addition, DDB1 recruits on the damage site the Cullin 4 (CUL4)/RING box protein 1 (RBX1) E3 ubiquitin ligase complex that ubiquitylates DDB2, XPC and the surrounding histones (Groisman et al., 2003). This results in proteasomal degradation of DDB2, stabilization of XPC binding and NER progression (Rüthemann et al., 2016).
Due to this unique binding-scanning mechanism, the presence of XPC on a DNA strand does not necessarily implicate the existence of a lesion. On the other side, UV-DDB can also bind to AP sites or mismatches (Fujiwara et al., 1999). Therefore, in order to prevent undesired cuts, this initial NER recognition phase is followed by “verification” process, operated through the ATPase/helicase function of TFIIH complex, and supported by the protein XPA (Li et al., 2015; Okuda et al., 2017). Although occurring through different mechanisms, the recruitment of TFIIH is a common event in GG-NER and TC-NER and it

represents the crucial step when the two subpathways converge on a unified process that will be described in the following section.

1.2.2 General mechanisms of NER

TFIIH is a ten-subunit complex that exerts a double function, as transcription initiation and repair factor. For its role in basal transcription, TFIIH requires a trimeric CDK-activating kinase subcomplex (CAK), that is, in turn, dispensable for DNA repair (Coin et al., 2008). Conversely, for its NER function, TFIIH mainly relies on the helicase activity of its two subunits XPB and XPD that bind to and unwind DNA in opposite directions (3'-5' and 5'-3', respectively), extending the DNA bubble around the complex and allowing the verification of the lesion (Tapias et al., 2004). However, while XPD helicase activity is necessarily required to unwind the damaged DNA, XPB seems to primarily promote ATP-dependent binding of TFIIH at the lesion site (Coin et al., 2007; Oksenych et al., 2009).

The DNA damage verification is additionally assisted by XPA protein that binds to the damaged nucleotides and promotes TFIIH helicase activity, thus favouring the generation of ssDNA stretches around the lesion (Sugasawa et al., 2009). At this stage, the trimeric ssDNA-binding protein RPA is recruited to the undamaged strand, where it helps the stabilization of the open structure, protecting the intact DNA and allowing the specific removal of damaged DNA by the NER endonucleases (Overmeer et al., 2011).

XPF-ERCC1 and XPG have been identified as the NER endonucleases able to incise the DNA at 5' and 3' of the lesion, respectively. XPG recruitment to the pre-incision complex depends on its direct interaction with TFIIH, and it is additionally needed to support the stabilization of the DNA opening and release of XPC-RAD23B (Evans et al., 1997). The binding of XPF-ERCC1 is the last event preceding the removal of the lesion and it depends on its direct interaction with XPA (Tsodikov et al., 2007; Orelli et al., 2010). The order of incisions in NER appears to be precisely defined. Although XPF-ERCC1 recruitment occurs downstream of XPG, it operates the first cut on the 5' side of the damaged strand (Staresincic et al., 2009). The released 3'-OH allows a DNA polymerase to extend the DNA and fill the gap. On the others side, the subsequent XPG incision at the 3' side, generates a 5'-phosphate end for the ligation. Following XPG and XPF-ERCC1 cuts, the ~30 nucleotides stretch containing the lesion is released and the correct DNA sequence is restored (Kemp et al., 2012). Pol δ, Pol ε or Pol κ operate the DNA gap filling synthesis together with PCNA and RFC (Ogi et al., 2010). LIG1, in replicating cells, or LIG3/XRCC1, in non-replicating cells, ligate DNA to complete the NER reaction (Marteijn et al., 2014).

1.2.3 Transcription-coupled NER (TC-NER)

TC-NER pathway is initiated by stalling of elongating RNAPII at a DNA lesion in the transcribed strand. The first observations indicating the existence of transcription-coupled DNA repair mechanisms were done in mammalian cells and, only afterwards, this pathway was uncovered in yeast and in bacteria (Bohr, 1985; Mellon, 1987; Mellon and Hanawalt, 1989; Smerdon and Thoma, 1990). Although the molecular mechanisms differ among the different living domains, the highly conserved underlying processes point out its biological relevance. Interestingly, TC-NER is the only DNA repair pathway where repair process is initiated by recognition of stalled RNAPII, rather than the lesion itself.

In humans, Cockayne syndrome group B (CSB) protein is the first sensor of the stall; indeed, CSB-RNAPII interaction is strongly induced by UV irradiation. CSB initiates transcription-coupled repair (TCR) and allows progressive and coordinate recruitment of downstream NER factors and lesion repair (van den Boom et al., 2004; van der Weegen et al., 2020). Structural studies conducted on CSB's *S. cerevisiae* homolog Rad26 shed light on TC-NER initiation mechanisms (Xu et al., 2017). In unstressed conditions, Rad26 binds upstream of RNA Pol II, favouring transcription elongation and small obstacles bypass. However, in the presence of a bulky lesion, persistent stalling of RNA Pol II results in the stabilization of RNA Pol II/ Rad26 complex and TCR activation (Xu et al., 2017). In line with this model, the Cramer group in 2021 solved the structure of five different RNAPII elongation complexes, expanding the understanding of the TCR assembly mechanisms in human cells (Kokic et al., 2021).

CSB is a 168 kDa protein, made up of 1493 amino acids; it belongs to the DNA-dependent ATPases family SWI2/SNF2 and it has ATP-dependent chromatin remodelling activity, but no helicase activity (Selby and Sancar, 1997). CSB has been implicated in a multitude of cellular processes, bridging transcription regulation and DNA repair (Tiwari et al., 2021). Earlier studies indicated that CSB-deficient cells exhibit a decreased elongation rate, even in absence of DNA damage, suggesting that it may play a role in regulation of basal transcription (Balajee et al., 1997; Dianov et al., 1997). CSB – but no other TC-NER factors – has been implicated in the recognition of transcription-blocking oxidative DNA damages that are subsequently processed by BER (Menoni et al., 2012). Furthermore, CSB interacts and regulates PARP1, stimulating its function in DNA repair (Flohr et al., 2003). CSB-deficient cells exhibit also a characteristic hypersensitivity to ICLs-inducing compounds, like cisplatin and mitomycin C (Furuta et al., 2002). In line with this, CSB has been shown to facilitate ICL repair, promoting SNM1A exonuclease activity on transcription-blocking lesions (Zheng et al., 2003; Iyama et al., 2015). The intimate connection between CSB and

a multitude of DNA repair mechanisms raises the possibility that a unique and broader transcription-coupled mechanism exists. In this speculation, CSB might act as a global sensor for transcription-interfering lesions, recruiting specialized downstream factors and thus ensuring DNA integrity and correct gene expression.

Following UV irradiation and stabilization of TCR initiation complex, CSB undergoes a conformational change and, after exposing a Cockayne syndrome group A (CSA)-interaction motif (CIM), it interacts with and targets CSA to the lesion site (van der Weegen et al., 2020). CSA is 44 kDa protein, consisting of 396 amino acids and, together with CUL4A, RBX1/ROC1 and DDB1, is part of a multi-subunit E3 ubiquitin ligase complex ($CRL4^{CSA}$); CSA does not have a functional homolog in yeast or in bacteria, conversely to CSB. Once recruited, $CRL4^{CSA}$ has been shown to ubiquitylate itself, CSB and RNAPII (Groisman et al., 2006; Nakazawa et al., 2020). The function and occurrence of CSB ubiquitylation in response to UV irradiation is a controversial topic. Indeed, some experiments showed that CSB ubiquitylation prompts it for valosin-containing protein (VCP)/p97-dependent extraction and proteasomal degradation, thus allowing release of the initiation complex and TC-NER progression (He et al., 2016). Other studies did not detect UV-dependent ubiquitylation and degradation of CSB, but rather SUMOylation. Whether SUMOylated CSB levels vary in the presence/absence of CSA is unclear (Sin et al., 2016; Liebelt et al., 2019).

Stabilization of CSB and protection from proteasomal degradation has been shown to depend on UV-stimulated scaffold protein A (UVSSA) and its interacting partner USP7. USP7 is a DUB involved in a multitude of DNA damage repair mechanisms and its UVSSA-mediated recruitment appears to be essential for TC-NER progression (Schwertman et al., 2013; Valles et al., 2020). Therefore, in the absence of UVSSA or USP7, upon UV-induced damage, CSB is degraded faster and TC-NER repair does not progress (Higa et al., 2016). UVSSA has been identified as a TC-NER protein by three research groups that demonstrated its interaction with RNAPII and CSB at UV-induced lesions (Nakazawa et al., 2012; Schwertman et al., 2012; Zhang et al., 2012). However, the mechanism of UVSSA recruitment to TCR complex has been object of debate. Live-cell imaging experiments showed that, upon UV irradiation, UVSSA binds to stalled RNAPII, independently of CSA and CSB (Schwertman et al., 2012). More recently, the systematic study of TCR sequential assembly revealed that UVSSA is recruited via association with CSA, through its N-terminal VHS domain. This interaction fully depends and it is stabilized in the presence of both CS proteins (van der Weegen et al., 2020). In turn, UVSSA contains a TFIIH-interacting region (TIR) that it is crucial for the recruitment of TFIIH, further stabilized in the presence of CSA

(van der Weegen et al., 2020). Subsequent monoubiquitylation of UVSSA at position K414 allows its displacement from TFIIH that is, in turn, transferred to stalled RNAPII to initiate repair (Nakazawa et al., 2020). The role of TFIIH in determining stalled RNAPII fate has also been investigated and it will be discussed in detail in the following section (1.2.4.1). After TFIIH recruitment, TC-NER and GG-NER branches converge in a unified pathway that proceeds to excise the damaged DNA and restore the correct sequence (Okuda et al., 2017).

Two recent studies by Greijer et al. and van der Weegen et al. identified the elongation factor 1 (ELOF1) as a novel TC-NER factor, that promotes recruitment of UVSSA and TFIIH to lesion sites (Geijer et al., 2021; van der Weegen et al., 2021) (Figure 5). ELOF1, similarly to its yeast homolog Elf1, behaves as an elongation factor in unperturbed conditions, where it constitutively binds to the transcription machinery (Ehara et al., 2017). In its absence, CSB and CSA can initiate TC-NER, however UVSSA and TFIIH recruitment is strongly reduced and RNAPII is not ubiquitylated, suggesting that ELOF1 is involved in the TCR assembly process and in the signalling events that allow RNAPII removal from the damage site. Additionally, the authors provided evidence for a second function of ELOF1 as a more general DNA damage sensor preventing transcription-replication conflicts site (Geijer et al., 2021; van der Weegen et al., 2021). Further studies will be required to clarify these aspects.

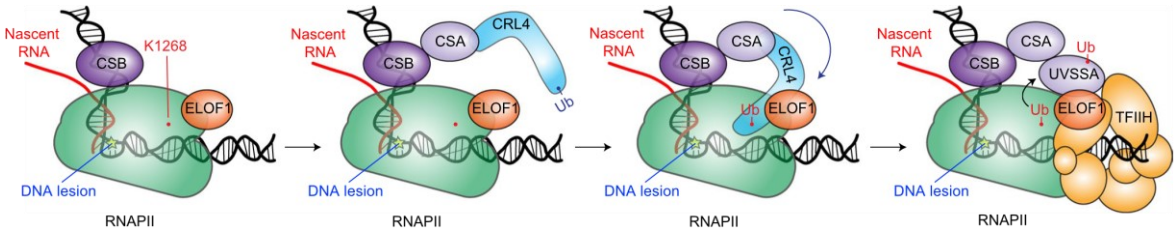

Figure 5. Assembly of TC-NER complex. The presence of a DNA lesion in the transcribed strand hampers the progression of transcription elongation. RNAPII stalling is detected by CSB that, in turn, recruits CSA to the lesion site. CSA is part of multi-subunit E3 ubiquitin ligase complex ($CRL4^{CSA}$) that ubiquitylates RNAPII on a single lysine (K1268) to permit TCR progression. ELOF1 behaves as an elongation factor in unperturbed conditions, where it constitutively binds to the transcription machinery and, following TCR activation, it interacts with $CRL4^{CSA}$. ELOF1 interaction with $CRL4^{CSA}$ allows the correct positioning of the complex and favours RNAPII ubiquitylation. ELOF1, subsequently, promotes CSA-dependent recruitment of UVSSA and its ubiquitylation, that is, in turn, required to transfer the TFIIH complex from UVSSA to stalled RNAPII. These events allow NER progression. Figure from van der Weegen et al., 2021.

1.2.4 Cellular responses to transcription-blocking DNA damage

The presence of a bulky lesion on the transcribed DNA strand blocks elongating transcription machineries. Stalled RNAPII locally activates TCR to remove the obstacle, thus allowing transcription resumption (*in cis* effect). In addition to this direct effect, in order to cope with transcriptional stress, cells activate specific regulative mechanisms and operate a finely tuned transcriptional reprogramming (*in trans* effect) (Geijer and Marteijn, 2018).

1.2.4.1 The fate of stalled RNAPII in TC-NER

Elongating RNAPII can act as a sensor of DNA damage and preserve correct gene expression. Indeed, in the presence of a DNA lesion in the transcribed strand, the stalled RNAPII provides an anchoring site to initiate and coordinate TCR. However, irreversibly stalled RNAPIIs can become toxic for the cell, as they impede further transcription of that gene (Saeki and Svejstrup, 2009). Moreover, the persistent presence of stalled RNAPII would physically hamper the verification and subsequent incision of the lesion (Li et al., 2015). To avoid undesired consequences and favour DNA repair, stalled elongation complexes need to be extracted from the lesion sites.

In vitro studies suggested that, upon recruitment of TFIIH, its ATPase subunits XPD and XPB translocate along the DNA and displace the stalled RNAPII (Sarker et al., 2005). Consistently, a more recent study showed that RNAPII is unable to resume transcription and it necessarily needs to dissociate during TCR (Chiou et al., 2018). This step would allow the recruitment and correct positioning of downstream NER repair factors, explaining why they do not directly associate with RNAPII after UV irradiation (van der Weegen et al., 2020; Kokic et al., 2021). However, whether RNAPII extraction occurs prior or simultaneously to NER repair has not been fully clarified yet.

Additionally, the release of stalled RNAPII depends on tightly regulated ubiquitylation and degradation mechanisms. Several studies in yeast and humans showed that in the presence of transcription-blocking lesions, RPB1, the largest subunit of RNAPII, is polyubiquitylated and degraded (reviewed in Wilson et al., 2013). In *S. cerevisiae*, Rpb1 undergoes coordinated ubiquitylation and deubiquitylation events that, initiated by Rsp5-dependent K63 monoubiquitylation, culminate in K48 polyubiquitylation mediated by an Elongin-Cul3-dependent ubiquitin ligase complex (Cul3-Rbx1-Elc1-Ela1) (Huibregtse et al., 1997; Beaudenon et al., 1999; Harreman et al., 2009). Poly-ubiquitylated Rpb1 can thus be extracted from chromatin by Cdc48-Ufd1-Npl4 segregase complex and delivered to the proteasome for degradation (Gillette et al., 2004; Verma et al., 2011).

In humans, RPB1 has been shown to undergo ubiquitylation and proteasomal degradation in response to UV irradiation (Bregman et al., 1996; Ratner et al., 1998). A multitude of E3 ubiquitin ligases have been shown to contribute to RPB1 ubiquitylation: NEDD4 ligase, Elongin A complex and BRCA1-BARD1 (BRCA1 Associated RING Domain 1) (Kleiman et al., 2005; Starita et al., 2005; Anindya et al., 2007; Yasukawa et al., 2008). It was also observed that CS-deficient cells show reduced RNAPII ubiquitylation level, suggesting that TCR initiation factors may be in some way implicated in the process (Bregman et al., 1996). In line, CSB appears to coordinate VCP/p97 recruitment and subsequent RNAPII degradation (He et al., 2016; He et al., 2017). Conversely, the Svejstrup lab suggested that CS proteins are not required for RBP1 ubiquitylation and degradation (Anindya et al., 2007). They also hypothesised that RNAPII degradation was not necessarily needed for TC-NER progression, but rather a “last resort” mechanism for those elongation complexes that could not be salvaged in any other way (Wilson et al., 2013). In any case, the regulation and biological significance of this post-translational modification (PTM) had remained enigmatic for long time.

Recently, a single DNA damage-induced ubiquitylation site in RNAPII has been identified: RPB1-K1268 has been shown to be conjugated with K48- and K63-linked ubiquitin chains in response to UV, with multiple effects (Nakazawa et al., 2020; Tufegdžić Vidaković et al., 2020). In line with previous studies in which reduced RPB1 ubiquitylation levels in CS-deficient cells were observed, $CRL4^{CSA}$ has been shown to directly contribute to K1268 ubiquitylation (Bregman et al., 1996; Nakazawa et al., 2020). However, loss of CSA only partially suppresses K1268 ubiquitylation that is, in turn, abolished by NEDD8 inhibitor, suggesting the contribution of an unknown second CRL-based E3 ligase (Nakazawa et al., 2020). Ubiquitylation of RPB1-K1268 has been shown to coordinate TCR assembly, stimulating the recruitment of UVSSA and TFIIH to stalled RNAPII. According to this model, UVSSA is initially recruited via interaction with CSA and then transferred to ubiquitylated RNAPII, to which it has higher affinity (Nakazawa et al., 2012). In the end, UVSSA K414 monoubiquitylation stimulates the transfer of TFIIH to stalled RNAPII (Nakazawa et al., 2020; Tufegdžić Vidaković et al., 2020). In addition, K1268 ubiquitylation seems to be required for UV-induced degradation of RPB1 (Tufegdžić Vidaković et al., 2020). Impairment of K1268 ubiquitylation in CSB- and CSA-deficient cells, could potentially explain why these cells are unable to degrade RNAPII after UV (Bregman et al., 1996). In contrast, in UVSSA-deficient cells RNAPII degradation occurs faster, possibly due to loss of USP7-dependent protective function of CSB (Nakazawa et al., 2012; Zhang et al., 2012). Although not fully clarified, the differences in RNAPII turnover in CS- and UVSSA-deficient

cells might contribute to explain the different clinical phenotypes associated with their loss (as discussed in section 1.2.5).

1.2.4.2 Transcription remodelling in response to UV

To cope with transcriptional stress, upon UV irradiation cells shut down transcription and reprogram gene expression (van den Heuvel et al., 2021).

An early study showed that upon UV irradiation there is a massive depletion of the hypophosphorylated form of RNAPII (RNAPIIa), in favour of an increase in hyperphosphorylated RNAPIIo pool. This might suggest that in the presence of a transcription-blocking lesion, cells at first attempt to reinitiate transcription (early response); however, the progressive stalling of elongating complexes at the lesion depletes the pool of RNAPII and shuts down transcription (late response) (Rockx et al., 2000). In line with this, it has recently been shown that immediately following UV irradiation, transcription initiation is restricted to the promoter-proximal 20-30 kb of genes (Williamson et al., 2017; Tufegdžić Vidaković et al., 2020).

At this stage, the expression of several small immediate early genes (IEGs) is increased (Bahrami and Drabløs, 2016). Among other genes, the transcriptional repressor activating transcription factor 3 (ATF3) is induced by UV light. ATF3 binds to near promoter CRE/ATF sites of about 5000 genes and inhibits their expression (Kristensen et al., 2013; Cui et al., 2016). ATF3-mediated gene repression contributes to shutdown transcription in an early stage, perhaps to allow efficient removal of DNA lesions. However, following DNA repair, to allow an efficient restart of transcription, ATF3 has to release the promoters. CSB and $CRL4^{CSA}$ together with the E3 ubiquitin ligase MDM2 ubiquitylate ATF3, that it subsequently degraded by the proteasome (Kristensen et al., 2013; Epanchintsev et al., 2017). Therefore, the persistent transcriptional repression in CS-deficient cells could also be potentially explained by their incapability to ubiquitylate and degrade ATF3 (Epanchintsev et al., 2017).

1.2.5 NER deficiencies and human health

NER deficiencies are associated with severe human diseases: mutations in GG-NER or TC-NER genes cause Xeroderma pigmentosum (XP) and Cockayne syndrome (CS), respectively. Patients affected by these syndromes, exhibit a broad spectrum of clinical phenotypes, ranging from skin cancer predisposition to neurodevelopmental defects and premature aging (Rapin et al., 2000). The molecular mechanisms responsible for these phenotypes have not been fully elucidated yet.

Xeroderma pigmentosum (XP) is a rare autosomal recessive disease caused by mutations in one of the following genes: *XPA*, *XPB*, *XPC*, *XPD*, *XPE*, *XPF*, *XPG* and *XPV*. According to the mutated gene patients are classified into 8 complementation groups. XP patients show a general NER deficiency, whose distinctive features are photosensitivity and increased cancer predisposition; however, clinical symptoms vary among the different groups (DiGiovanna and Kraemer, 2012). Patients with mutations in GG-NER genes *XPC* and *XPE* are only mildly sensitive to UV radiation. However, they show a 1000-fold increased risk to develop skin cancer and internal tumours, possibly due to the accumulation of DNA lesions generated by endogenous reactive metabolites (Barnes and Lindahl, 2004; Sethi et al., 2013). In turn, patients with mutations in *XPA*, *XPB*, *XPD*, *XPF* and *XPG* are dramatically sensitive to UV light exposure, developing sunburns immediately after brief exposures (Bradford et al., 2011). Lastly, patients of the XPV group typically show increased skin cancer susceptibility. They have normal NER, but mutated *POLH*: this gene encodes DNA TLS polymerase Pol η, that allows error-free bypass of unrepaired photoproducts during DNA replication (Masutani et al., 1999; Lange et al., 2011).

TC-NER deficiencies predispose to very heterogenous phenotypes caused by impairment of cell functions that accelerates cell death. Mutations in genes encoding CSB and CSA (*ERCC6* and *ERCC8*, respectively) are causative for Cockayne syndrome (CS) (Cockayne, 1936). CS is a severe autosomal recessive disorder, whose typical symptoms are abnormal development, neurological defects, microcephalia, progressive cachexia, premature aging, sunlight sensitivity and renal-cardiovascular disorders. Due to the severe progeroid phenotype, the average life expectancy of CS patients is 12 years (Karikkineth et al., 2017). Mutations in *UVSSA* are responsible for a milder form of TCR deficiency, known as UV-sensitive syndrome ($UV^{S}S$). Patients affected by this disorder, are hypersensitive to UV radiation, but completely lack progeroid phenotypes, neurological and developmental alterations (Spivak, 2005). The strong difference between CS and $UV^{S}S$ manifestations is surprising, since in both syndromes TC-NER is impaired; several hypotheses have been formulated to possibly explain this divergence. According to one model, the more severe clinical spectrum of CS patients depends on the compromised degradation of lesion-stalled elongation complexes in the absence of CS proteins. Indeed, the persistent presence of stalled RNAPII not only physically hampers NER, but it also impedes any other repair system to detect, access and remove the transcription-blocking lesions (photoproduct and oxidative damages). In contrast, loss of UVSSA impairs TCR, but it still permits degradation of stalled RNAPII. This allows BER factors to detect and remove oxidative lesions (but not photolesions), therefore explaining the exclusive sensitivity of $UV^{S}S$ patients to UV

photoproducts (Marteijn et al., 2014). It has also been proposed that CS progeroid phenotypes depend on the transcriptional misregulation generated by loss of function of CSA or CSB (e.g. ATF3-dependent repression of transcription) (Proietti-De-Santis et al., 2006; Wang et al., 2014; Epanchintsev et al., 2020). The Luijsterburg group proposes that CS is a consequence of transcription restart failure, caused by impaired RPB1-K1268 ubiquitylation (van den Heuvel et al., 2021). In this model, RPB1-K1268 ubiquitylation, altered in CS-deficient cells, is first required to shut down transcription, and then to coordinate RNAPII degradation. Indeed, CS patients' fibroblasts cannot degrade RNAPII, in contrast to UV^{S}S ones, that show even faster turnover (Bregman et al., 1996; Fei and Chen, 2012; Nakazawa et al., 2012; Schwertman et al., 2012; Zhang et al., 2012).

Mutations in NER downstream core factors genes (*XPB*, *XPD*, *XPF*, *XPG*) affect both GG- and TC-NER. Patients in these groups have heterogenous phenotypes and usually exhibit either pure XP or a XP-CS syndrome, with a combination of XP and CS symptoms (Natale and Raquer, 2017). *XPB* and *XPD* mutations can also cause trichothiodystrophy (TTD), whose manifestations might depend on the additional role played by TFIIH complex in transcription initiation (Marteijn et al., 2014). Mutations in *XPF-ERCC1* are responsible for the most complex clinical manifestations, possibly due to its additional function in ICL repair. Patients and mice models with impaired ERCC1 function, exhibit a combination of symptoms of XP, CS and Fanconi anemia, with characteristic premature aging of post-replicative (neurons) and proliferative tissues (haematopoietic stem cells) (Kashiyama et al., 2013).

1.3 DNA-protein crosslinks (DPCs)

DNA-protein crosslinks (DPCs) are highly toxic DNA lesions that consist of a protein covalently attached to DNA. DPCs can be considered unique DNA lesions, not only because they constitute very large adducts, but also because they are very diverse in nature. DPCs are highly toxic and interfere with every chromatin transaction, such as replication and transcription. Accordingly, DPCs have been shown to hamper RNAPII progression on the transcribed strand *in vitro* and to interfere with replication fork advancement *in vivo* (Hong and Kreuzer, 2000; Pohlhaus and Kreuzer, 2005; Kuo et al., 2007; Nakano et al., 2012; Ji et al., 2019). In order to prevent genomic alteration, DPCs need to be efficiently repaired (Klages-Mundt and Li, 2017; Stingele et al., 2017).

1.3.1 Types and sources of DPCs

DPCs can originate both from exogenous and endogenous sources and through enzymatic or non-enzymatic mechanisms (Tretyakova et al., 2015; Kühbacher and Duxin, 2020). Importantly, the existence of many sources of DPCs suggests that every protein in the vicinity of DNA can become crosslinked (Stingele et al., 2017). The most significant sources and types of DPCs will be discussed in this section (Figure 6).

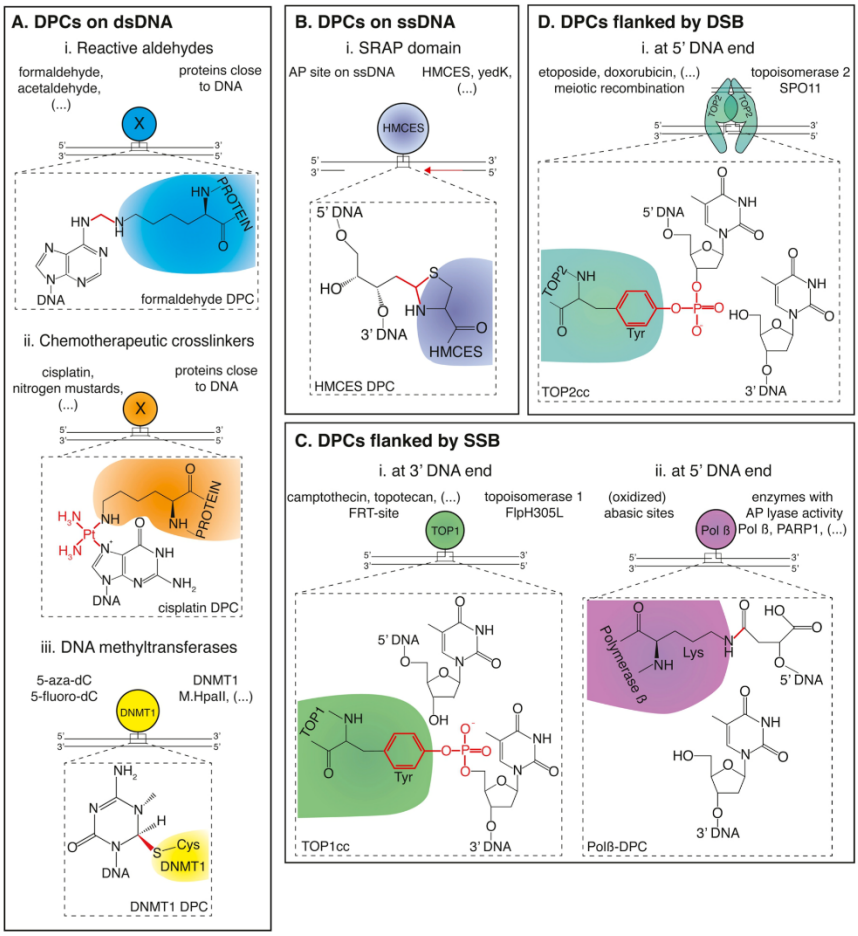

Figure 6. Types of DPCs. A, i) Reactive aldehydes generate unspecific non-enzymatic DPCs. Particularly, FA-induced DPCs are bridged via a methylene linkage that can preferentially form between the amino or thiol group of an amino acid and the exocyclic amine of a DNA base. **A, ii)** Chemotherapeutic agents with double functional reactive groups, such as cisplatin or nitrogen mustards can react with a DNA base and an amino acid side chain to form a DPC. **A, iii)** The chemotherapeutic 5-azadC behaves as pseudosubstrate for DNMT1, irreversibly entrapping this enzyme on the DNA. **B, i)** The SRAP domain of HMCES crosslinks to an AP site via a thiazolidine linkage in order to prevent undesired DNA strand breaks. **C, i)** The antineoplastic drugs topotecan and irinotecan can intercalate in the enzyme-DNA interface and inhibit TOP1 religation, covalently trapping TOP1 at the 3' end of a SSB. **C, ii)** BER enzymes, such as Pol β, APE1 and PARP1, can be accidentally crosslinked to the 5' end of AP sites during their reaction. **D, i)** Intercalating agents doxorubicin and etoposide covalently trap TOP2 homodimer via its two active site tyrosines to both 5' ends of a DSB. Figure from Kühbacher and Duxin, 2020.

1.3.1.1 Enzymatic DPCs

Enzymatic DPCs are formed when normally transient covalent enzyme-DNA intermediates get trapped during their reaction cycles. This can either occur spontaneously, due to DNA structural alterations, or because of exposure to exogenous crosslinking agents. Currently, several chemotherapeutics used in the clinic kill cancer cells by inducing DPC formation (Stingele et al., 2017).

Relevant enzymatic crosslinks are produced by trapping of topoisomerase 1 and 2 (TOP1/2). These enzymes are utilized by the cells to resolve DNA topological stress and, during the reaction, a tyrosine of their active site covalently binds the phosphate group of the DNA backbone (Champoux, 2001; Wang, 2002). In physiological conditions, this transient covalent intermediate, referred to as a TOP1/2-cleavage complex (cc), is quickly resolved and the DNA is religated. However, in the presence of DNA distortions or crosslinking agents, the enzyme release fails, thus resulting in its permanent trapping on the DNA (Pommier et al., 2014). TOP1 cleaves only one strand of the DNA, therefore TOP1-cc is attached at the 3' end of a SSB. The antineoplastic drugs topotecan and irinotecan, derived from the alkaloid camptothecin (CPT), can intercalate in the enzyme-DNA interface, therefore inhibiting TOP1 religation (Pommier, 2006; Pommier and Marchand, 2012). By contrast, TOP2 operates as a dimer in which each subunit introduces a SSB, generating a DSB. As a consequence, TOP2-cc is attached via two active site tyrosines to both 5' ends of a DSB (Stingele et al., 2017). The chemotherapeutic agents etoposide, anthracyclines (doxorubicin) and mitoxantrone, similarly to TOP1 inhibitors, trap TOP2 and hamper its DNA release (Nitiss, 2009; Pommier and Marchand, 2012).

Another chemotherapeutic agent that generates DPCs is the cytidine analogue 5-aza-2'-deoxycytidine (5-azadC), commonly used in the treatment of myelodysplastic syndromes (Fenaux et al., 2009). 5-azadC is incorporated in the DNA during replication and it exerts its toxicity by entrapping the enzyme DNA methyltransferase 1 (DNMT1) on the DNA (Santi

et al., 1984; Maslov et al., 2012). The methyltransferase activity of DNMT1 is essential to maintain methylation patterns upon replication (Gujar et al., 2019). The DNA-incorporated 5-azadC is methylated by DNMT1, however, following the reaction, DNMT1 remains covalently trapped through a cysteine residue forming a DNMT1-DPC. Inhibition of DNMT1 reduces the DNA methylation levels and consequently causes the re-expression of pathologically silenced tumour suppressor genes (Wilson et al., 1983; Robert et al., 2003). BER enzymes, such as Pol β and APE1, can be accidentally crosslinked to oxidized AP sites during their reaction (DeMott et al., 2002; Quiñones et al., 2015; Quiñones et al., 2020). PARP1, due to its "first responder" function to DNA strand breaks and AP sites, appears to be intrinsically prone to covalently bind DNA (Prasad et al., 2014). PARP1 crosslinking occurs through the formation of a Schiff base between the C1 atom of deoxyribose in the AP site and a primary amine in PARP1. Then, if the Schiff base is reduced (perhaps due to PARP1 intrinsic reducing capacity), PARP1 remains covalently attached to 3' end of the DNA (Prasad et al., 2019). Alternatively, PARP1 can accidentally crosslink to the 5' end following APE1 cleavage during BER (Prasad et al., 2020). PARP1 can also be trapped by cancer drugs, such as olaparib, rucaparib, niraparib, or talazoparib, comprehensively referred to as PARP inhibitors (PARPi) (Pommier et al., 2016). PARPi are currently approved for the treatment of BRCA1/2 mutated breast, ovarian, pancreatic and prostate cancers (Rose et al., 2020). All PARPi exert their action through competition inhibition with NAD+, however these agents can additionally trap PARP1 on DNA and their different efficacy appears to strictly depend on their "trapping" ability. Therefore, the presence of trapped PARP molecules can pathologically hamper transcription and replication progression, improving tumour cells death (Murai et al., 2012b; Zandarashvili et al., 2020). AP sites are also dangerous due to their instability, therefore they can easily convert into undesired strand breaks (Loeb and Preston, 1986). Recent studies showed that cells prevent this event by converting AP sites in ssDNA into intentional DPCs. The protein 5-hydroxymethylcytosine binding, ES cell specific (HMCES) recognizes an AP site and crosslinks to it through its SOS response-associated peptidase (SRAP) domain via a thiazolidine linkage (Mohni et al., 2019; Thompson et al., 2019). This genome protection strategy appears to be highly conserved, as indicated by the existence in bacteria of a similar mechanism depending on HMCES ortholog yedK (Wang et al., 2019; Hu et al., 2021).

1.3.1.2 Non-enzymatic DPCs

Non-enzymatic DPCs are formed by unspecific covalent binding of any protein in the vicinity of DNA in the presence of DPCs-inducing agents. Common sources of crosslinking are endogenously produced reactive metabolites, such as ROS and aldehydes, but also exogenous agents, such as IR, UV radiation and chemotherapeutics (Tretyakova et al., 2015; Stingele et al., 2017).

A significant endogenous source of DPCs is represented by FA, produced in the cells during several metabolic reactions. Thus, even in physiological conditions, high concentrations of FA can be detected in human blood (Heck et al., 1985; Zhang et al., 2009). Importantly, FA is generated near the DNA as by-product of histone demethylation and AlkB-dependent repair, thus it represents a significant and constant risk for genomic integrity (Shi et al., 2004; Shen et al., 2014; Pontel et al., 2015). The generation of FA-induced DPCs occurs as a multi-step reaction: first FA reacts with the amino or thiol group of an amino acid (nucleophile) to form a methylol adduct on the protein, then, this is dehydrated to a Schiff base. The reaction of the Schiff base with an amino group of a DNA base (second nucleophile) forms a methylene-bridged DPC (Nakamura and Nakamura, 2020). Recently, the introduction of a new sensitive method to study crosslinked-protein identity revealed that FA-induced DPCs are mainly crosslinked nucleosomes (Weickert et al., 2023).

Free radicals generated by ROS reaction with DNA bases or amino acid side chains have been shown to react with another molecule to form a DPC. How strong the contribution of ROS to DPC formation *in vivo* has not be assessed yet (Barker et al., 2005; Tretyakova et al., 2015).

UV and IR radiation have also been shown to induce DPC formation, however the precise mechanisms are still poorly understood (Fornace and Little, 1977; Peak and Peak, 1986; Moss et al, 1997; Gueranger et al., 2011). The effect of IR on DNA-protein crosslinking strongly depends on molecular oxygen conditions. It has been observed that the efficiency of DPC formation is higher in hypoxic tumours compared to normoxic tumours (Nakano et al., 2015). Conversely, in the presence of oxygen, IR promotes base damages, SSBs, and DSBs. Although these effects are not fully understood, the reverse oxygen effect appears to be a unique characteristic of radiation-induced DPCs (Zhang and Wheeler, 1993; Shoulkamy et al., 2012; Nakano et al., 2017).

Several chemotherapeutic agents exert their toxicity also through DPC formation. For example, nitrogen mustards, due to their bifunctional reactive groups, can react with a DNA base and an amino acid side chain to form DPCs (Ewig and Kohn, 1977; Loeber et al. 2008; Groehler et al., 2016). In addition, platinum-based agents, such as cisplatin, that are mainly

known as DNA-DNA crosslinkers, are also able to form DPCs. For instance, cisplatin, once entered in the cell, is subjected to displacement of its chloride atoms, in the presence of water. The activated hydrolysed product can react with side chains of cysteine, lysine and arginine and nitrogen donor atoms on nucleic acids, introducing a DPC (Woźniak and Walter, 2000; Chválová et al., 2007; Ming et al., 2017).

1.3.2 DPC repair strategies

Due to their huge diversity and considerable bulky nature, DPCs represent a significant challenge for the cell. In order to prevent deleterious consequences, a multitude of general and dedicated DPC repair mechanisms cooperate to remove the crosslinked-protein and restore DNA integrity (Stingele et al., 2017; Zhang et al., 2020).

1.3.2.1 Hydrolytic repair of TOP1-ccs and TOP2-ccs

Since cells rely on TOP1 and TOP2 to resolve DNA torsional stress, their aberrant covalent trapping is a relatively frequent event. To avoid deleterious complications, cells possess two specialized enzymes, tyrosyl-DNA phosphodiesterase 1 and 2 (TDP1/2), that release TOP1-cc and TOP2-cc, respectively (Figure 7). However, the action of TDP1 and TDP2 appears to be not sufficient to resolve the damage, which in addition requires the multiple other DNA repair factors (Pommier et al., 2014).

TDP1 was initially discovered in *S. cerevisiae* and, subsequently, it was found to be expressed in all the organisms (Pouliot et al., 1999; Murai et al., 2012a). TDP1 is able to hydrolyse 3'-tyrosine preferably at ssDNA structures (Raymond et al., 2005). *In vitro* experiments showed that TDP1 was not able to release full length TOP1-cc, in absence of a pre-processing, such as denaturation (Yang et al., 1996; Interthal et al., 2005). This observation suggested that in the cell some interventions might be required to permit TDP1-mediated hydrolysis. In addition, TDP1 can only cleave a shortened fragment of TOP1-cc that is produced *in vivo* by the proteasome (Lin et al., 2008; Interthal and Champoux, 2011). Accordingly, more recent studies showed that, in order to be subjected to proteasomal degradation, TOP1-cc is first SUMOylated by the SUMO E3 ligase PIAS4 and subsequently polyubiquitylated by the SUMO-targeted ubiquitin ligase (STUbL) RING finger protein 4 (RNF4) (Sun et al., 2020).

This proteasomal pre-processing allows TDP1 to finally access and release TOP1-cc through the generation of a transient covalent intermediate between the active site histidine His263 (humans) and the 3' end of the substrate. This is then followed by His493-mediated hydroxylation of the covalent intermediate and subsequent release of TDP1 and a 3'-

phosphate DNA product (Pommier et al., 2014). His493Arg substitution in TDP1 prevents the disassembly of the covalent TDP1-DNA intermediate and it is, therefore, causative for a severe autosomal recessive disease, called spinocerebellar ataxia with axonal neuropathy (SCAN1) (Takashima et al., 2002). Following TDP1 release, PNPK dephosphorylates and phosphorylates the 3' and 5' ends, respectively. These are then recognized and religated by SSBR machinery (PARP1, XRCC1, LIG3 and Pol β) (Caldecott, 2008). Several PTMs coordinate TDP1 and SSBR activity. More in detail, TDP1 is stabilized at TOP1-cc lesion by SUMOylation and PARylation, whereas its subsequent phosphorylation allows the recruitment of XRCC1 and LIG3 to ultimate repair (Chiang et al., 2010; Hudson et al., 2012; Das et al., 2014).

TDP2 is involved in the repair of TOP2-cc, that is trapped via two 5'-phosphotyrosyl-DNA bonds. TDP2 hydrolyses the covalent bonds, thus generating a DSB with 5'-phosphate and 3'-OH groups that can be immediately religated by NHEJ pathway factors (Gómez-Herreros et al., 2013). TDP2-mediated catalysis does not involve the formation of a covalent catalytic intermediate but it requires two divalent metals (such as Mg^{2+}, Mn^{2+} or Co^{2+}). The two ions attack the phosphotyrosyl bond, coordinated by the catalytic residues of the active site, and allow the release of TOP2 and free DNA (Gao et al., 2012). TDP2 activity, similarly to TDP1, was shown to require TOP2-cc proteasomal pre-processing, depending on PIAS4-RNF4 (Mao et al., 2001; Sun et al., 2020). Another study revealed that SUMOylation regulates TDP2 through a proteasomal-independent mechanism. The SUMO E3 ligase ZATT (ZNF451) binds and repositions TDP2 in a lesion-accessible conformation; subsequently ZATT binds and SUMOylates TOP2-cc. TDP2 is recruited to the SUMOylated TOP2-cc where it is able to resolve the covalent bonds (Schellenberg et al., 2017).

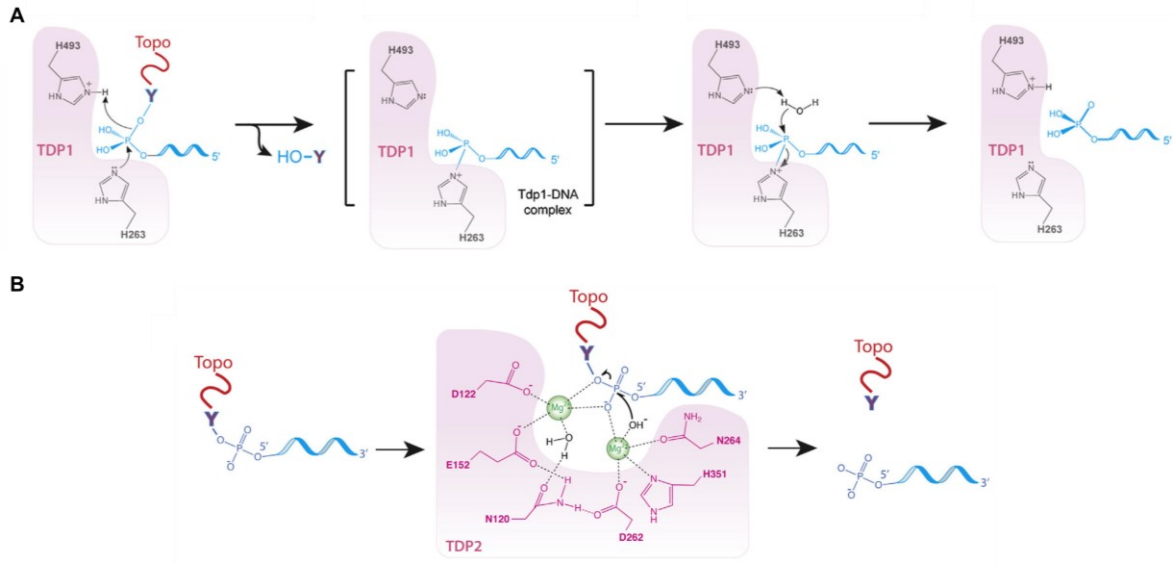

Figure 7. TDP1 and TDP2 catalytic cycles. A) The imidazole N2 atom of TDP1 His263 attacks the phosphodiester backbone (first nucleophilic attack), while His493 donates a proton and allows the release of TOP1 (leaving group). TDP1 forms a transient covalent intermediate (Tdp1-DNA complex) between its active site His263 and the 3'-phosphate end of the substrate DNA. This is followed by His493-mediated hydroxylation of the covalent intermediate phosphate group (second nucleophilic attack) and subsequent release of TDP1 and a 3'-phosphate DNA product. **B)** Conversely to TDP1, TDP2-mediated catalysis does not involve the formation of a covalent catalytic intermediate. Following the entry of the covalent TOP2-DNA substrate in TDP2 active site, two magnesium ions coordinated by TOP2 catalytic residues attack the phosphotyrosyl bond (nucleophilic attack). This reaction allows the release of TOP2 and free DNA with a 5′-phosphate end. Figure adapted from Pommier et al., 2014.

1.3.2.2 Nuclease-dependent repair of DPCs

In addition to the multitude of dedicated DPC repair mechanisms, several studies indicated that canonical DNA repair pathways, such us HR or NER, differentially contribute to resolve these toxic lesions.

1.3.2.2.1 HR contribution to DPC repair

First indications of HR participation in DPC repair came from studies in bacteria and yeast. The bacterial MRN ortholog SbcCD complex was shown to cleave DNA and allow the release of proteins at DNA termini (Connelly et al., 2003). In yeast, the MRN counterpart (Mre11-Rad50-Xrs2) is required to remove Top1, Top2 and Spo11 adducts (Keeney et al., 1997; Hartsuiker et al., 2009a; Hartsuiker et al., 2009b). In humans, it was initially observed that the MRN complex and CtIP promote repair of DSBs induced by etoposide treatment in G1 phase, independently of HR (Quennet et al., 2011).

It was shown that TDP2-deficient cells do not accumulate significant amount of TOP2-cc in absence of TOP2 inhibitors, suggesting the existence of a parallel repair mechanism to resolve this DPC (Pommier et al., 2014). Further studies confirmed that, in addition to TDP2-mediated catalysis, TOP2-cc can be processed by the MRN (MRE11-RAD50-NBS1) complex. Accordingly, loss of function of MRN or NBS1 compromises TOP2-cc repair, causing accumulation of these intermediates, which, in turn, can be rescued by TDP2 overexpression (Lee et al., 2012; Hoa et al., 2016). *In vitro* studies showed that to release protein adducts covalently attached to DNA ends, the MRN multifunctional complex utilizes its endo and exonuclease and ATPase activities, coordinated by the NBS1 subunit. The complex operates through a multistep process that is initiated by a DNA incision in proximity of the trapped protein. Then, the exonuclease activity of MRN stimulates a 3'-5' DNA resection; this is followed by a second incision on the complementary DNA strand. This event removes the DPC and allows DSB repair by NHEJ machinery (Deshpande et al., 2016; Hoa et al., 2016).

Interestingly, even though many studies addressed the specific contribution of MRN to TOP2-cc repair, it seems that the complex can act in the presence of a broad range of protein adducts, suggesting that it might represent a general cell protection mechanism towards DPCs (Aparicio et al., 2016; Deshpande et al., 2016). In line with this, HR-deficient cells are highly sensitive to the non-enzymatic DPCs-inducing agent FA and accumulate DSBs (Nakano et al., 2007; Nakano et al., 2009).

1.3.2.2.2 NER contribution to DPC repair

The contribution of NER to DPC repair remains a controversial topic. An early study showed that the bacterial NER complex (UvrABC) is able to excise *in vitro* a 16 kDa protein covalently bound to a DNA AP site (Minko et al., 2002). Then, the same authors systematically analysed NER excision efficiency of different-sized peptides, observing that small peptide-crosslinks are preferable substrates. Therefore, they speculated that a proteolytic pre-processing might be required for repair *in vivo* (Minko et al., 2005). In line with this, further studies showed that deficiencies of UvrABC sensitize the cells to the DPCs-inducing agent FA, but not to 5-azadC. The authors observed that the bacterial NER machinery can excise DPCs, but only if the protein adduct size does not exceed 12-14 kDa. This would explain why it is “blind” to the bulky 5-azadC-induced DNMT1-DPCs that are, in turn, resolved by HR (Nakano et al., 2007).

In yeast, two independent studies showed that deficiencies in NER factors result in sensitivity to FA, suggesting the contribution of NER pathway to DPC repair (de Graaf et al., 2009; Stingele et al., 2014). More in detail, de Graaf et al. observed that deficiencies in NER factors sensitize cells to high-dose short treatment with FA, whereas loss of HR function increases sensitivity towards low-dose chronic exposure to FA. This observation indicates that, according to the duration and intensity of the insult, the two pathways differentially contribute to repair FA-induced lesions; however the underlying mechanistic details were not fully clarified (de Graaf et al., 2009). In agreement, Stingele et al. discovered that yeast strains lacking Rad4 (XPC homolog) displayed a significant delay in DPC removal (Stingele et al., 2014).

The first study to investigate NER function in DPC repair in humans was performed by Quievryn and Zhitkovich. The authors analysed the *in vivo* repair kinetics of FA-induced DPCs in XPA and XPF-deficient fibroblasts and observed that this was unchanged compared to WT cells (Quievryn and Zhitkovich, 2000). In contrast, proteasomal inhibition significantly affected DPC repair, suggesting that a proteolytic digestion, rather than excision, was required to resolve these lesions. Interestingly, the researchers observed that

loss of XPF function, but not of XPA, increased sensitivity towards FA. This was interpreted as an indication of XPF involvement in the repair of different FA-induced lesions, rather than DPCs (Quievryn and Zhitkovich, 2000). By contrast, a later study showed that XPA provides resistance to nitrogen mustard-induced DPCs (Groehler et al., 2016). The controversy regarding NER factors contribution to DPC repair was further enhanced by *in vitro* studies, proving that NER endonucleases can exclusively excise DNA-peptides crosslinks, while they cannot operate on a fully folded 16 kDa protein. This indicated that a proteasomal pre-proteolytic degradation might be required to allow NER to access to the lesion (Reardon and Sancar, 2006; Reardon et al., 2006). Baker et al. confirmed that *in vitro* XPG-dependent excision requires a proteolytic pre-processing and, additionally, they provided the first evidence for NER *in vivo* contribution to DPC repair (Baker et al., 2007). In this study, the rate of DPC repair was assessed by quantifying the expression of a fluorescent GFP reporter in cells. Thus, these experiments indicated that DPCs in transcribed genes are also repaired. Furthermore, since *in vivo* DPC repair was not fully abolished by XPG deficiency, the authors concluded that, together with NER, other pathways might play a significant role in repairing DPCs (Baker et al., 2007). The work from Nakano et al. in 2009 analysed the respective contribution of NER and HR to DPC repair in bacteria and mammals. NER machineries in mammals appear to be greatly limited by the size of the proteins that can be excised (8-10 kDa). The authors concluded that, for this reason, *in vivo* NER pathway does not significantly contribute to chromosomal repair of FA-induced DPCs (Nakano et al., 2009). This was in contrast with the data obtained by the same authors in bacterial system, suggesting a distinct involvement of NER to DPC repair in different organisms (Nakano et al., 2007). Additionally, in this study, the DPCs were not polyubiquitylated, discouraging the hypothesis that proteasomal degradation contributes to repair (Nakano et al., 2009).

The reason why a unified model about NER function in DPC repair was missing at the time of these studies might depend on technical limitations in studying DPC repair kinetics. A more recent work established a quantitative PCR-based assay (SSPE-qPCR) to investigate DPC repair *in vivo*, upon cell transfection with a plasmid harboring a site-specific DPC (Chesner and Campbell, 2018). The experiments provided the evidence that, both in Chinese hamster ovary (CHO) cells and in human cells, the NER factor XPD is required to repair DPCs. The authors also observed, in contrast with previous studies, that NER can repair DPCs up to 38 kDa, even though it operates more efficiently on smaller adducts. Moreover, by monitoring the repair of a DPC inserted in an actively transcribed locus, the authors provided the first indication of the existence of a transcription-coupled DPC repair mechanism (Chesner and Campbell, 2018).

1.3.2.3 Dedicated DPC-proteases

Although canonical DNA repair pathways have been shown to participate to a certain extent in DPC repair, over the last years, specialized DPC-proteases have been identified in eukaryotes (Figure 8). Their functions will be examined in this section.

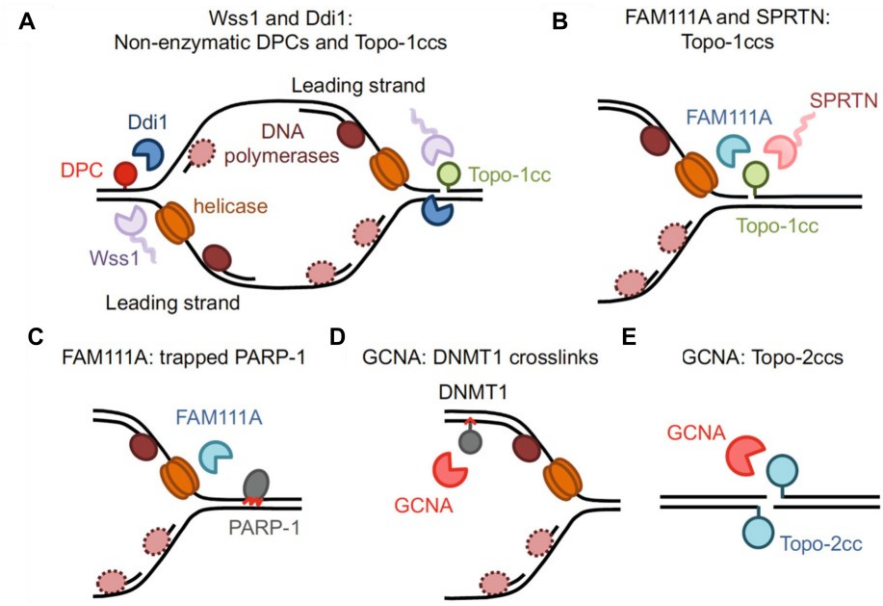

Figure 8. Overview of DPC-proteases. A) Yeast Wss1 and Ddi1 are required for replication-coupled repair of Top1-ccs and non-enzymatic DPCs. **B)** In mammals, the putative DPC-protease FAM111A has been implicated, together with the extensively characterized DPC-protease SPRTN, in the removal of fork obstacles, such as TOP1-ccs. **C)** FAM111A has also been proposed to resolve trapped PARP1. **D)** GCNA ectopically expressed in mammalian cells appears to colocalize with DNMT1 upon 5-azadC treatment; this suggests a role for GCNA in DNMT1-DPCs resolution. **E)** GCNA has a protective function towards etoposide treatment in *C. elegans*, thus it is plausibly involved in TOP2-cc resolution. Figure from Ruggiano and Ramadan, 2021.

1.3.2.3.1 The DPC-protease SPRTN

A synthetic interaction screen conducted in 2014 allowed Stingele et al. to identify the yeast protein Wss1 as the first dedicated DPC-protease (Stingele et al., 2014). In detail, cells lacking Wss1 showed a strong negative genetic interaction with Tdp1, resulting in a dramatic growth defect and sickness. Interestingly, *Δwss1 Δtdp1* cells were extremely sensitive to CPT, and this phenotype was rescued by deleting *Δtop1*. This finding suggested that Wss1 acts in parallel to Tdp1 to resolve toxic Top1-ccs (Stingele et al., 2014). Further *in vitro* experiments showed that Wss1 is activated in a DNA-dependent manner and it is able to cleave several DNA-bound proteins and itself *in trans*, perhaps as a regulatory inactivation step. In addition, loss of Wss1 sensitizes the cells to the DPCs-inducing agent FA, proving that this protease represents a general and crucial protection mechanism towards enzymatic and non-enzymatic DPCs (Stingele et al., 2014; Stingele and Jentsch, 2015).

A few years later, the metalloprotease SprT-like N-terminal domain (SPRTN), also known as C1orf124 or DVC1, was identified as dedicated replication-coupled DPC-protease in higher eukaryotes (Lopez-Mosqueda et al., 2016; Stingele et al., 2016; Vaz et al., 2016; Maskey et al., 2017; Mórocz et al., 2017). SPRTN was initially characterized as a p97 and PCNA-interactor, involved in regulation of TLS in the presence of UV-induced lesions (Centore et al., 2012; Davis et al., 2012; Ghosal et al., 2012; Juhasz et al., 2012; Machida et al., 2012). Although SPRTN function was not clear at the time, these works anticipated its implication in replication-coupled mechanisms for DNA damage tolerance.

SPRTN is a 489 amino acids DNA-dependent metalloprotease with an N-terminal SprT protease domain and a C-terminal tail region harboring various protein-protein interaction modules. Specifically, SPRTN has VCP/p97 binding motif (SHP-binding motif), a site for interaction with the replication clamp PCNA (PCNA-interacting protein box, PIP-box) and a ubiquitin binding site (ubiquitin-binding zinc finger, UBZ). The crystal structure of human SPRTN revealed that this protease has two DNA-binding domains (DBDs): a basic region (BR), binding to dsDNA, and a zinc-binding domain (ZBD), recognizing ssDNA (Li et al., 2019). SPRTN has an open active site and appears to be active towards a multitude of protein substrates, therefore, to avoid toxic undesired cuts, its activation needs to be tightly regulated. Similarly to Wss1, SPRTN activity is strictly dependent on DNA (Stingele et al., 2016; Vaz et al., 2016). *In vitro* experiments showed that, upon DNA-binding, SPRTN proteolytic function is activated towards the substrate, but also towards another SPRTN molecule (Stingele et al., 2016). This *in trans* autocleavage has additionally been observed *in vivo* upon treatment with DPCs-inducing agents and it represents an autoinhibitory mechanism to evict SPRTN from DNA and prevent undesired degradation events (Zhao et al., 2021; Weickert et al., 2023). Moreover, SPRTN *in vitro* activation only occurs in the presence of specific DNA structures, such as bubbles, gaps, junctions or DSBs, but not if the DPC is linked to an unperturbed ssDNA or dsDNA region (Reinking et al., 2020). This might be interpreted as an additional layer of regulation, mediated by the correct positioning of SPRTN DNA-binding regions towards the substrate (Li et al., 2019; Reinking et al., 2020).

Ubiquitylation events play a crucial role in the *in vivo* regulation of SPRTN activation and turnover. In the cell, SPRTN is constitutively present as unmodified and monoubiquitylated. DPC induction by FA treatment triggers SPRTN deubiquitylation and subsequent chromatin recruitment (Stingele et al., 2016). An early model proposed that, since monoubiquitylated SPRTN is excluded from chromatin, the ubiquitin switch might regulate its access to DPCs and subsequent activation (Stingele et al., 2016). A more recent study showed that monoubiquitylation of SPRTN is a constitutive process to negatively regulate the enzyme

through two parallel processes. First, this modification primes SPRTN for proteasomal degradation, increasing its turnover, second, it activates SPRTN auto-catalytic cleavage *in trans*, keeping the enzyme in an inactive state (Zhao et al., 2021). Upon DPC induction, USP7-dependent deubiquitylation stabilizes and activates the catalytic activity of SPRTN, favouring repair (Zhao et al., 2021). Other DUBs have been involved in SPRTN deubiquitylation, however, whether they represent alternative or redundant mechanisms has not been clarified (Huang et al., 2020; Perry et al., 2021; Zhao et al., 2021).

Lastly, there is still a big open question about the signalling events that trigger chromatin relocalization of SPRTN in the presence of a DPC. Therefore, it is known that SPRTN forms nuclear foci upon treatment with DPCs-inducing agents, but the molecular mechanisms orchestrating this recruitment are currently unknown (Stingele et al., 2016). In its C-terminal tail, SPRTN harbours various protein-protein interaction modules that might regulate its chromatin access. Early studies showed that SPRTN can interact with ubiquitinated-PCNA through its PIP and UBZ domains, being thus involved in replication-coupled DPC repair mechanisms (Centore et al., 2012; Vaz et al., 2016). In addition, SPRTN can interact with VCP/p97 through a SHP-box (Davis et al., 2012; Mosbech et al., 2012). However, these domains appear to be dispensable for SPRTN chromatin enrichment upon DPC induction (Stingele et al., 2016). Several PTMs have been proposed to regulate SPRTN recruitment. Ubiquitylation, as previously discussed, seems to be primarily involved in the regulation of SPRTN stability, however, at the moment, a role in SPRTN DPC-relocation cannot be excluded (Borgermann et al., 2019; Ruggiano et al., 2021; Zhao et al., 2021). It has been also shown that, upon FA treatment, SPRTN can be acetylated by the acetyltransferases PCAF/GCN5, following its deubiquitylation mediated by valosin-containing protein interacting protein 1 (VCPIP1). Therefore, mutations of the acetylation site prevent SPRTN chromatin accumulation, suggesting a critical role for this modification (Huang et al., 2020). CHK1-mediated phosphorylation of SPRTN has also been observed to promote its chromatin recruitment (Halder et al., 2019). New insights finally suggested that SUMOylation might play a crucial role in coordinating DPC repair and, thereby, SPRTN function (Ruggiano et al., 2021). A recent study showed that testis expressed 264 (TEX264) protein recruits VCP/p97 and SPRTN to SUMO-conjugated TOP1ccs in a replication-dependent manner (Fielden et al., 2020). However, whether this is a general recruitment mechanism or it is an exclusive TOP1-cc repair strategy has not been clarified. In conclusion, although several studies suggest that protein-protein interactions and PTMs regulate SPRTN recruitment, how these mechanisms are precisely orchestrated is currently unknown.

1.3.2.3.1.1 Defects in SPRTN function

SPRTN is essential for viability, therefore *Sprtn KO* causes early embryonic lethality in mice. Conditional KO in mouse embryonic fibroblasts (MEFs) determines aberrant phenotypes, such as growth defects, genome instability and cell death (Maskey et al., 2014). In human, *SPRTN* loss of function mutations are causative for Ruijs-Aalfs syndrome (RJALS), a serious disease characterized by genomic instability, premature aging and early-onset hepatocellular carcinoma (Ruijs et al., 2003). Analysis of the mutations found in RJALS patients, revealed that one patient had a biallelic 1 bp deletion resulting in a premature stop codon at amino acid 249, while the other two patients were heterozygous for a missense mutation (c.350A > G) resulting in Tyr117Cys substitution (close to the active site) and a 4 bp deletion producing a premature stop codon at amino acid 246 (Lessel et al., 2014). The C-terminal truncated variant of SPRTN, referred to as SPRTN-ΔC, lacks all the protein-protein interaction motifs (PIP-box, SHP-box, UBZ domain) mentioned above, as well as the nuclear localization signal (NLS), but it retains the protease activity (Stingele et al., 2016; Vaz et al., 2016). SPRTN-ΔC is mislocalized to the cytoplasm and its DPC repair function is compromised *in vitro* and *in vivo*, thus viability of cells carrying this mutation is affected (Lessel et al., 2014; Stingele et al., 2016; Vaz et al., 2016). Restoration of SPRTN-ΔC nuclear localization (by fusing SPRTN-ΔC to NLS) partially rescues the DPC repair defect *in vivo*, suggesting that it might, at least in part, depend on SPRTN-ΔC mislocalisation (Lopez-Mosqueda et al., 2016). Conversely, new mechanistic insights demonstrated that the main defect of SPRTN-ΔC relies on the loss of UBZ domain and on the consequential functional deregulation (Weickert et al., 2023). Moreover, the paradigm that SPRTN exclusively operates as a replication-coupled protease, has been challenged by new evidence of its participation in the repair of the post-replicative DNMT1-DPCs. This finding could explain the defects observed in non-replicative tissues of Ruijs-Aalf syndrome patients, finally helping to shed light on the pathogenesis of this severe syndrome (Lessel et al., 2014; Weickert et al., 2023).

1.3.2.3.2 GCNA

Following the identification of Wss1 in yeast and SPRTN in humans, additional proteases have been implicated in DPC repair (Ruggiano and Ramadan, 2021).

Germ cell nuclear antigen (GCNA), also known as acid repeat-containing protein (ACRC) has been for long time used as a marker to identify mouse germ cells, however its identity and function were unknown. In 2016, Carmell et al. discovered that GCNA belongs to an evolutionary conserved family containing a SprT-like protease domain, multiple SUMO

interacting motives (SIMs) and an intrinsically disordered region (IDR) (Carmell et al., 2016). GCNA is almost exclusively expressed in germ cells and, even though it is not strictly required for cell viability in mammalian cells, its loss of function predisposes to genome instability in flies, worms, zebrafish, and human germ cell tumours (Bhargava et al., 2020; Dokshin et al., 2020). An increased amount of DPCs was observed in ovaries and embryos of *Drosophila Gcna* mutants. In addition, in *C. elegans*, loss of *gcna-1* (GCNA homolog) and *dvc-1* (SPRTN homolog, dispensable for cell viability) results in an additive effect on embryonic lethality, suggesting that GCNA-1 and DVC-1 might operate as two independent DPC-proteases (Bhargava et al., 2020). Furthermore *gcna-1* loss of function sensitizes worms to DPCs-inducing agents, such as FA and cisplatin (Borgermann et al., 2019). GCNA-1 interacts with TOP-2 on condensed chromosomes during embryonic cell divisions in *C.* and its loss of function determines etoposide sensitivity (Dokshin et al., 2020). Furthermore, ectopically expressed GCNA was shown to be recruited to chromatin upon DPC induction and to colocalize with DNMT1 following 5-azadC treatment (Borgermann et al., 2019). SUMOylation inhibition abolished GCNA recruitment to chromatin upon DPC induction by FA, suggesting that GCNA colocalizes with DPCs in a SUMO-dependent manner (Borgermann et al., 2019). Taken together, these data suggest that GCNA participates in DPC repair likely in parallel to SPRTN, however further studies will be required to clarify the molecular mechanisms.

1.3.2.3.3 FAM111A

The serine protease family with sequence similarity 111 member A (FAM111A) has recently been proposed to act as a DPC-protease (Kojima et al., 2020). FAM111A has a trypsin-like protease domain, a DBD and a PIP-box and it has been initially identified as a replication fork protein, interacting with PCNA (Alabert et al., 2014). The study conducted by Kojima et al. showed that FAM111A loss of function sensitizes tumour cells to TOP1 and PARP1 inhibitors, and (mildly) to FA, etoposide and 5-azadC. In addition, FAM111A exhibits DNA-dependent proteolytic activity and, similarly to SPRTN, can undergo autocleavage (Stingele et al., 2016; Hoffmann et al., 2020; Kojima et al., 2020). Altogether, these data suggested that FAM111A is a replication-coupled protease, implicated in the removal of fork obstacles, such as TOP1-cc and trapped PARP (Kojima et al., 2020). Interestingly, FAM111A depletion does not dramatically affect cell viability and fork speed, conversely to SPRTN (Lessel et al., 2014; Vaz et al., 2016; Kojima et al., 2020). This suggests that FAM111A might represent a “back-up” mechanism, able to assist SPRTN, in case of DPCs overload (Ruggiano and Ramadan, 2021).

Mutations in *FAM111A* are causative for the rare autosomal dominant Kenny-Caffey syndrome, whose patients suffer from hypoparathyroidism, skeletal development abnormalities and subsequent short stature (Unger et al., 2013). Gain of function mutations causing Kenny-Caffey syndrome are located in proximity of catalytic residues and result in hyperactivation of FAM111A proteolytic activity, with aberrant consequences on cell fitness (Eren et al., 2021; Nie et al., 2021). Both 5-Ethynyl-uridine (EU) and 5-Ethynyl-2'-deoxyuridine (EdU) incorporation are reduced upon FAM111A overexpression, suggesting that this protease inhibits both replication and transcription (Hoffmann et al., 2020). Expression of catalytically active FAM111A (carrying the dominant missense mutation Asp439Asn) decreased the amount of RPB1 localized at chromatin, plausibly due to increased proteolysis (Hoffmann et al., 2020). However, although a few studies suggest that FAM111A is a DPC-protease, this still need to be formally confirmed.

1.3.2.3.4 DDI1 and DDI2

The yeast aspartate protease DNA damage inducible 1 (Ddi1) has recently been implicated in DPC repair. Ddi1 has a ubiquitin binding-like domain (UBL), a helical domain (predicted DNA-binding domain), a retroviral-like protease domain (RVP), and a ubiquitin-associated domain (UBA), thus it structurally belongs to a family of proteins involved in the transfer of polyubiquitinated substrates to the proteasome (Finley, 2009; Nowicka et al., 2015). However, UBA domain is lost in its vertebrates orthologs, indicating a putative functional divergence (Nowicka et al., 2015). Recent studies showed that Ddi1 has a strong genetic interaction with Wss1, in protecting the cells from replication stress (Svoboda et al., 2019). In addition, *Δwss1 Δddi1* are further sensitized towards the DPCs-inducing agents CPT and FA compared to single mutants; the RVP domain is indispensable to rescue this phenotype (Svoboda et al., 2019). Taken together, these data strongly suggested that Ddi1 plays a role in repairing Top1-ccs and non-enzymatic DPCs (Serbyn et al., 2020). Furthermore, *Δwss1 Δddi1* cells showed an increased accumulation of proteasome subunits on chromatin. This suggests that when both Wss1 and Ddi1 are impaired, the proteasome might operate as an additional DPC-protease to compensate their function (Serbyn et al., 2020). Lastly, loss of Ddi1 impairs Rpb1 degradation upon hydroxyurea (HU) treatment, indicating that this protease is required to evict stalled RNA Pol II from chromatin during replication stress (Serbyn et al., 2020). However, evidence that Ddi1 operates on crosslinked rather than chromatin bound-proteins are lacking and, therefore, its DPC proteolytic activity has never been confirmed *in vitro* (Sirkis et al., 2006; Trempe et al., 2016; Serbyn et al., 2020).

A direct role for Ddi1 human homologs DDI1/2 in DPC repair has not been described. However, similarly to Ddi1, both proteins appear to be essential for cell viability upon replication stress (Kottemann et al., 2018). In the presence of stalled replication forks, DDI1 and DDI2 mediate the interaction between the stalled ubiquitylated replication termination factor 2 (RTF2) and the proteasome. This allows the proteolytic removal of the obstacle and replication resumption (Kottemann et al., 2018). Whether these proteases have a similar function in the presence of a DPC obstacle is unknown. Additionally, due to their proteolytic activity, it would be interesting to explore the possibility of a direct DPC-proteolytic function (Dirac-Svejstrup et al., 2020). Further studies will be required to clarify these questions.

1.3.3 Interplay of DPC repair mechanisms

DPCs are bulky lesions that can hamper replication fork progression. Therefore, to remove these obstacles, cells developed tightly regulated replication-coupled mechanisms (Perry and Ghosal, 2022). However, even though the replicative machinery is particularly crucial in the detection of DPCs, recent studies showed that these lesions can also be repaired independently of DNA replication. In the global genome DPC repair pathway, DPC sensing mainly relies on PTMs (Leng and Duxin, 2022).

1.3.3.1 Replication-coupled DPC repair

The first evidence of the existence of a replication-coupled DPC repair pathway came from a study conducted in *Xenopus laevis* eggs extract (Duxin et al., 2014). Interpreting their results, the authors hypothesised the existence of a replication-dependent protease involved in the repair of DPCs (Duxin et al., 2014). This hypothesis was confirmed a few years later by the identification of the dedicated DPC-protease SPRTN (Stingele et al., 2016; Vaz et al., 2016). Duxin et al. showed that in the presence of a DPC on the leading strand, the helicase CMG initially stalls. In the beginning it was assumed that the crosslinked protein is proteolytically reduced to a short peptide that can be bypassed by the CMG helicase. Subsequently, the intervention of a TLS polymerase allows DNA extension past the lesion and replication resumption. Repair of a DPC on the lagging strand also requires proteolytic digestion, but it is initiated by replisome stall (Duxin et al., 2014). This study opened the way to a series of further investigations, that progressively shed light on replication-coupled DPC repair.

According to the current model, in the first instance, the presence of a DPC on the leading strand hampers CMG progression. At this stage, the E3 ubiquitin ligase TRAF-interacting protein (TRAIP), associated with the replisome, orchestrates the ubiquitylation of the DPC

and the surrounding proteins (Larsen et al., 2019). Conversely to the initial model, it has now been shown that CMG can bypass the ubiquitylated DPC prior to its proteolytic digestion, in the presence of the helicase regulator of telomere elongation helicase 1 (RTEL1) (Vannier et al., 2014; Sparks et al., 2019). RTEL1 presumably travels with the replisome and unwinds the DNA around the DPC, thus allowing CMG to bypass the lesion (Sparks et al., 2019). The ssDNA generated following CMG bypass is immediately coated with RPA, associated with the E3 ubiquitin ligase RFWD3 (Gallina et al., 2021). RFWD3-mediated ubiquitylation of the DPC primes it for proteasomal degradation (Larsen et al., 2019). In parallel, DNA polymerase approach to the lesion activates SPRTN proteolytic activity, that degrades the protein adduct independently of DPC ubiquitylation (Larsen et al., 2019). Further insights showed that following CMG bypass, RTEL1-mediated unwinding allows the engagement of the 5'-3' helicase FANCJ downstream of the adduct. FANCJ translocation towards the lesion unfolds the DPC to allow its proteolytic processing by SPRTN. Finally, TLS allows the extension past the remanent peptide (Yaneva et al., 2023). These studies revealed that the proteasome and SPRTN are both involved in replication-coupled DPC repair (Larsen et al., 2019). However, the mechanisms underlying the pathway choice are still under investigation. Additionally, although SPRTN seems to play a relevant role in the process, the contribution of other proteases, such as FAM111A or DDI1/2 cannot be excluded.

1.3.3.2 Replication-independent DPC repair

Replication-independent DPC repair is initiated by signalling events finely regulated by PTMs. DPC induction triggers a dynamic and significant SUMOylation response in the proximity of the damage. SUMO signals promote detection of DPCs and coordinate their proteolytic repair (Borgermann et al., 2019; Serbyn et al., 2020; Ruggiano et al., 2021).

For instance, in yeast, Siz1 and Mms21 have been shown to SUMOylate Top1-cc, followed by Slx5/Slx8-dependent ubiquitylation (Serbyn et al., 2020; Sun et al., 2020). In parallel, the SUMO E3 ligase Siz2 SUMOylates surrounding proteins (Serbyn et al., 2020). SUMOylation promotes Wss1 recruitment to the DPC locus, while ubiquitylation targets Top1-cc for proteasomal degradation (Serbyn et al., 2020).

Similarly, in human cells, TOP1-cc and TOP2-cc are SUMOylated by the E3 ligase PIAS4 and subsequently polyubiquitylated by RNF4, independently of replication and transcription (Sun et al., 2020). The resolution of post-replicative DNMT1-DPCs occurs through the same pathway, however, it is currently unclear whether PIAS4 or other SUMO E3 ligases are involved in the process (Liu et al., 2021; Weickert et al., 2023). Lastly, to restore DNA

integrity, ubiquitylated TOP1/2-cc and DNMT1-DPC are targeted for proteasomal degradation (Sun et al., 2020; Liu et al., 2021; Weickert et al., 2023).

A recent study showed that DNMT1-DPC is also cleaved by SPRTN, demonstrating that this protease can surprisingly operate in the global genome DPC repair pathway (Figure 9) (Weickert et al., 2023). SPRTN cleavage occurs independently of replication and transcription and relies on SUMO-targeted ubiquitylation operated by RNF4. Genetic interaction of *SPRTN-ΔC* and *RNF4 KO* cells suggests that SPRTN cleavage of DNMT1-DPC occurs in order to facilitate its proteasomal degradation (Weickert et al., 2023).

Moreover, the ectopically expressed putative DPC-protease GCNA colocalizes with DNMT1 upon 5-azadC treatment, suggesting that it might contribute to replication-independent DPC repair (Borgermann et al., 2019).

To conclude, DPCs can be repaired by replication-coupled or by global genome mechanisms. SPRTN and the proteasome functions appear to be crucial in both processes, whereas the involvement of additional/alternative factors has not been clarified yet.

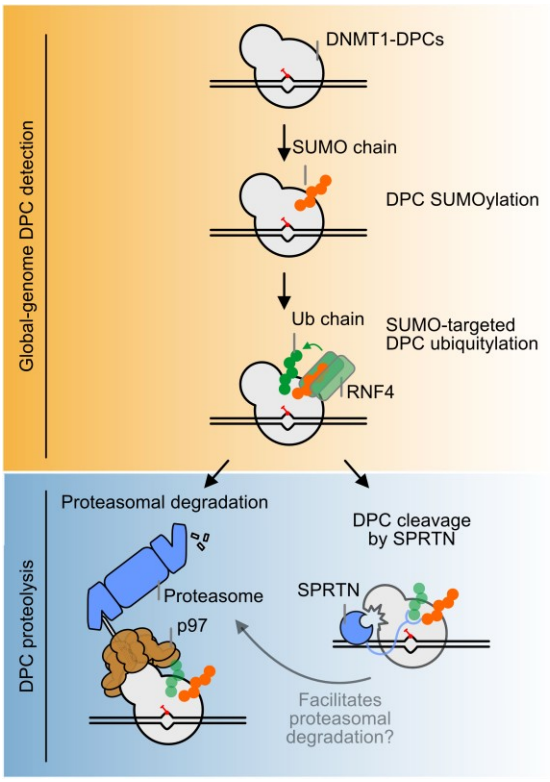

Figure 9. Model of global genome DPC repair. DNMT1-DPC is initially SUMOylated and subsequently ubiquitylated by the STUbL RNF4. Next, DNMT1-DPC can be either processed by p97 and the proteasome or cleaved by SPRTN. SPRTN cleavage may facilitate further p97-proteasomal degradation. Figure from Weickert et al., 2023.

2 AIM OF THE STUDY

DNA-protein crosslinks (DPCs) are covalent linkages between DNA and protein that can originate by several endogenous and exogenous sources. DPCs are highly toxic, since they can interfere with physiological chromatin processes, including replication and transcription. Therefore, cells developed a plethora of processes to resolve DPCs, thus preserving genome stability. Proteolysis of crosslinked proteins is ensured by the interplay of the DPC-dedicated protease SPRTN and the proteasome, while canonical DNA repair pathways – such as NER and HR pathways – contribute to restore the correct DNA sequence. DPC repair can be initiated in replication-coupled and global genome manners. Replication-coupled DPC repair operates in the presence of a bulky crosslinked protein that interferes with replication fork progression. Conversely, replication-independent global genome DPC repair is initiated by SUMOylation of the DPC and subsequent ubiquitylation mediated by RNF4. In any case, both pathways rely on proteasomal and SPRTN-mediated degradation of the crosslinked protein.

DPCs have additionally been shown to hamper RNA polymerases progression on the transcribed strand *in vitro* (Nakano et al., 2012). Experiments assessing the repair of DPC-containing plasmids upon transfection in human cells suggest that transcription contributes to repair (Chesner and Campbell, 2018). However, the consequences of transcription blockage by DPCs *in vivo* have not been extensively investigated.

Transcription-blocking lesions, such as UV-induced DNA bulky adducts, which can hamper elongating RNAPII progression, have been shown to activate TC-NER. Stalled RNAPII is sensed by CSB which in turn recruits CSA and subsequent NER factors to orchestrate degradation of stalled RNAPII, excision of the damage and restoration of DNA sequence.

This study aimed to investigate the consequences of DPC induction on transcription in human cells. In addition, we aimed to explore whether cells possess transcription-coupled DPC repair mechanisms and to identify any involved factors. Furthermore, we intended to assess the genetic interaction between putative transcription-coupled DPC repair factors and established DPC repair mechanisms.

3 RESULTS

3.1 FA-induced DPCs cause transcription stress

FA is a highly reactive aldehyde and a significant source of DPCs (Heck et al., 1990; Huang and Hopkins, 1993). The recently established method Purification of x-linked Proteins (PxP) combined with label-free quantitative proteomics revealed that the most abundant FA-induced crosslinks are histones (Weickert et al., 2023). In order to establish DPC repair kinetics of histones-DNA crosslinks, HAP1 cells were treated for 1h with FA prior to cell harvesting and PxP processing. Dose-dependent induction of histone H3-DNA crosslink was detected by western blotting (Figure 10A). Upon DPC induction, cells were allowed to repair in drug-free media for 3 and 6h. H3-DNA crosslinks were largely repaired after 6h of recovery, suggesting that they are not exclusively resolved through replication-coupled mechanisms; therefore replication-dependent repair would require more time for all cells to pass through S phase at least once. Accordingly, RPE1-iCas9 (from now on referred to as RPE1) WT cells G1-arrested by contact inhibition showed similar repair kinetics when compared to asynchronous cycling cells (Figure 10B).

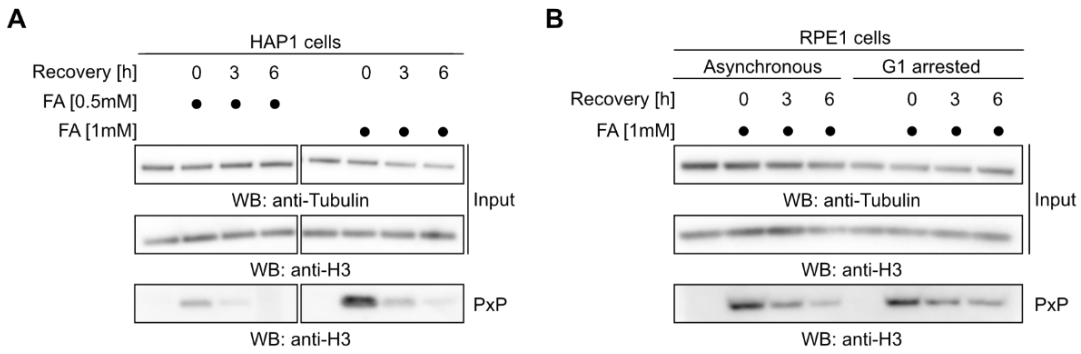

Figure 10. FA treatment induces H3-DNA crosslinks that are repaired in 6 hours. A) PxP-Western blotting monitoring histone-H3 crosslinks repair in HAP1 cells treated for 1h with FA 0.5mM and FA 1mM. Following 1h DPC induction, cells were let recover in drug-free media for 3 and 6h before harvesting. **B)** PxP-Western blotting monitoring histone H3-crosslinks repair in RPE1 cells asynchronous and G1-arrested by contact inhibition treated for 1h with FA 1mM. Following 1h DPC induction, cells were let recover in drug-free media for 3 and 6h before harvesting.

FA has recently been shown to induce transcription stress, however the nature of the responsible FA-induced lesions – ICLs, monoadducts or DPCs – is currently unclear (Mulderrig et al., 2021). On the other hand, DPCs have been reported to block the progression of RNA polymerases *in vitro*, but the extent to which DPCs perturb transcription in mammalian cells is unknown (Nakano et al., 2012). Therefore, we aimed to explore the interplay between transcription and DPC repair.

In order to investigate the effect of DPC induction by FA treatment on transcription and replication, newly synthesized RNA and DNA were labelled by incorporation of 5-Ethynyl-uridine (EU) and 5-Ethynyl-2'-deoxyuridine (EdU), respectively. EU and EdU are subsequently conjugated with a fluorescent azide (Click-iT labelling), thus allowing to measure transcription or replication levels by fluorescent microscopy. Using this assay, we found that in RPE1 cells, both transcription and replication were strongly inhibited by a pulse of FA in a dose-dependent manner (Figure 11A-D).

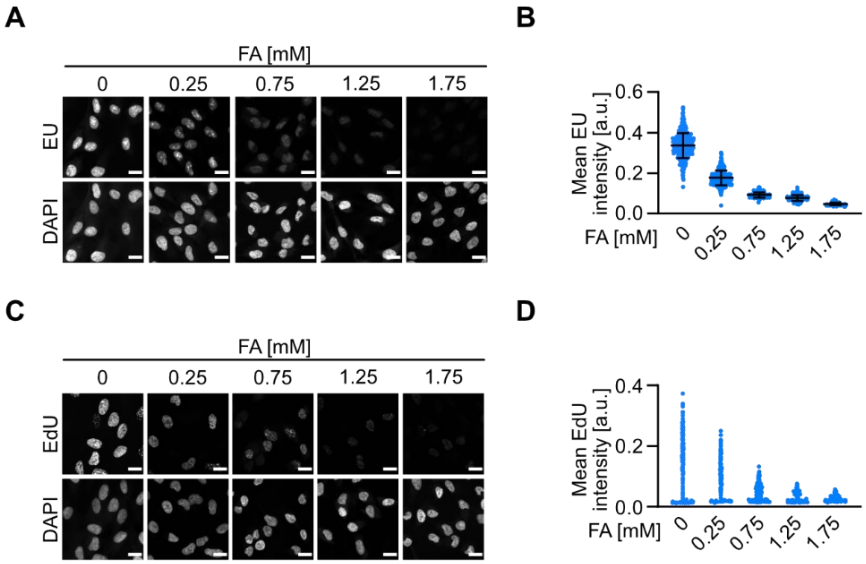

Figure 11. FA treatment inhibits transcription and replication. A) Representative microscopy pictures of RPE1 cells treated with FA and labelled by EU incorporation. Cells were treated for 1h with indicated concentration of FA prior to 1h EU incorporation and Click-iT reaction. Nuclei were stained with DAPI. Scale bar: 20µm **B)** Quantification of A). Values represent EU fluorescence intensities of single nuclei; error bars: mean ± SD; a.u.=arbitrary units; the experiment has been repeated three times with similar result. **C)** Representative microscopy pictures of RPE1 cells treated with FA and labelled by EdU incorporation. Cells were treated for 1h with indicated concentration of FA prior to 1h EdU incorporation and Click-iT reaction. Nuclei were stained with DAPI. Scale bar: 20 µm **D)** Quantification of C). Values represent EU fluorescence intensities of single nuclei; error bars: mean ± SD; a.u.=arbitrary units; the experiment has been repeated three times with similar result.

Then we used Recovery of RNA synthesis (RRS) assay to assess whether cells were able to recover from transcription stress and in which timeframe (Jia et al., 2015). To this end, G1-synchronized RPE1 cells were treated with FA for 1h, followed by recovery in drug-free media for 6 and 16h. In addition, RPE1 cells were irradiated with UVC prior to EU incorporation, as control; UVC irradiation induces a transcriptional shutdown (Gregersen and Svejstrup, 2018; Lans et al., 2019). Release from FA – like recovery from a UVC treatment – enabled transcription to progressively recover from the shutdown, with cells regaining normal rates of EU incorporation by 16h post-release (Figure 12A-D). Importantly, recover from transcription stress occurred independently of replication and in a similar time

window than DPC repair (Figure 10). This correspondence suggested that among other lesions, FA-induced DPCs contribute to transcriptional stress. In addition, recovery from FA occurred on a similar time scale than after UVC irradiation.

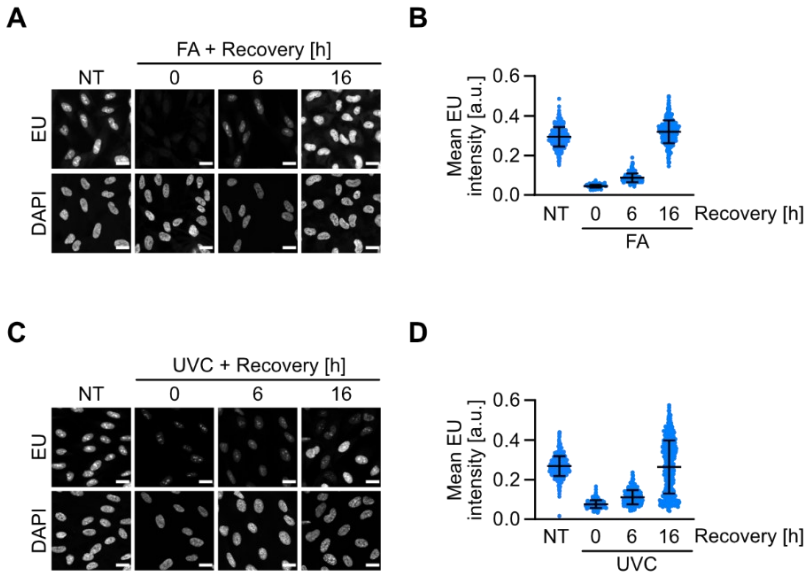

Figure 12. FA-induced transcription inhibition is reversible. A) Representative microscopy pictures of G1-arrested RPE1 cells treated with FA 1.75mM for 1h and let recover for 6 and 16h in drug-free media. Newly synthesised RNA was labelled by EU incorporation followed by Click-iT reaction. Nuclei were stained with DAPI. Scale bar: 20µm. **B)** Quantification of A). Values represent EU fluorescence intensities of single nuclei; error bars: mean ± SD; a.u.=arbitrary units; the experiment has been repeated three times with similar result. **C)** Representative microscopy pictures of G1-arrested RPE1 cells irradiated with UVC 20J/m^2 and let recover for 6 and 16h. Newly synthesised RNA was labelled by EU incorporation followed by Click-iT reaction. Nuclei were stained with DAPI. Scale bar: 20µm. **D)** Quantification of C). Values represent EU fluorescence intensities of single nuclei; error bars: mean ± SD; a.u.=arbitrary units; the experiment has been repeated three times with similar result.

UVC-induced lesions block elongating RNAPII progression, resulting in transient transcription inhibition. Stalling of RNAPII triggers TC-NER activation and allows lesion repair. Given that we observed that transcription is inhibited by FA treatment, we hypothesized that this compound could trigger a similar cellular response than UVC.

To address whether FA-induced transcription arrest causes recruitment of TC-NER complex to stalled RNAPII, we employed a recently described method to isolate the endogenous elongating form of RNAPII (RNAPIIo) and its associated factors (van der Weegen et al., 2020). RPE1 cells were treated with FA for 1h or UVC-irradiated 1h prior to RNAPII immunoprecipitation using an antibody that specifically recognizes the Ser2-phosphorylated form of RNAPII (RNAPII-S2). FA treatment, like UVC irradiation, caused efficient recruitment of CSB and CSA to stalled RNAPII. Conversely, TFIIH complex (p89) binding upon FA was slightly reduced compared to UVC (Figure 13A). In addition, FA-

dependent recruitment of CSA occurred in a CSB-dependent manner (Figure 13B). TC-NER assembly following FA treatment and UVC irradiation occurred transiently and was resolved after 6h. Proteasome inhibition by MG-132 treatment inhibited the release of TC-NER factors from RNAPII, suggesting that proteolysis might regulate their turnover following repair (Figure 13C).

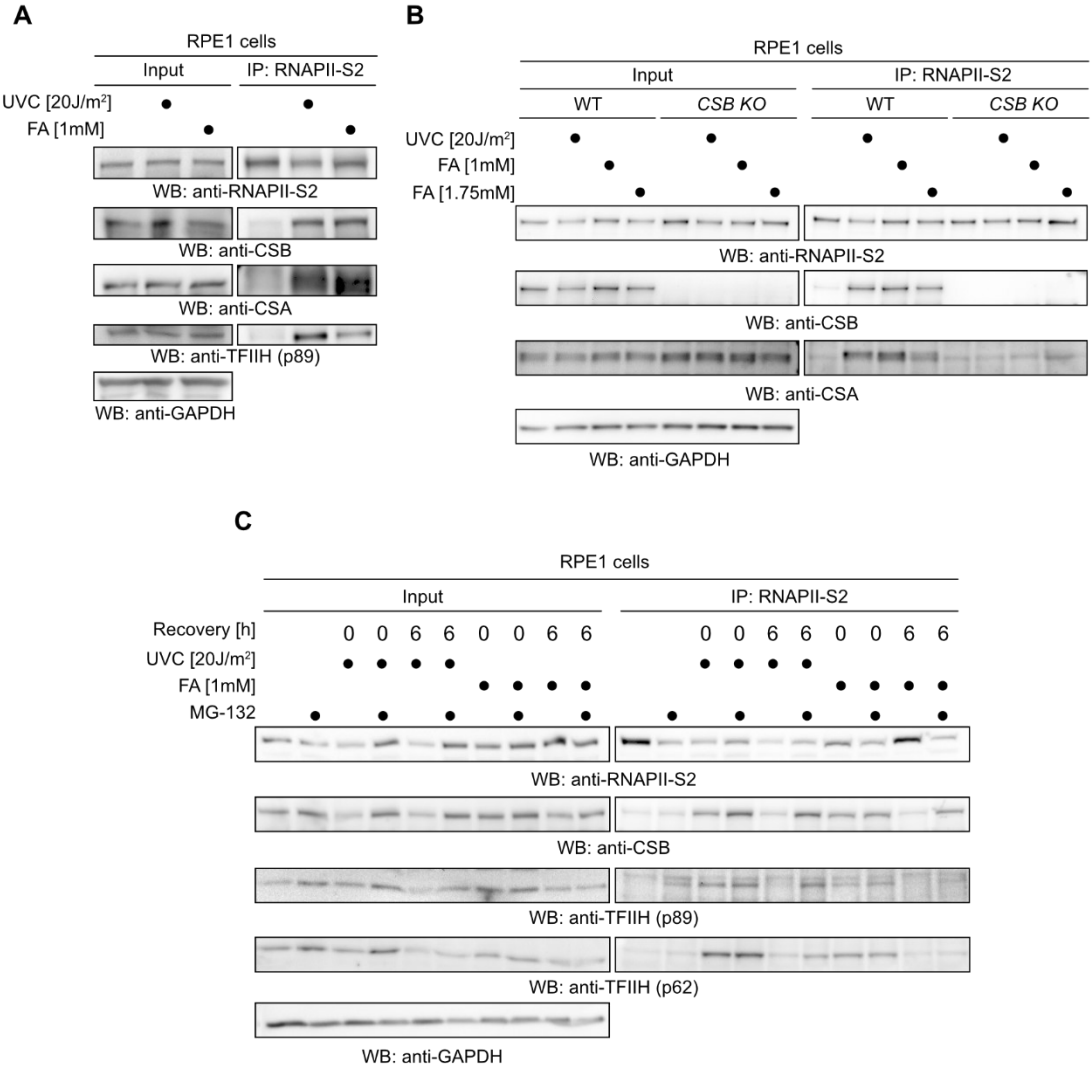

Figure 13. TC-NER is activated by FA in CSB-dependent manner. A) Western blotting of endogenous RNAPII-S2 Co-immunoprecipitation (Co-IP) on WT cells stained for the indicated TCR proteins. RPE1 WT cells treated with FA 1mM for 1h or irradiated with UVC 20J/m^2 1h prior to phospho-S2-RNAPII immunoprecipitation. **B)** Western blotting of endogenous RNAPII-S2 Co-IP on RPE1 WT vs *CSB KO* cells treated with FA 1mM, 1.75mM for 1h or irradiated with UVC 20J/m^2 1h prior to phospho-S2-RNAPII immunoprecipitation. **C)** Western blotting of endogenous RNAPII-S2 Co-IP on RPE1 WT cells treated with FA 1mM 1h or irradiated with UVC 20J/m^2. Phospho-S2-RNAPII immunoprecipitation was performed immediately after treatment/irradiation (0h) or following 6h recovery (6h). Where indicated, proteasome inhibitor MG-132 5μM was added to media during treatment and recovery.

Transcription stress induces polyubiquitylation of RPB1, the largest subunit of RNAPII. This has recently been highlighted as a critical step to orchestrate TC-NER activation and

degradation of stalled RNAPII (Nakazawa et al., 2020; Tufegdžić Vidaković et al., 2020). Therefore, we aimed to investigate RPB1 degradation dynamics in RPE1 cells upon FA treatment. In RPE1 cells treated with cycloheximide (CHX), a 1h FA pulse induced RPB1 degradation with similar kinetics to that caused by UVC. In both conditions, the degradation was abolished by cotreatment with the proteasome inhibitor MG-132 or the NEDDylation inhibitor (NEDDi) MLN-4924 (Figure 14A-H).

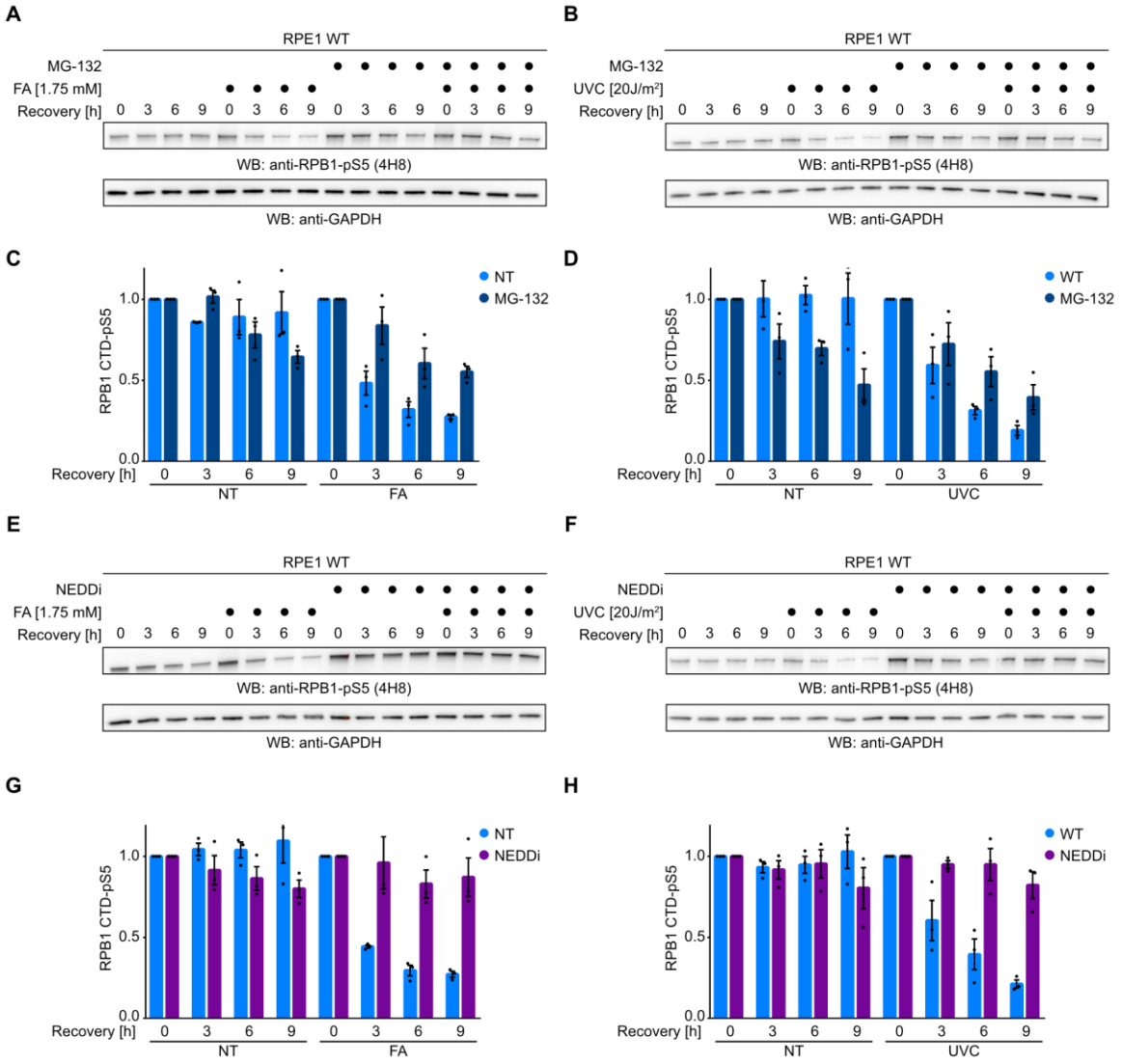

Figure 14. FA treatment induces proteasomal and NEDDylation-dependent RPB1 degradation. **A)** CHX chase of endogenous RPB1 in RPE1 WT cells treated with FA 1.75mM for 1h and let recover for the indicated time (h). Where indicated, MG-132 5μM was added to media during the entire duration of treatment and recovery. **B)** CHX chase of endogenous RPB1 in RPE1 WT cells irradiated with UVC 20J/m^2 and let recover for the indicated time (h). Where indicated, MG-132 5μM was added to media during recovery. **C)** Quantification of A), error bars ± SEM, n=3 replicates. **D)** Quantification of B), error bars ± SEM, n=3 replicates. **E)** CHX chase of endogenous RPB1 in RPE1 WT cells treated with FA 1.75mM for 1h and let recover for the indicated time (h). Where indicated, NEDDi 2μM was added to media during the entire duration of treatment and recovery. **F)** CHX chase of endogenous RPB1 in RPE1 WT cells irradiated with UVC 20J/m^2 and let recover for the indicated time (h). Where indicated, NEDDi 2μM was added to media during recovery. **G)** Quantification of E), error bars ± SEM, n=3 replicates. **H)** Quantification of F), error bars ± SEM, n=3 replicates.

Furthermore, RPB1 degradation induced by FA was compromised in *CSB KO* and *CSA KO* cells, as observed after UVC irradiation (Figure 15A-H). Interestingly, in *UVSSA KO* cells RPB1 was efficiently degraded, upon FA and UVC treatment (Figure 15I-L).

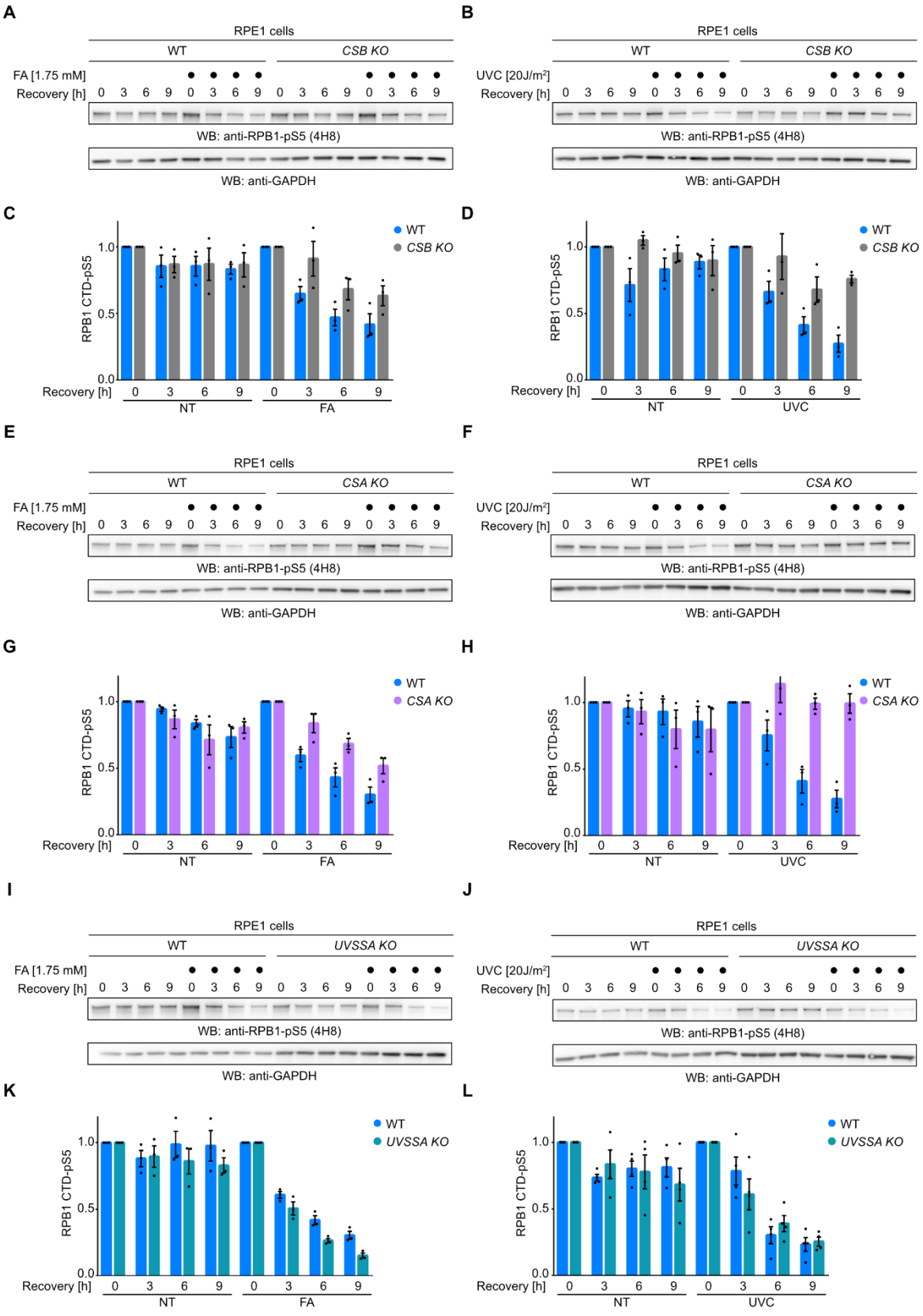

Figure 15. FA-dependent RPB1 degradation is affected in *CSB KO* and *CSA KO*, but not in *UVSSA KO* cells. A) CHX chase of endogenous RPB1 in RPE1 WT vs *CSB KO* cells treated with FA 1.75mM for 1h and let recover for the indicated time (h). **B)** CHX chase of endogenous RPB1 in RPE1 WT vs *CSB KO* cells irradiated with UVC 20J/m^2 and let recover for the indicated time (h). **C)** Quantification of A), error bars ± SEM, n=3 replicates. **D)** Quantification of B), error bars ± SEM, n=3 replicates. **E)** CHX chase of endogenous RPB1 in RPE1 WT vs *CSA KO* cells treated with FA 1.75mM for 1h and let recover for the indicated time (h). **F)** CHX chase of endogenous RPB1 in RPE1 WT vs *CSA KO* cells irradiated with UVC 20J/m^2 and let recover for the indicated time (h). **G)** Quantification of E), error bars ± SEM, n=3 replicates. **H)** Quantification of F), error bars ± SEM, n=3 replicates. **I)** CHX chase of endogenous RPB1 in RPE1 WT vs *UVSSA KO* cells treated with FA 1.75mM for 1h and let recover for the indicated time (h). **J)** CHX chase of endogenous RPB1 in RPE1 WT vs *UVSSA KO* cells irradiated with UVC 20J/m^2 and let recover for the indicated time (h). **K)** Quantification of I), error bars ± SEM, n=3 replicates. **L)** Quantification of J), error bars ± SEM, n=4 replicates.

Taken together, these data demonstrate that FA treatment induces a robust transcription stress response that correlates with DPC induction. Cellular responses to FA-dependent inhibition of transcription are mediated by CSB and CSA following their recruitment to stalled RNAPII.

3.2 TC-NER upstream factors support transcription recovery following DPC induction independently of downstream machinery

Having discovered that TC-NER factors respond to FA treatment, we aimed to investigate CSB's function in cellular tolerance to DPCs. To this purpose, RPE1 and HAP1 WT and *CSB KO* cells were subjected to low dose continuous treatment with the DPCs-inducing agents FA and 5-azadC, prior to Alamar blue viability assay. RPE1 and HAP1 *CSB KO* cells were hypersensitive to both DPCs-inducing agents compared to WT, indicating an important function for CSB in cellular DPC tolerance (Figure 16A-D).

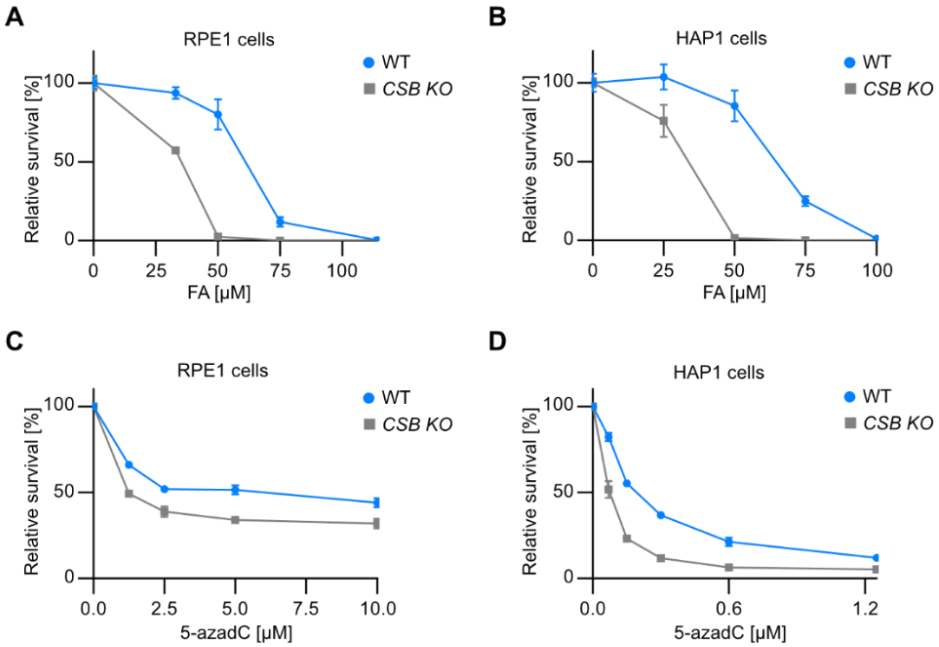

Figure 16. *CSB KO* cells are sensitive to DPCs-inducing agents. A) Alamar blue assay of RPE1 WT vs *CSB KO* cells upon 5 days incubation with FA [μM]. Values represent the mean ± SD of three technical replicates. **B)** Alamar blue assay of HAP1 WT vs *CSB KO* cells upon 4 days incubation with FA [μM]. Values represent the mean ± SD of three technical replicates. **C)** Alamar Blue assay of RPE1 WT vs *CSB KO* cells upon 5 days incubation with 5-azadC [μM]. Values represent the mean ± SD of three technical replicates. **D)** Alamar blue assay of HAP1 WT vs *CSB KO* cells upon 4 days incubation with 5-azadC [μM]. Values represent the mean ± SD of three technical replicates. Every experiment (A-D) has been repeated at least three times with similar result.

Having established that *CSB KO* cells are sensitive the DPCs-inducing agent 5-azadC, we hypothesized that 5-azadC-induced DNMT1-DPCs trigger transcriptional stress response, similarly to FA-induced lesions. In order to assess the effect of DNMT1-DPCs on transcription, RPE1 WT cells were synchronized in S phase through a double thymidine block and subsequently treated with 5-azadC prior to EU incorporation and Click-iT labelling. In this experimental setup, no effect on transcription was observed (Figure 17A,B). We hypothesized that the lack of transcription stress might be due to the primary role of

RNF4/proteasome-dependent pathway in removing post-replicative DNMT1-DPCs. Therefore, we siRNA-depleted RNF4 prior to 5-azadC incorporation in WT vs *CSB KO* genetic background. However, also inactivation of global genome DPC repair pathway did not affect transcription after 5-azadC exposure (Figure 17C,D). We suspect that the difficulty in detecting 5-azadC induced transcription stress might be caused by the highly localized nature of 5-azadC lesions, in comparison to those caused by FA. Furthermore, since DNMT1 acts during S phase at hemi-methylated sites and therefore at transcriptionally 'quiet' loci, it is likely that the majority of DNMT1-DPCs do not substantially affect transcription (Bashtrykov et al., 2012; Liu et al., 2013).

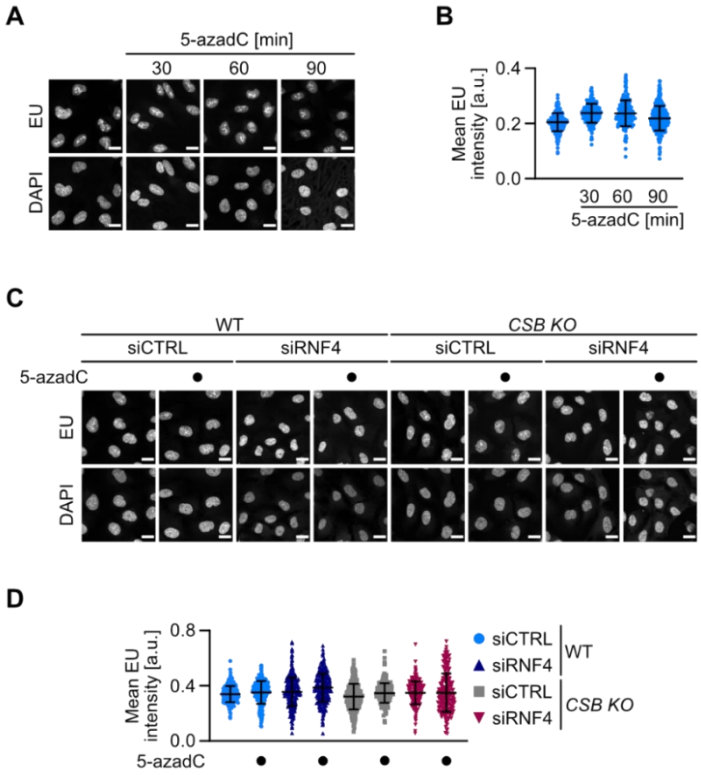

Figure 17. 5-azadC treatment does not inhibit transcription. A) Representative microscopy pictures of S phase synchronized RPE1 cells treated with 5-azadC 10μM for the indicated time (min). Newly synthesised RNA was labelled by EU incorporation (30min), followed by Click-iT reaction. Nuclei were stained with DAPI. Scale bar: 20μm. **B)** Quantification of A). Values represent EU fluorescence intensities of single nuclei; error bars: mean ± SD; a.u.=arbitrary units; the experiment has been repeated two times with similar result. **C)** Representative microscopy pictures of S phase synchronized RPE1 WT vs *CSB KO* cells transfected with siCTRL/siRNF4 and treated with 5-azadC 10μM for 1h prior to 30min EU incorporation and Click-iT reaction. Nuclei were stained with DAPI. Scale bar: 20μm. **D)** Quantification of D). Values represent EU fluorescence intensities of single nuclei; error bars: mean ± SD; a.u.=arbitrary units; the experiment has been repeated three times with similar result.

To further dissect CSB's role in transcription recovery from FA-induced transcription stress, we decided to employ RRS assays following FA treatment in CSB-deficient cell lines. In line with the sensitivity phenotype, we observed a substantial delay in transcription recovery

following release from FA in RPE1 and HAP1 *CSB KO* cells compared to WT (Figure 18A-D). Taken together these findings suggest an important role for CSB in cellular DPC tolerance and in recovery from FA-dependent transcription stress.

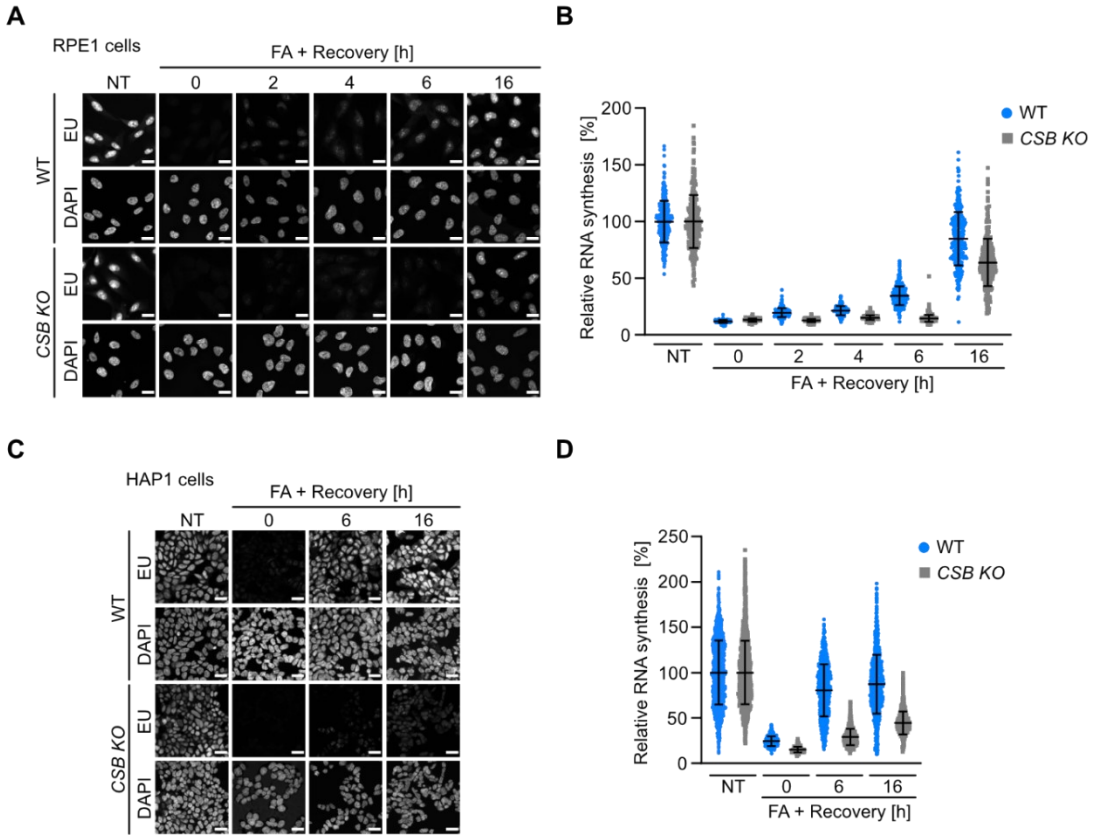

Figure 18. CSB supports transcription recovery following FA treatment. A) Representative microscopy pictures of G1-arrested RPE1 WT vs *CSB KO* cells treated with FA 1.75mM for 1h and let recover for 2, 4, 6 and 16h in drug-free media. Newly synthesised RNA was labelled by EU incorporation followed by Click-iT reaction. Nuclei were stained with DAPI. Scale bar: 20µm. **B)** Quantification of A). Values represent EU fluorescence intensities of single nuclei normalized to the mean of untreated controls (NT) of each cell line and set to 100%. Error bars: mean ± SD; the experiment has been repeated three times with similar result. **C)** Representative microscopy pictures of HAP1 WT vs *CSB KO* cells treated with FA 0.75mM for 1h and let recover for 6 and 16h in drug-free media. Newly synthesised RNA was labelled by EU incorporation followed by Click-iT reaction. Nuclei were stained with DAPI. **D)** Quantification of C). Values represent EU fluorescence intensities of single nuclei normalized to the mean of untreated controls (NT) of each cell line and set to 100%. Error bars: mean ± SD; the experiment has been repeated three times with similar result.

Subsequently, we asked whether in addition to TC-NER branch, GG-NER was required for DPC tolerance. Strikingly we observed that in RPE1 cells, loss of the GG-NER initiator XPC did not sensitize cells to FA or 5-azadC, even in absence of CSB (Figure 19A,B,G). As expected, loss of CSB but not of XPC also sensitized RPE1 cells to illudin S, an alkylating agent that causes DNA lesions specifically requiring TC-NER but not GG-NER for their repair (Figure 19C) (Jaspers et al., 2002). In our cell system, *CSB KO* and *XPC KO* were not sensitive to TOP1/2 poisons CTP and etoposide, suggesting that resolution of TOP1/2-

cc mainly relies on DPC repair pathways independent of NER (Figure 19E,F). By contrast, RPE1 *XPC KO* cells were hypersensitive to UVC irradiation, in agreement with the essential role played by GG-NER in removing UVC-dependent lesions (Figure 19D). Taken together, these data demonstrate that DPCs exclusively require TC-NER branch for their resolution, suggesting that these lesions specifically hamper elongating RNAPII progression.

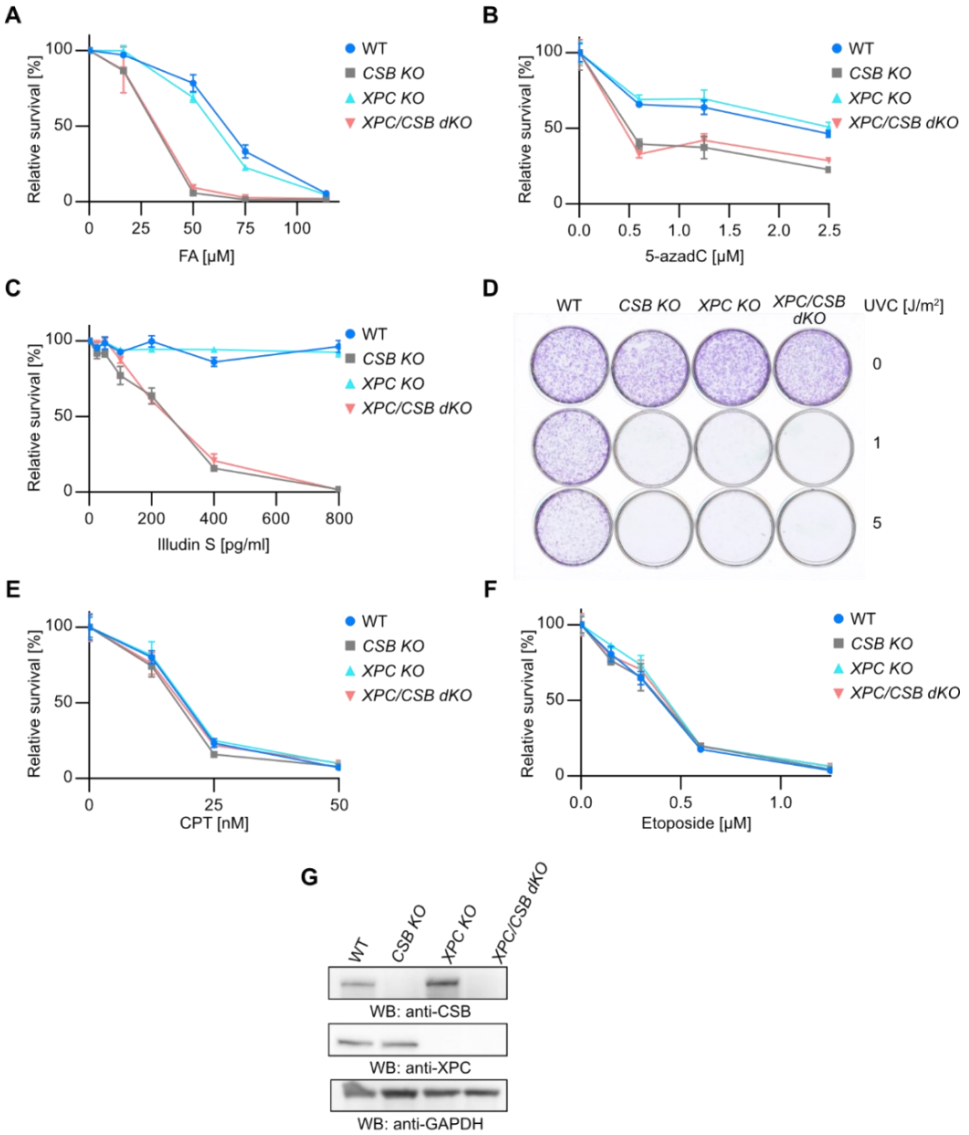

Figure 19. DPC tolerance does not require GG-NER. A) Alamar blue assay of RPE1 WT vs *CSB KO* vs *XPC KO* vs *CSB/XPC dKO* cells upon 5 days incubation with FA [μM]. Values represent the mean ± SD of three technical replicates. **B)** Alamar blue assay of RPE1 WT vs *CSB KO* vs *XPC KO* vs *CSB/XPC dKO* cells upon 5 days incubation with 5-azadC [μM]. Values represent the mean ± SD of three technical replicates. **C)** Alamar blue assay of RPE1 WT vs *CSB KO* vs *XPC KO* vs *CSB/XPC dKO* cells upon 5 days incubation with illudin S [pg/ml]. Values represent the mean ± SD of three technical replicates. **D)** Clonogenic assay of RPE1 WT vs *CSB KO* vs *XPC KO* vs *CSB/XPC dKO* cells after 7 days from UVC irradiation. **E)** Alamar blue assay of RPE1 WT vs *CSB KO* vs *XPC KO* vs *CSB/XPC dKO* cells upon 5 days incubation with CPT [nM]. Values represent the mean ± SD of three technical replicates. **F)** Alamar blue assay of RPE1 WT vs *CSB KO* vs *XPC KO* vs *CSB/XPC dKO* cells upon 5 days incubation with etoposide [μM]. Values represent the mean ± SD of three technical replicates. **G)** Western blotting of RPE1 WT vs *CSB KO* vs *XPC KO* vs *CSB/XPC dKO* cells. Every experiment (A-F) has been repeated three times with similar result.

Having discovered that TC-NER but not GG-NER is required for DPC tolerance and that CSB promotes transcription-coupled responses to FA treatment, we next aimed to determine which additional factors are required for transcription recovery. Using the RRS assay, we systematically analysed the contribution of upstream and downstream TC-NER factors to transcription recovery upon stress.

In the first instance, we observed that, similarly to RPE1 *CSB KO* and *CSA KO*, *ELOF1 KO* cells showed a delay in transcription recovery following release from FA. However, while *CSB KO* and *CSA KO* cells recovered only to a certain extent, *ELOF1 KO* cells displayed an intermediate transcription recovery defect, being able to fully recover after 16h (Figure 20A,C). In agreement with previous studies UVC-irradiated *CSB KO*, *CSA KO* and *ELOF1 KO* cells failed to recover any transcription after 16h recovery (Figure 20B,D) (van der Weegen et al., 2021).

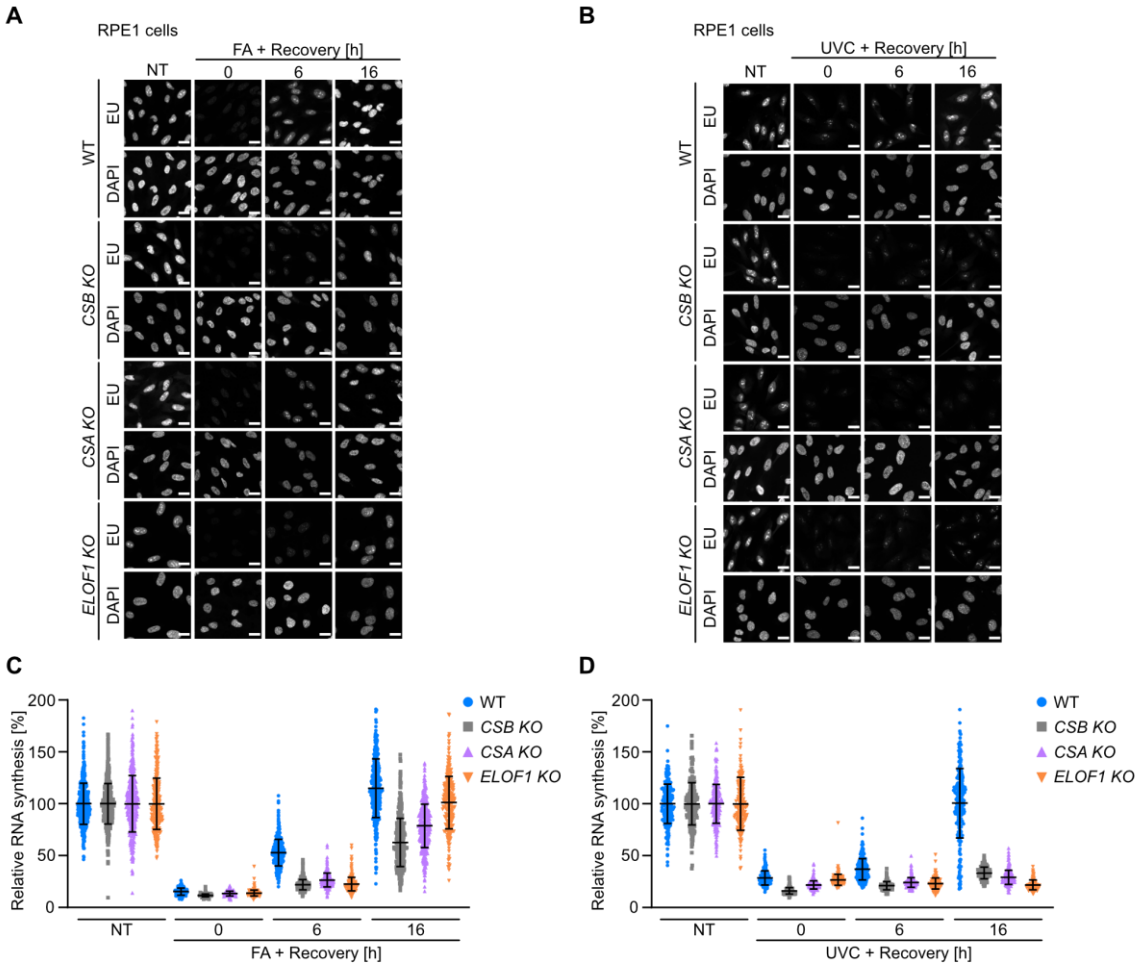

Figure 20. CSA and ELOF1 support transcription recovery following FA treatment to a different extent. A) Representative microscopy pictures of G1-arrested RPE1 WT vs *CSB KO* vs *CSA KO* vs *ELOF1 KO* cells treated with FA 1.75mM for 1h and let recover for 6 and 16 h in drug-free media. Newly synthesised RNA was labelled by EU incorporation followed by Click-iT reaction. Nuclei were stained with DAPI. Scale bar: 20µm. **B)** Representative microscopy pictures of G1-arrested RPE1 WT vs *CSB KO* vs *CSA KO* vs *ELOF1 KO* cells irradiated with UVC 20J/m^2 and let

recover for 6 and 16h. Newly synthesised RNA was labelled by EU incorporation followed by Click-iT reaction. Nuclei were stained with DAPI. Scale bar: 20µm. **C)** Quantification of (A). Values represent EU fluorescence intensities of single nuclei normalized to the mean of untreated controls (NT) of each cell line and set to 100%. Error bars: mean ± SD; the experiment has been repeated three times with similar result. **D)** Quantification of (B). Values represent EU fluorescence intensities of single nuclei normalized to the mean of untreated controls (NT) of each cell line and set to 100%. Error bars: mean ± SD; the experiment has been repeated two times with similar result.

In line with the RRS phenotypes, RPE1 *CSB KO*, *CSA KO* and *ELOF1 KO* cells were hypersensitive to FA and, as expected, to illudin S (van der Weegen et al., 2020; van der Weegen et al., 2021). *CSB KO* and *CSA KO* cells are hypersensitive to 5-azadC, conversely to *ELOF1 KO* cells, that are only mildly affected by this treatment, suggesting that ELOF1 might be not involved in the repair of DNMT1-DPCs (Figure 21A). Interestingly, loss of ELOF1 function in *CSB KO* cells caused an additive sensitivity to FA and 5-azadC, as well as illudin S (Figure 21B). This data is in agreement with previous observations and suggest that ELOF1 also has an additional CSB-independent role in DNA repair (Geijer et al., 2021; van der Weegen et al., 2021).

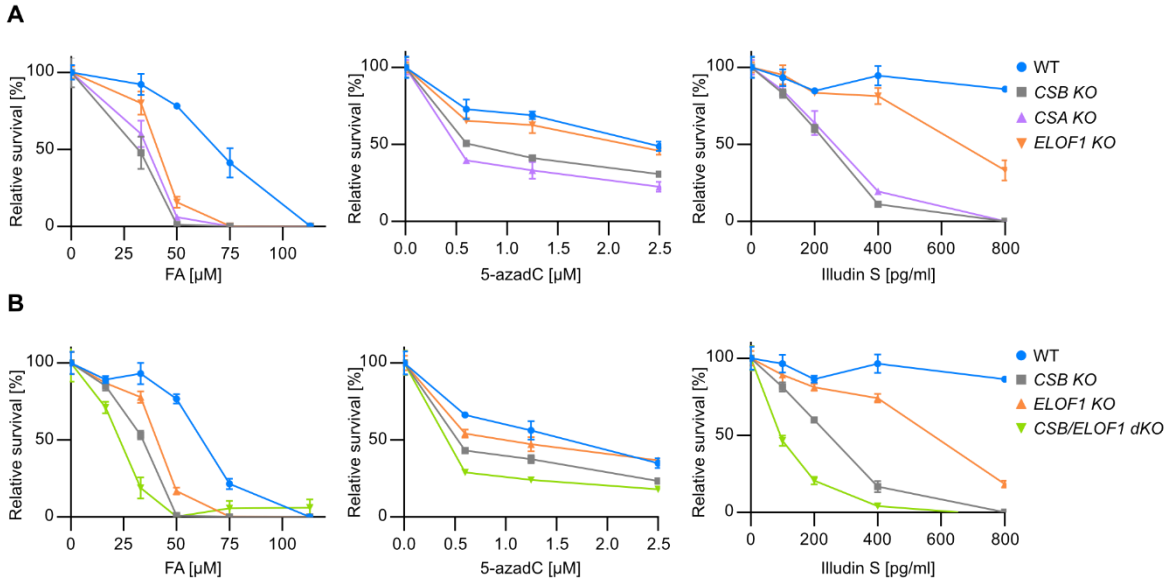

Figure 21. CSA and ELOF1 are required for DPC tolerance to a different extent. A) Alamar blue assay of RPE1 WT vs *CSB KO* vs *CSA KO* vs *ELOF1 KO* cells upon 5 days incubation with FA [µM], 5-azadC [µM] and illudin S [pg/ml]. Values represent the mean ± SD of three technical replicates. **B)** Alamar blue assay of RPE1 WT vs *CSB KO* vs *ELOF1 KO* vs *CSB/ELOF1 dKO* cells upon 5 days incubation with FA [µM], 5-azadC [µM] and illudin S [pg/ml]. Values represent the mean ± SD of three technical replicates. Every experiment (A-B) has been repeated three times with similar result.

Similarly to *ELOF1 KO* cells, *UVSSA KO* cells showed an intermediate transcription recovery defect following FA release, despite being completely unproficient in restarting transcription following UVC-irradiation (Figure 22A-D). Furthermore, loss of UVSSA sensitized cells to both FA and 5-azadC (Figure 22E), even though it did not compromise FA-induced degradation of RPB1 (Figure 15I,K).

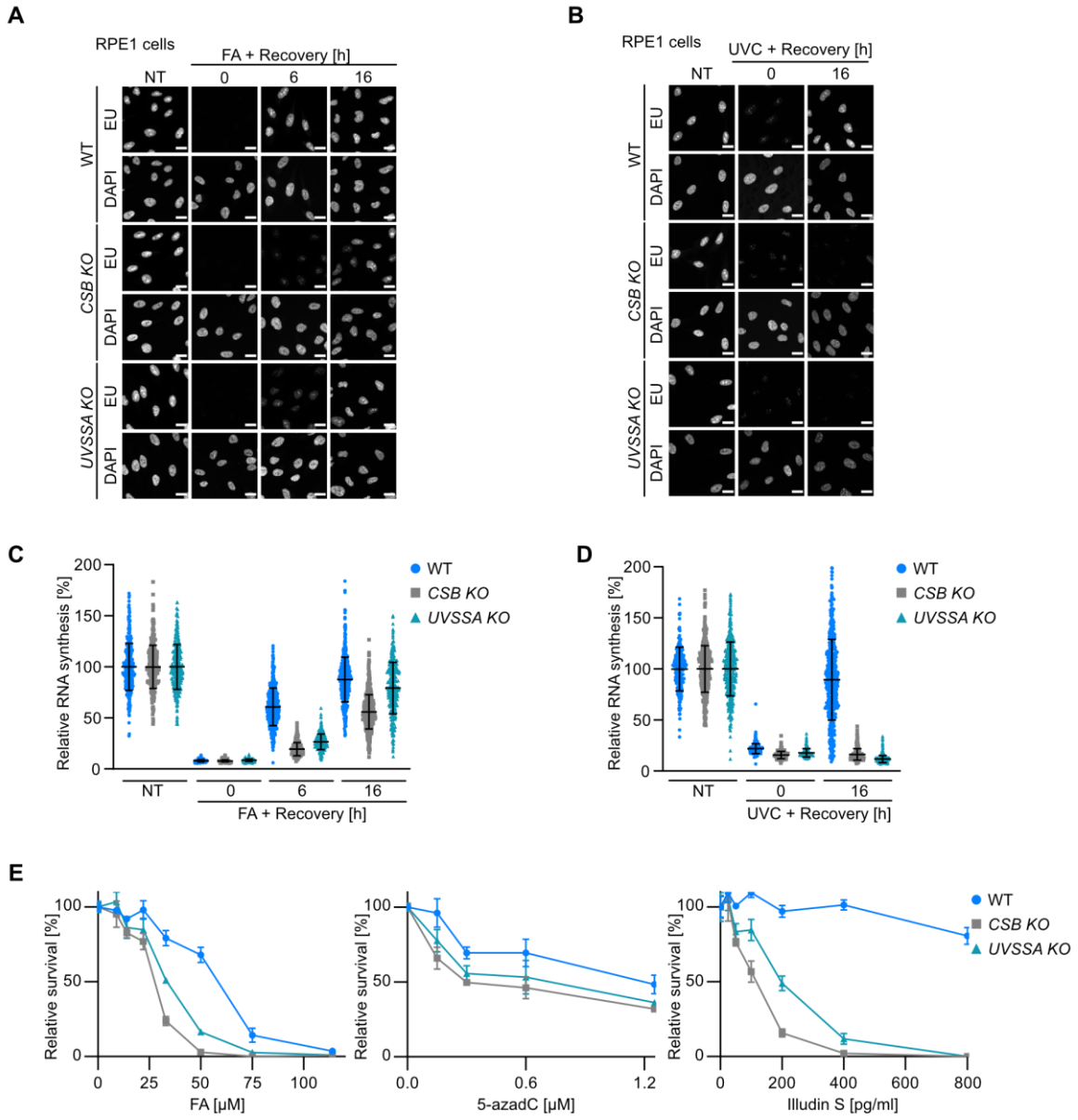

Figure 22. UVSSA supports transcription recovery following FA treatment. A) Representative microscopy pictures of G1-arrested RPE1 WT vs *CSB KO* vs *UVSSA KO* cells treated with FA 1.75mM for 1h and let recover for 6 and 16h in drug-free media. Newly synthesised RNA was labelled by EU incorporation followed by Click-iT reaction. Nuclei were stained with DAPI. Scale bar: 20µm. **B)** Representative microscopy pictures of G1-arrested RPE1 WT vs *CSB KO* vs *UVSSA KO* cells irradiated with UVC 20J/m^2 and let recover for 16h. Newly synthesised RNA was labelled by EU incorporation followed by Click-iT reaction. Nuclei were stained with DAPI. Scale bar: 20µm. **C)** Quantification of (A). Values represent EU fluorescence intensities of single nuclei normalized to the mean of untreated controls (NT) of each cell line and set to 100%. Error bars: mean ± SD; the experiment has been repeated three times with similar result. **D)** Quantification of (B). Values represent EU fluorescence intensities of single nuclei normalized to the mean of untreated controls (NT) of each cell line and set to 100%. Error bars: mean ± SD; the experiment has been repeated two times with similar result. **E)** Alamar blue assay of RPE1 WT vs *CSB KO* vs *UVSSA KO* cells upon 5 days incubation with FA [µM], 5-azadC [µM] and illudin S [pg/ml]. Values represent the mean ± SD of three technical replicates. Every experiment has been repeated three times with similar result.

Subsequently, we compared the effect of XPA and CSB deficiencies on transcription recovery in *XPC KO* genetic background. We observed that *XPC/XPA dKO* showed no transcription recovery defect upon FA treatment, in contrast to UVC irradiation (van Den Heuvel et al., 2023). This was in contrast with *XPC/CSB dKO* cells that were deficient in transcription recovery upon both treatments (Figure 23A-D). Furthermore, *XPC/XPA dKO* cells were hypersensitive to FA, but not to 5-azadC, in contrast to *XPC/CSB dKO* (Figure 23E). Due to the correlation between sensitivity to the DPCs-inducing agent 5-azadC and the RRS assay data, we concluded that the *XPA KO* cells are likely sensitive to ICLs or monoadducts lesions induced by FA, rather than DPCs.

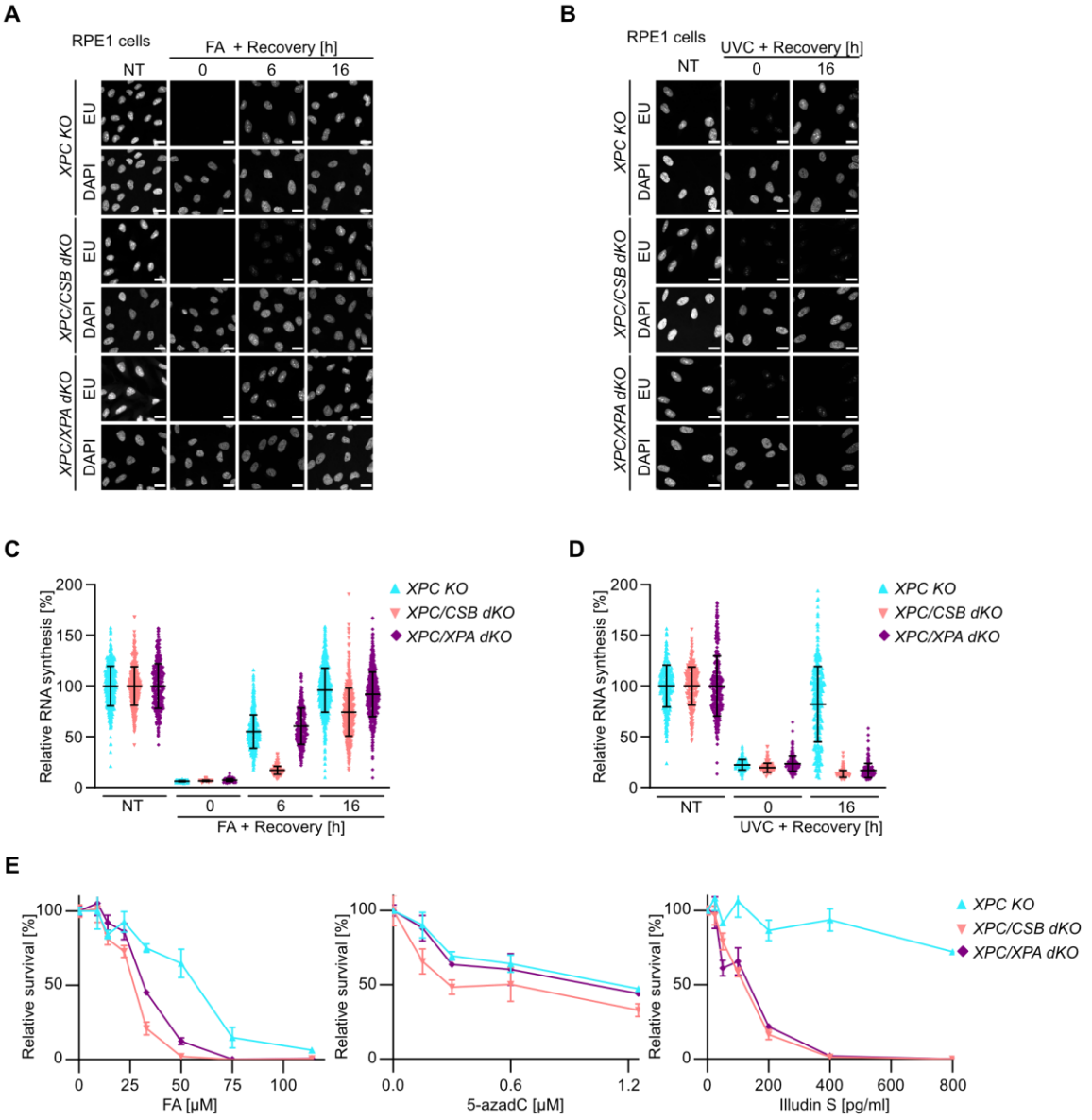

Figure 23. XPA is not needed for transcription recovery following FA treatment. A) Representative microscopy pictures of G1-arrested RPE1 *XPC KO* vs *CSB/XPC dKO* vs *XPA/XPC dKO* cells treated with FA 1.75mM for 1h and let recover for 6 and 16h in drug-free media. Newly synthesised RNA was labelled by EU incorporation followed by Click-iT reaction. Nuclei were stained

with DAPI. Scale bar: 20µm. **B)** Representative microscopy pictures of G1-arrested RPE1 *XPC KO* vs *CSB/XPC dKO* vs *XPA/XPC dKO* cells irradiated with UVC 20J/m^2 and let recover for 16h. Newly synthesised RNA was labelled by EU incorporation followed by Click-iT reaction. Nuclei were stained with DAPI. Scale bar: 20µm. **C)** Quantification of (A). Values represent EU fluorescence intensities of single nuclei normalized to the mean of untreated controls (NT) of each cell line and set to 100%. Error bars: mean ± SD; the experiment has been repeated three times with similar result. **D)** Quantification of (B). Values represent EU fluorescence intensities of single nuclei normalized to the mean of untreated controls (NT) of each cell line and set to 100%. Error bars: mean ± SD; the experiment has been repeated two times with similar result. **E)** Alamar blue assay of RPE1 *XPC KO* vs *CSB/XPC dKO* vs *XPA/XPC dKO* cells upon 5 days incubation with FA [µM], 5-azadC [µM] and illudin S [pg/ml]. Values represent the mean ± SD of three technical replicates. Every experiment has been reapeted three times with similar result.

Lastly, we examined the role of XPF-ERCC1 and XPG, the two endonucleases which perform the dual incision step in NER. Similarly to *XPA KO* cells phenotypes, loss of ERCC1 or XPG did not affect transcription recovery after FA treatment, unlike UVC irradiation (Figure 24A-D) (Apelt et al., 2021). *ERCC1 KO* and *XPG KO* cells displayed FA hypersensitivity and a mild 5-azadC sensitivity phenotype (Figure 24E).

Taken together, these data showed that transcription recovery following FA-induced transcriptional stress depends on the upstream TC-NER factors CSB and CSA, while downstream TC-NER factors are dispensable. This observation suggests that upstream TC-NER factors are recruited to FA lesion-stalled RNAPII and activate a non-canonical TC-NER pathway that is distinct to the pathway activated upon UVC irradiation. The consistency between RRS phenotypes and sensitivity to 5-azadC treatment strongly suggests that DPCs are the main lesions involved in transcription arrest.

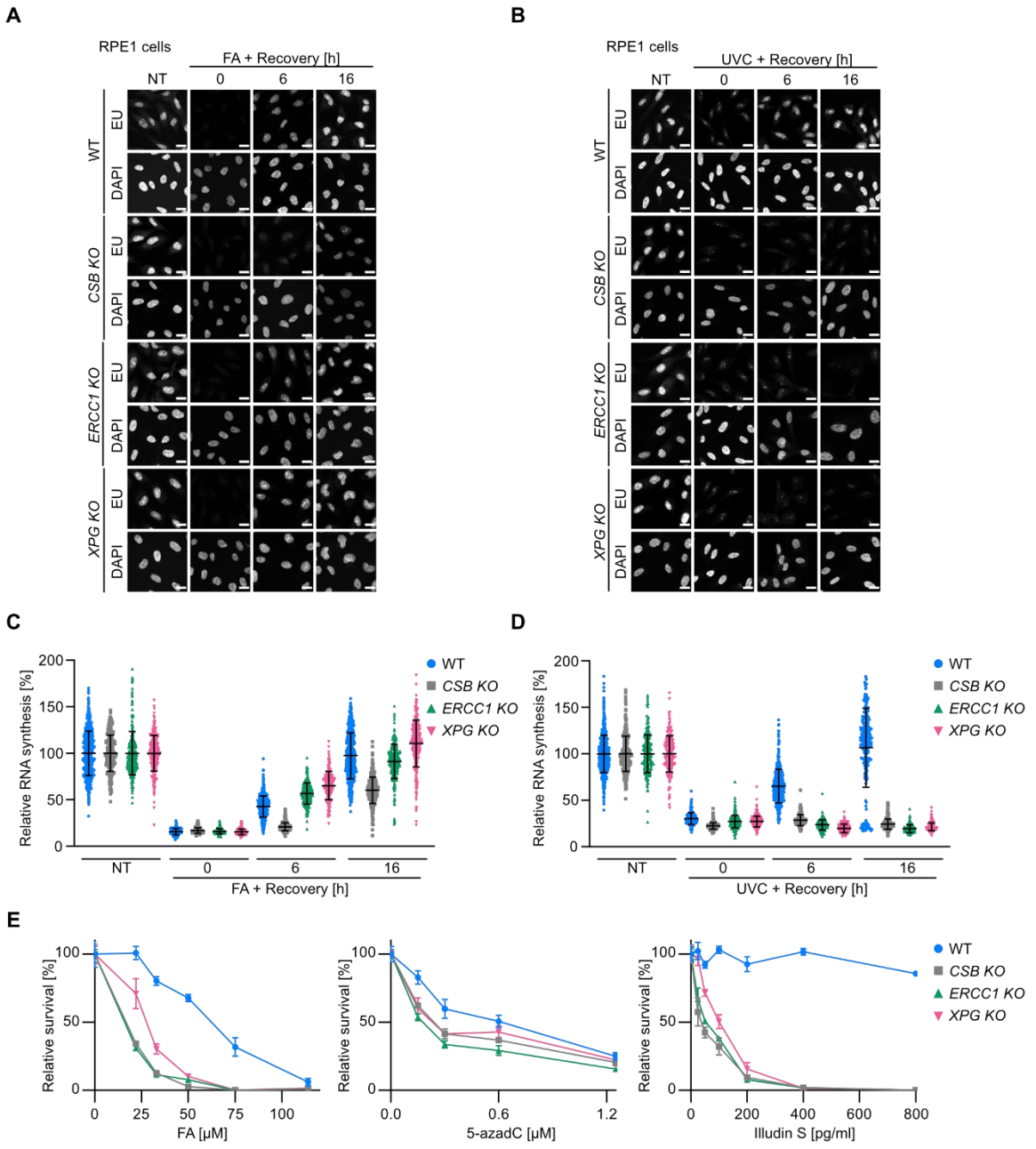

Figure 24. ERCC1 and XPG are not needed for transcription recovery following FA treatment. **A)** Representative microscopy pictures of G1-arrested RPE1 WT vs *CSB KO* vs *ERCC1 KO* vs *XPG KO* cells treated with FA 1.75mM for 1h and let recover for 6 and 16h in drug-free media. Newly synthesised RNA was labelled by EU incorporation followed by Click-iT reaction. Nuclei were stained with DAPI. Scale bar: 20μm. **B)** Representative microscopy pictures of G1-arrested RPE1 WT vs *CSB KO* vs *ERCC1 KO* vs *XPG KO* cells irradiated with UVC 20J/m^2 and let recover for 6 and 16h. Newly synthesised RNA was labelled by EU incorporation followed by Click-iT reaction. Nuclei were stained with DAPI. Scale bar: 20μm. **C)** Quantification of (A). Values represent EU fluorescence intensities of single nuclei normalized to the mean of untreated controls (NT) of each cell line and set to 100%. Error bars: mean ± SD; the experiment has been repeated three times with similar result. **D)** Quantification of (B). Values represent EU fluorescence intensities of single nuclei normalized to the mean of untreated controls (NT) of each cell line and set to 100%. Error bars: mean ± SD; the experiment has been repeated two times with similar result. **E)** Alamar blue assay of RPE1 WT vs *CSB KO* vs *ERCC1 KO* vs *XPG KO* cells upon 5 days incubation with FA [μM], 5-azadC [μM] and illudin S [pg/ml]. Values represent the mean ± SD of three technical replicates. Every experiment has been repeated three times with similar result.

3.3 CSB promotes DPC tolerance independently of known DPC repair mechanisms

Having identified a role for CSB in DPC repair distinct from its classical role in TC-NER, we sought to explore the relationship of CSB with other known DPC repair mechanisms. First, we edited the endogenous *SPRTN* locus in RPE1 WT or *CSB KO* cells using two gRNAs resulting in mutations in the coding region of exon 5. The resulting mutant cells express a C-terminal truncated variant (SPRTN-ΔC) that mimics SPRTN variants found in RJALS patients (Lessel et al., 2014) (Figure 25A). *CSB KO/SPRTN-ΔC* cells displayed enhanced sensitivity to FA compared to either *SPRTN-ΔC* or *CSB KO* cells (Figure 25B). We also noticed that *CSB KO/SPRTN-ΔC* cells displayed a general proliferation defect compared to *SPRTN-ΔC*, *CSB KO* or WT cells, indicating synthetic defects upon combined loss of SPRTN and CSB function (Figure 25C).

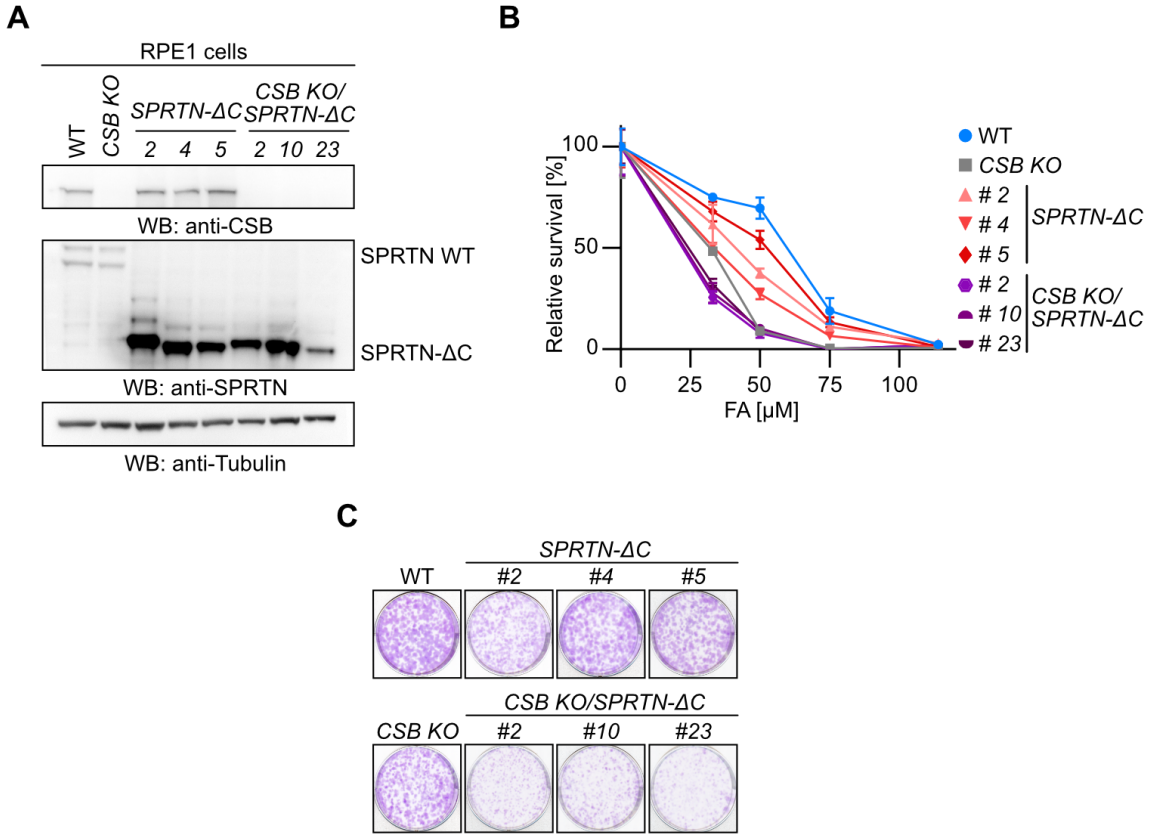

Figure 25. *CSB* and *SPRTN* show an additive genetic interaction. A) Western blotting analysis of RPE1 WT and *CSB KO* cells genetically engineered to express SPRTN-ΔC variant. **B)** Alamar blue assay of RPE1 WT, *SPRTN-ΔC, CSB KO, CSB KO/SPRTN-ΔC* cells upon 5 days incubation with FA [μM]. Values represent the mean ± SD of three technical replicates. The experiment has been repeated four times with similar result. **C)** Clonogenic assay of RPE1 WT, *SPRTN-ΔC, CSB KO, CSB KO/SPRTN-ΔC* cells 8 days after UVC irradiation.

The additive interaction between SPRTN and CSB suggests that SPRTN does not participate in CSB-dependent DPC repair. In agreement with this, we found that RPE1 *SPRTN-ΔC* cells were fully competent in transcription recovery following FA treatment and UVC irradiation (Figure 26A-D).

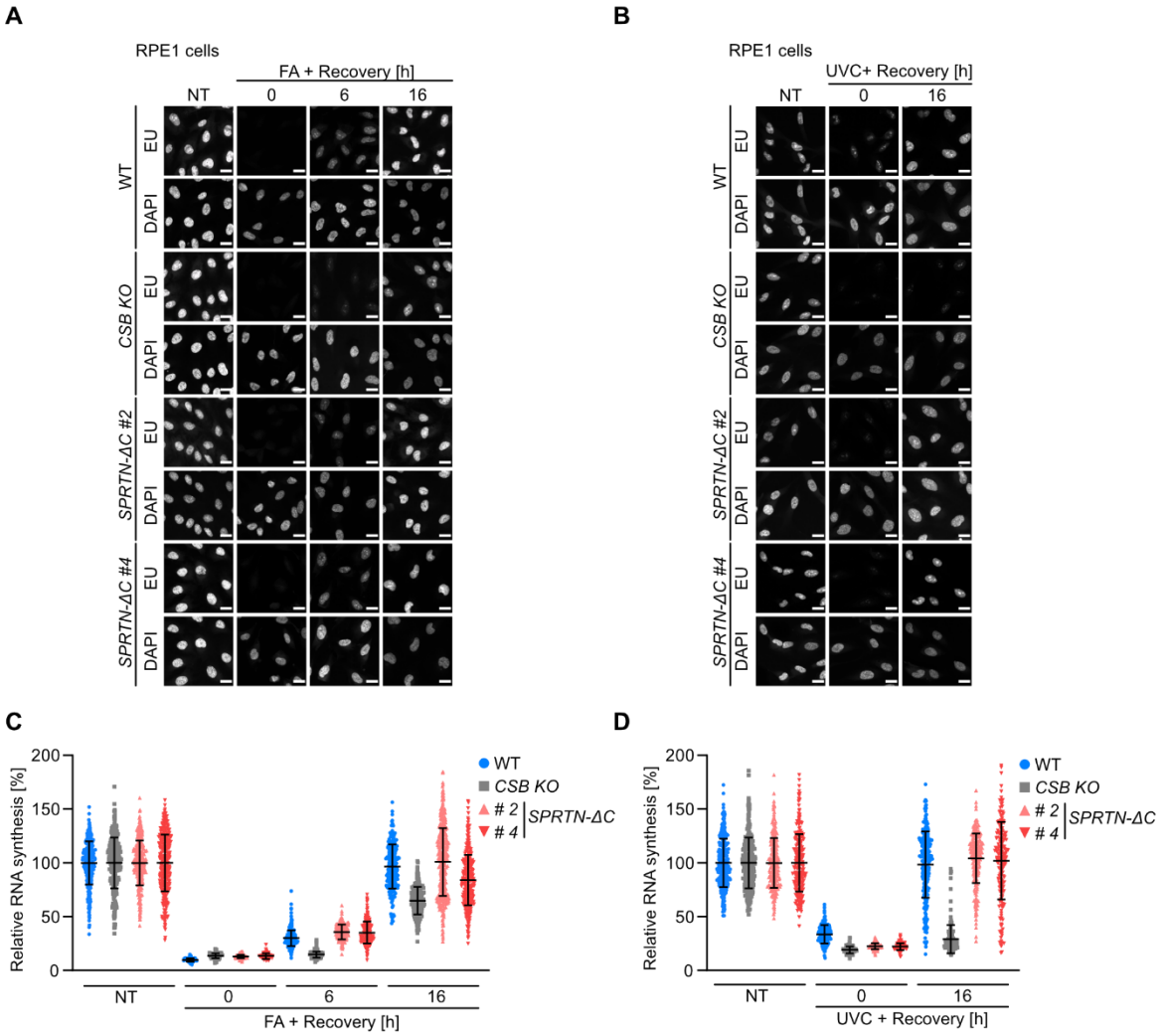

Figure 26. SPRTN function is not required to restart transcription after FA treatment. A) Representative microscopy pictures of G1-arrested RPE1 WT vs *CSB KO* vs *SPRTN-ΔC* cells treated with FA 1.75mM for 1h and let recover for 6 and 16h in drug-free media. Newly synthesised RNA was labelled by EU incorporation followed by Click-iT reaction. Nuclei were stained with DAPI. Scale bar: 20µm. **B)** Representative microscopy pictures of G1-arrested RPE1 WT vs *CSB KO* vs *SPRTN-ΔC* cells irradiated with UVC 20J/m^2 and let recover for 16h. Newly synthesised RNA was labelled by EU incorporation followed by Click-iT reaction. Nuclei were stained with DAPI. Scale bar: 20µm. **C)** Quantification of (A). Values represent EU fluorescence intensities of single nuclei normalized to the mean of untreated controls (NT) of each cell line and set to 100%. Error bars: mean ± SD; the experiment has been repeated three times with similar result. **D)** Quantification of (B). Values represent EU fluorescence intensities of single nuclei normalized to the mean of untreated controls (NT) of each cell line and set to 100%. Error bars: mean ± SD.

In order to validate our findings with a complementary approach, we knocked down CSB in WT and *SPRTN-ΔC* cells and observed increased FA hypersensitivity in *SPRTN-ΔC* cells (Figure 27A,C). Additionally, we siRNA-depleted SPRTN in WT and *CSB KO* cells, observing further sensitisation of both cell lines to FA (Figure 27B,D). These data suggest that CSB's role in DPC repair is independent of SPRTN.

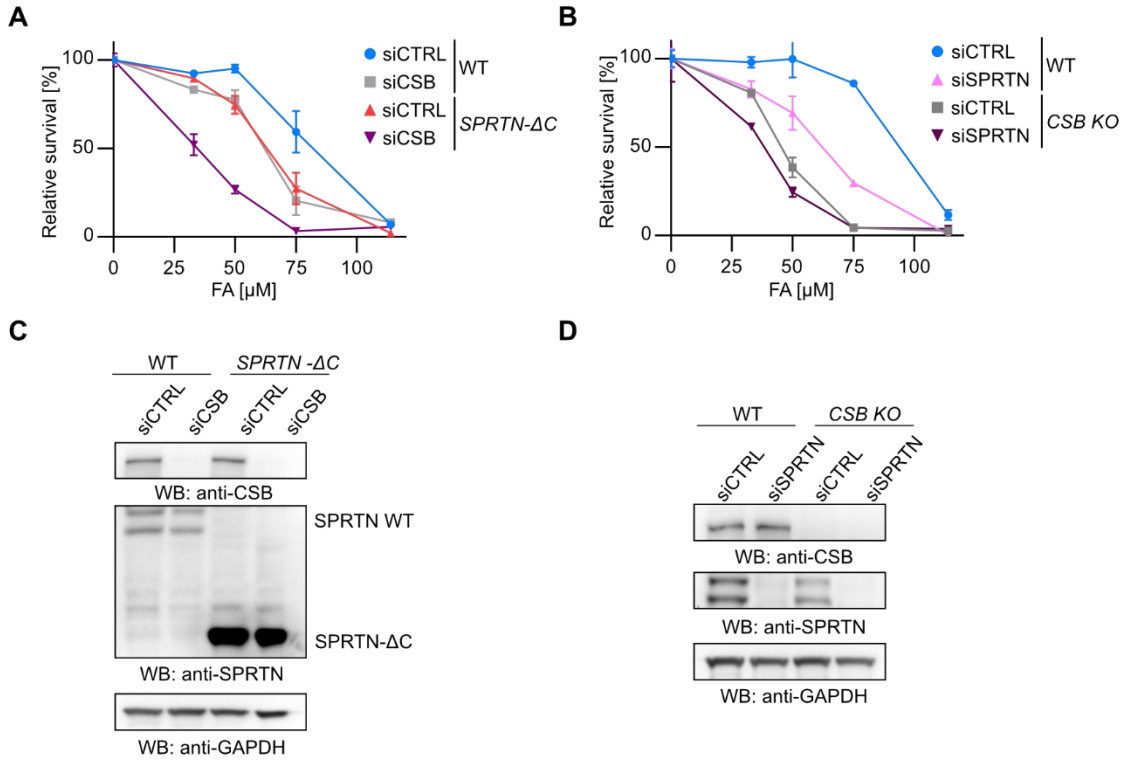

Figure 27. CSB and SPRTN are not epistatic. A) Alamar blue assay of RPE1 WT vs *SPRTN-ΔC* + siCTRL/siCSB upon 4 days incubation with FA [μM]. Values represent the mean ± SD of three technical replicates. The experiment has been repeated four times with similar result. **B)** Alamar blue assay of RPE1 WT vs *CSB KO* + siCTRL/siSPRTN upon 4 days incubation with FA [μM]. Values represent the mean ± SD of three technical replicates. The experiment has been repeated four times with similar result. **C)** Western blotting analysis of RPE1 WT vs *SPRTN-ΔC* + siCTRL/siCSB 72h after siRNA transfection. **D)** Western blotting analysis of RPE1 WT vs *CSB KO* + siCTRL/siSPRTN 72h after siRNA transfection.

Given recent findings that RNF4-mediated proteasomal degradation is critical for replication-independent DPC repair, we next aimed to explore the relationship between CSB and RNF4 in DPC repair (Liu et al., 2021; Weickert et al., 2023). RNAi-mediated depletion of RNF4 from RPE1 *CSB KO* cells caused further sensitisation to both FA and 5-azadC (Figure 28A-C). Taken together, these findings strongly suggest that CSB operates in a DPC repair pathway distinct from the established SPRTN- and RNF4-dependent repair pathways.

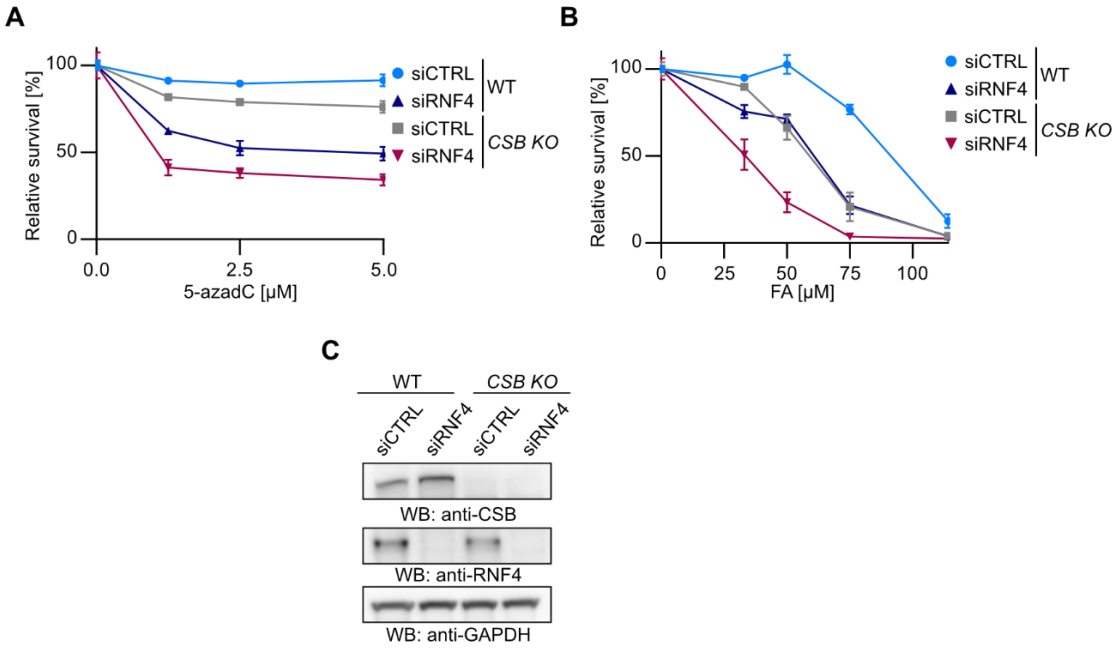

Figure 28. CSB and RNF4 are not epistatic. A) Alamar blue assay of RPE1 WT vs *CSB KO* siCTRL/siRNF4 upon 4 days incubation with 5-azadC [µM]. Values represent the mean ± SD of three technical replicates. The experiment has been repeated three times with similar result. **B)** Alamar blue assay of RPE1 WT vs *CSB KO* siCTRL/siRNF4 upon 4 days incubation with FA [µM]. Values represent the mean ± SD of three technical replicates. The experiment has been repeated three times with similar result. **C)** Western blotting analysis of RPE1 WT vs *CSB KO* + siCTRL/siRNF4 72h after siRNA transfection.

3.4 DPC-seq reveals the existence of a transcription-coupled DPC repair pathway that depends on CSB

Our results pointed to a transcription-coupled DPC repair pathway coordinated by CSB and CSA. However, while pulsed FA treatments are known to cause substantial DNA-protein crosslinking, other DNA lesions are induced as well, complicating the interpretation of our results. In order to specifically monitor FA-induced DPCs, we decided to employ the recently established PxP assay (Weickert et al., 2023). To this aim, repair of histone H3-DNA crosslinks induced by FA treatment was monitored in RPE1 and HAP1 WT vs *CSB KO* cells. In this experimental setup, no substantial difference in total H3-DNA crosslinks resolution was observed (Figure 29A-B). This result is consistent with the fact that only a small portion of the genome is transcribed, therefore the contribution of CSB in repairing H3-DNA crosslinks may not be detectable by looking at the repair of the total amount of histone-DNA crosslinks.

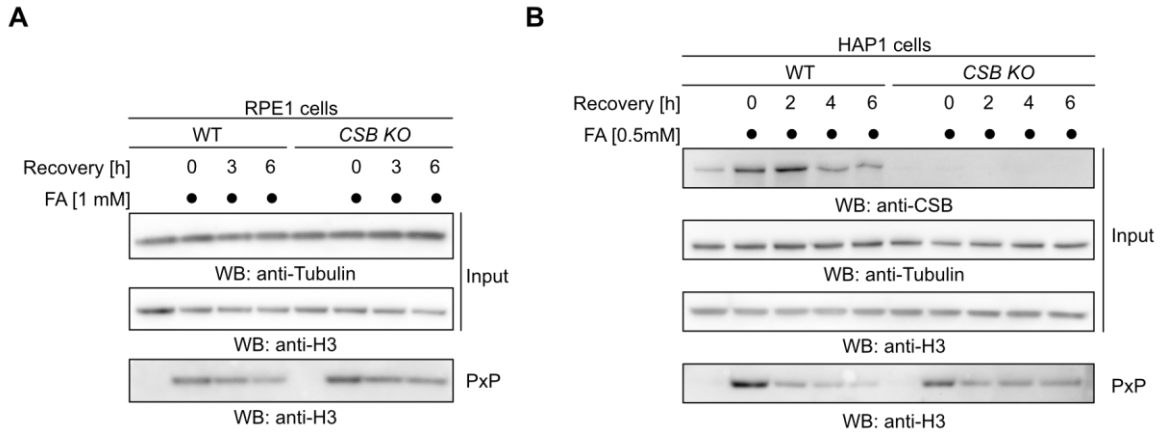

Figure 29. Histone H3-DNA crosslink is repaired to a similar extent in WT vs *CSB KO* cells. A) PxP-Western blotting to monitor histone H3-DNA crosslinks repair in RPE1 WT vs *CSB KO* cells treated for 1h with FA 1mM. Following 1h DPC induction, cells were let recover in drug-free media for 3 and 6h before harvesting. **B)** PxP-Western blotting to monitor histone H3-DNA crosslinks repair in HAP1 cells WT vs *CSB KO* treated for 1h with FA 0.5mM. Following 1h DPC induction, cells were let recover in drug-free media for 2, 4 and 6h before harvesting.

In order to examine the relation between transcription and DPC repair, we established a DPC-sequencing (DPC-seq) assay that enables genome-wide mapping of FA-induced DPCs (Figure 30). In brief, cells are seeded and synchronized in G1 phase by 24h serum starvation. To induce DPCs, cells are treated with FA; after 1h, FA-containing media is washed away and cells are either harvested immediately (0h recovery) or allowed to recover for 6h in drug-free media (6h recovery). Cells are collected in SDS-containing lysis buffer and DNA is sheared by sonication. Crosslinked DNA is separated from free DNA through

KCl addition, that precipitates proteins and covalent protein-DNA complexes. Following proteinase K treatment and DNA library preparation, in-depth next generation sequencing (NGS) is performed. This approach enabled us to monitor DPC formation and repair across the genome, by using read coverage as a proxy for DPCs presence. The assay has been established in collaboration with Prof. Sir Steve Jackson's lab (Cancer Research UK Cambridge Institute). I performed cell treatments and isolated crosslinked DNA fragments using the KCl/SDS precipitation assay, while Dr. Aldo Bader performed library preparation, NGS sequencing and bioinformatic analysis.

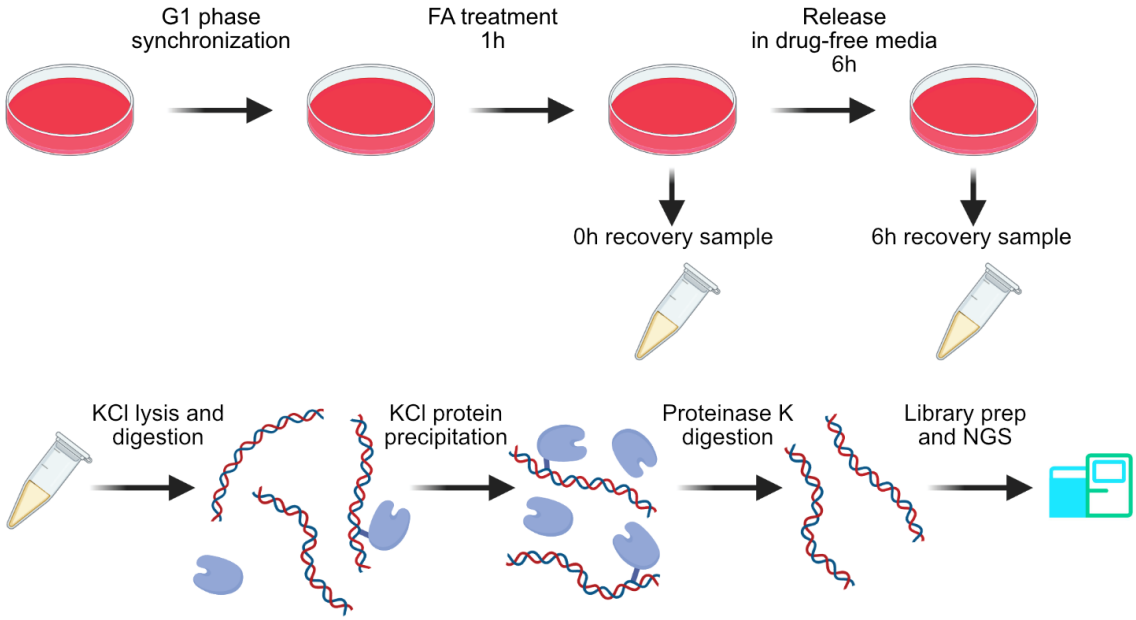

Figure 30. DPC-seq strategy outline. Synchronized G1 RPE1 WT vs *CSB KO* cells are treated with FA and harvested in SDS-containing lysis buffer immediately after the treatment (0h) or following 6h release in drug-free media. Crosslinked DNA is separated from free DNA through KCl addition, that precipitates proteins and covalent protein-DNA complexes. Following proteinase K treatment, DNA library preparation and NGS enables to monitor the loci at which DPCs are induced and repaired.

To address our question, G1-synchronised RPE1 WT vs *CSB KO* cells were subjected to KCl/SDS-precipitation, followed by DPC-seq analysis. In order to verify that our assay allows to monitor induction and repair of DPCs, after KCl/SDS precipitation, relative DPC amounts were calculated using the ratio between crosslinked DNA and total DNA (crosslinked + soluble DNA). We observed that FA treatment induced the formation of DPCs at a similar extent in RPE1 WT and *CSB KO* cells, which was reduced 6h after FA release (Figure 31A). Therefore, in depth-NGS was performed and mapping of our sequencing data onto human genomic features allowed us to assess DPC coverage across gene bodies. We observed a peak in DPC coverage immediately following FA treatment (0h recovery) that

was significantly reduced 6h after release (6h recovery), indicating DPC repair. Moreover, this analysis showed that FA-induced DPCs formed preferentially at transcription start site (TSS). Since TSS are typically nucleosome-free while enriched for RNAPII, our data suggest that FA treatment causes robust DNA crosslinking of RNAPII (RNAPII-DPC) (Figure 31B,C). To understand whether transcription affects DPC repair rates, we separated genes into quartiles of relative RNAPII occupancy based on existing RNAPII ChIP-seq data (Herrero-Ruiz et al., 2021). We observed that the higher the RNAPII occupancy in genes, the stronger DPC coverage dropped over the 6h recovery period, strongly suggesting the existence of transcription-coupled DPC repair (Figure 31D).

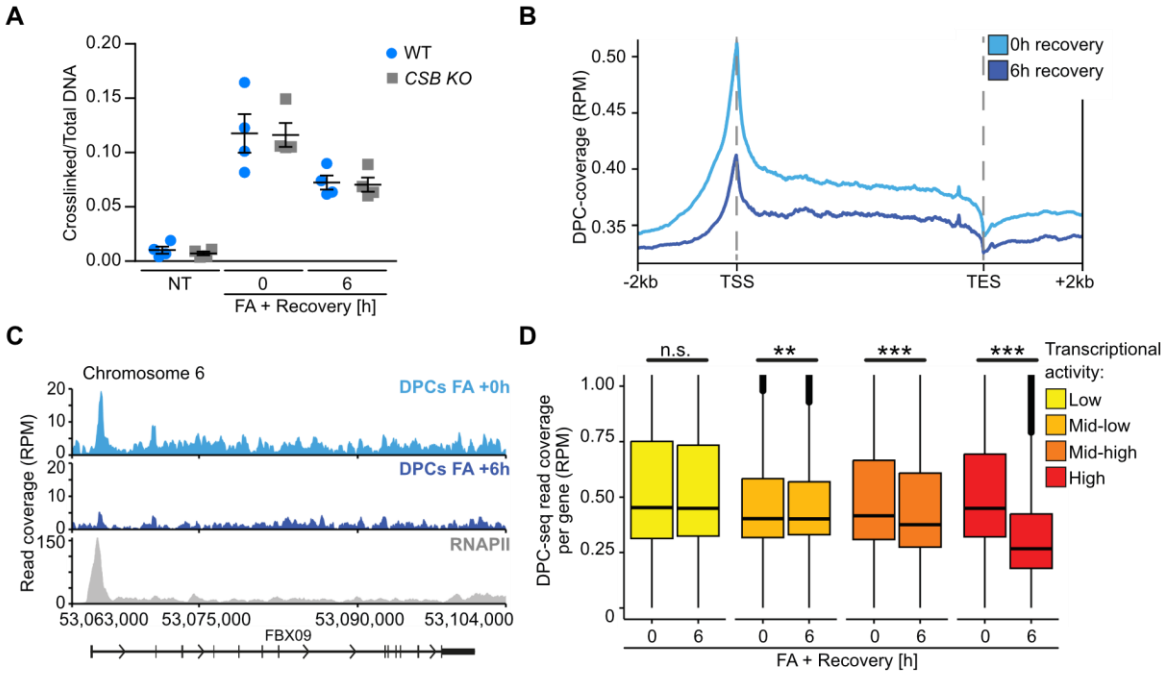

Figure 31. Analysis of DPC induction and resolution using DPC-seq. A) Quantification of crosslinked/total DNA upon KCl/SDS DPCs precipitation. Values represent mean ± SEM of four independent experiments. **B)** Metagene profile of DPC-seq in FA treated RPE1 cells with or without 6h recovery, coverage calculated as reads per million (RPM). **C)** Genome browser plot showing DPC-seq coverage at a specific region of chromosome 6 with RNAPII ChIP-seq coverage added for comparison (GEO: GSE141798; Herrero-Ruiz et al., 2021). **D)** DPC-seq coverage per gene, with or without 6h recovery after FA treatment, in genes grouped by transcriptional activity as determined by RNAPII ChIP-seq (GEO: GSE141798; Herrero-Ruiz et al., 2021), statistics via paired Wilcoxon test ** $p<0.01$ *** $p<0.001$. Box-plot shows upper and lower quartile boundaries, a line at the median and total distribution.

Having determined that our newly established DPC-seq assay allows to investigate DPC repair dynamics at genome-wide resolution, we employed this method to finally assess CSB's contribution to transcription-coupled DPC repair. Therefore, we compared DPC coverage after FA treatment and release in WT vs *CSB KO* cells and observed, that even

though there was little difference in DPC induction between these cell lines, 6h after FA release a subset of 1154 genes displayed a statistically significant increase in DPC coverage in *CSB KO* compared to WT cells (Figure 32A). Strikingly, we noticed that the most dramatic differences between WT and *CSB KO* cells occurred within gene bodies (Figure 32B). To further investigate the features that specifically promote CSB-dependent DPC repair, we dissected the relative levels of different genomic features in genes whose DPC repair depended on CSB. These analyses revealed that protein coding genes were significantly enriched in CSB-dependent genes, conversely to genes encoding for rRNA and tRNA. We concluded that CSB predominantly acts in an RNAPII (rather other RNA polymerases) dependent manner (Figure 32C). Next, comparing DNA-accessibility (ATAC-seq data) and RNAPII occupancy per gene, we identified a defined group of genes with both high transcriptional activity and high accessibility (Figure 32D). Remarkably, 50% of genes at which DPCs were repaired in a CSB-dependent manner belong to this high-accessibility, high-activity population, while only 19% of genes whose repair was CSB-independent fell into this category. Conversely, 45% of genes whose repair was not CSB-dependent display low transcriptional activity and low accessibility (Figure 32E). Accordingly, we found that CSB loss did not impact DPC repair in inactive genes but, as transcriptional activity increases, *CSB KO* cells showed increasing enrichment of DPCs 6h after FA treatment (Figure 32F). Finally, we quantified the fold change in DPC coverage of WT vs *CSB KO* cells across the length of CSB-dependent genes to investigate the role of CSB more precisely in relation to the gene body (Figure 32G,H). This clearly demonstrated that CSB loss specifically enriches for DPCs' persistence across the gene body, but not particularly upstream or downstream of the gene. In addition, the enrichment is only seen 6h after FA treatment, showing that this is specifically a DPC resolution and not a formation phenotype.

In conclusion, our newly established DPC-seq assay provided direct evidence for the existence of a CSB-dependent transcription-coupled DPC repair mechanism in human cells.

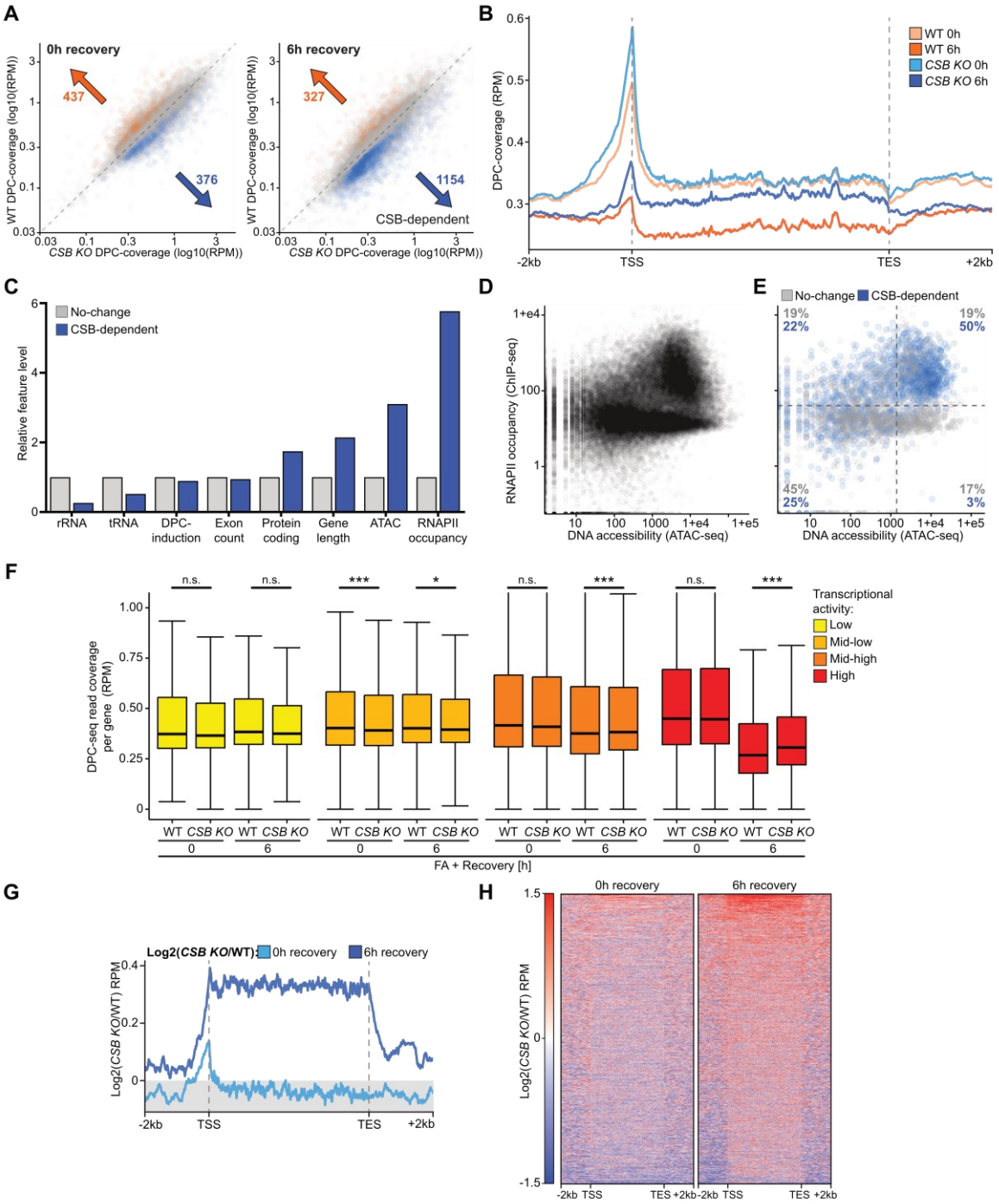

Figure 32. CSB is required for the repair of DPCs at transcriptionally active loci. A) DPC-seq coverage per gene in RPE1 WT vs *CSB KO* cells immediately (0h) and 6h after FA treatment, coloured based on significantly changing in either WT or *CSB KO* cells and the number of significantly changing genes indicated on the plot. **B)** Metagene plot of DPC-seq coverage in RPE1 WT vs *CSB KO* cells treated with FA and with or without 6h recovery, metagene specifically shows CSB-dependent genes from A). **C)** The level of different genomic features in CSB-dependent genes from A) relative to the non-changing group. **D)** Per gene RNAPII occupancy vs DNA accessibility, as determined via ATAC-seq in RPE1 cells (GEO: GSE209659). **E)** Same as D) but only showing CSB-dependent and non-changing genes, also with the percentage of each group that are present in the shown quadrants. **F)** Box-plot of DPC-seq coverage per gene in WT and *CSB KO* cells with 1h 1.75mM FA treatment with or without 6h recovery split into quartiles of transcriptional activity, statistics via Dunn test (paired) * p<0.05 *** p<0.001. Box-plot shows upper and lower quartile boundaries, a line at the median and total distribution. **G)** Same as B) but showing log2 fold change coverage for WT vs *CSB KO* cells with or without 6h recovery after FA treatment. **H)** Heatmap of coverage for each gene individually from G) for 0h (left) and 6h (right) recovery after FA treatment.

4 DISCUSSION

DPCs are highly toxic lesions that, due to their diverse and bulky nature, can interfere with every chromatin process. In the last decade, replication-dependent and global genome repair mechanisms of DPCs have been extensively investigated (Stingele et al., 2017; Zhang et al., 2020; Leng and Duxin, 2022; Perry and Ghosal, 2022; Weickert et al., 2023). However, although DPCs have been shown to hamper RNAPII progression *in vitro*, the cellular responses to DPCs-dependent transcription inhibition are unknown (Nakano et al., 2012). In this study, through a combination of genetic, biochemical and genome-wide approaches, we demonstrate the existence of a transcription-coupled pathway that repairs DPCs (Figure 33).

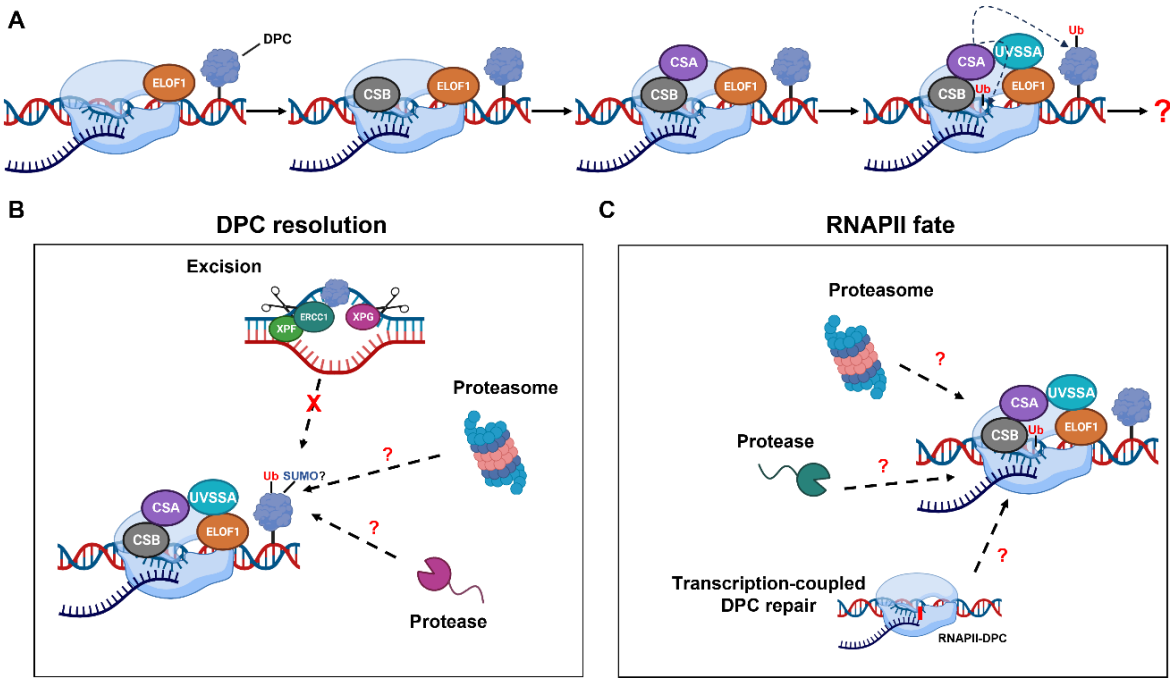

Figure 33. Model of transcription-coupled DPC repair. A) The presence of a DPC hampers the progression of elongating RNAPII. Transcriptional arrest induces the stabilization of RNAPII interaction with CSB, that is recruited to the stalling site. CSB interacts with CSA that, in turn, targets the E3 ubiquitin ligase complex $CRL4^{CSA}$ to the lesion site. $CRL4^{CSA}$ and/or other(s) E3 ligases ubiquitylate(s) RNAPII and/or the DPC itself in the presence of UVSSA and ELOF1. This allows the repair of the DPC and the release of stalled RNAPII via unknown mechanisms. **B)** Our data suggest that in transcription-coupled DPC repair, upon CSB/CSA-mediated recognition of the lesion, conventional TC-NER does not progress and XPF-ERCC1/XPG-mediated excision does not occur. Therefore, how the transcription-blocking DPC is released is currently unclear. We hypothesise that PTMs – such as ubiquitylation and/or SUMOylation – orchestrate the proteolytic digestion of the DPC, plausibly operated by a protease and/or by the proteasome. **C)** In order to allow transcription resumption, stalled RNAPII needs to be displaced from the lesion site. We speculate that the proteasome and/or an unknown protease is involved in this process, that is likely orchestrated by $CRL4^{CSA}$-mediated ubiquitylation. Another possibility is that the elongating RNAPII gets crosslinked itself to DNA. In this case, it is likely that another elongating RNAPII encounters and stalls at the RNAPII-DPC site and initiates – like in the presence of any other DPC – its transcription-coupled repair.

4.1 Transcription-coupled DPC repair pathway

The presence of a UV-induced bulky lesion on the transcribed DNA strand hampers the progression of elongating RNAPII. Transcriptional arrest causes the local stabilization of the RNAPII-CSB interaction and the subsequent formation of TCR initiation complex (van den Boom et al., 2004). CSB undergoes a conformational change and interacts with CSA, thus targeting the E3 ubiquitin ligase complex $CRL4^{CSA}$ to the lesion site (van der Weegen et al., 2020). The presence of CSA is crucial to recruit UVSSA, the TFIIH complex and, finally, the downstream TC-NER factors XPG and XPF-ERCC1 that excise the damaged DNA stretch to ultimate repair (Scharer, 2013).

It was speculated that also DPCs, due to their bulky nature, might act as physical barriers to RNAPII progression *in vivo*. The results of this thesis directly confirmed this hypothesis in cells and identified CSB and CSA as two essential factors for the resumption of transcription upon FA-induced RNAPII stalling. In addition, our DPC-seq data provided direct evidence that CSB is specifically required to repair FA-induced DPCs across gene bodies. Surprisingly, XPA, XPG and XPF-ERCC1 are all dispensable for transcription restart after FA treatment, suggesting that, in the presence of a DPC, progression of canonical TC-NER does not occur. Accordingly, whereas DPC induction by FA triggers recruitment of CSB and CSA to stalled RNAPII, the subsequent binding of the TFIIH complex is slightly reduced compared to UVC response (Figure 13A,C). Several models may explain why TC-NER does not progress: the bulky nature of DPCs might 1) impede the correct positioning of TFIIH or 2) prevent XPA lesion recognition and recruitment. Alternatively, it is likely that the presence of crosslinked nucleosomes hampers DNA unwinding by TFIIH and the subsequent positioning of XPG and XPF-ERCC1. Whatever the scenario, transcription-coupled DPC repair seems to substantially diverge from canonical TC-NER, raising the important question: how is the lesion eventually removed?

4.1.1 Resolution of transcription-blocking DPCs

Depending on the nature and localization of the DPCs, unspecific and dedicated repair mechanisms operate to restore DNA integrity. Early studies showed that NER contributes to a certain extent to DPC removal in different organisms (Minko et al., 2002; Minko et al., 2005; Reardon and Sancar, 2006; Reardon et al., 2006; Baker et al., 2007; Nakano et al., 2007; de Graaf et al., 2009; Stingele et al., 2014; Chesner and Campbell, 2018). The results of this thesis revealed a crucial role for the upstream TC-NER factors CSB and CSA in transcription-coupled DPC repair. However, given that XPG and XPF-ERCC1 are

dispensable, it seems plausible that, upon lesion recognition, the transcription-blocking DPC is resolved by proteolysis.

The DPC-protease SPRTN, initially characterized for its exquisite role in replication-dependent repair of DPCs, has recently been shown to be able to cleave DPCs in cells also independently of replication (Weickert et al., 2023). Furthermore, *in vitro* studies showed that, in the presence of a DPC placed in a bubble, SPRTN becomes activated (Reinking et al., 2020). Since transcription elongation unwinds the DNA helix locally, creating a bubble, it is reasonable to speculate that SPRTN may play a role in the removal of transcription-blocking DPCs. However, our experimental data discouraged this hypothesis. Cells expressing the hypomorphic SPRTN-ΔC variant show no transcription recovery defect after FA treatment. Additionally, *SPRTN* and *CSB* show a synthetic sick genetic interaction, indicating that they act in two independent pathways to ensure DPC clearance and genome stability.

PTMs on the DPC itself or on the surrounding proteins play important roles in orchestrating DNA repair (Leng and Duxin, 2022). It has been shown that when a DPC stalls the replicative machinery progression, TRAIP-dependent polyubiquitylation stimulates the proteasomal degradation of the crosslinked protein (Larsen et al., 2019). The requirement for CSA to restart transcription after FA treatment suggests a similar role for polyubiquitylation in transcription-coupled DPC repair. It is, therefore, plausible that $CRL4^{CSA}$ modifies the DPC to trigger its degradation by the proteasome. UVSSA may participate in this process, helping to direct CSA-dependent ubiquitylation to the DPC in front of the polymerase. Alternatively, $CRL4^{CSA}$-mediated polyubiquitylation of the DPC and/or the surrounding proteins may allow the recruitment of unknown factors to the lesion site. Therefore, at present, we cannot exclude that transcription-blocking DPCs can be repaired by a novel DPC-protease (Ruggiano and Ramadan, 2021). The putative DPC-proteases FAM111A, DDI1 and DDI2 are all reasonable candidates for transcription-coupled repair of DPCs. However, at present, no experimental evidence can support this hypothesis (Ruggiano and Ramadan, 2021).

Recent studies have additionally highlighted the importance of SUMOylation in coordinating replication-independent DPC repair. TOP1-ccs, TOP2-ccs and DNMT1-DPCs are SUMOylated prior to RNF4-dependent polyubiquitylation and subsequent degradation by the proteasome and/or SPRTN (Sun et al., 2020; Liu et al., 2021; Weickert et al., 2023). Moreover, FA treatment induces a significant increase in chromatin SUMOylation levels, suggesting a role for this PTM in the repair of all DPCs (Borgermann et al., 2019). In addition, a few studies showed that SUMOylation plays a role in CSB regulation and TC-

NER progression, however a consensus on SUMO's function has not been established (Sin et al., 2016; Liebelt et al., 2019). However, our experiments revealed a negative genetic interaction between *CSB* and *RNF4*, suggesting that this STUbL is not involved in the same pathway than CSB. This result indicates that transcription-coupled repair of DPCs substantially diverges from global genome DPC repair (Weickert et al., 2023).
In conclusion, TC-NER pathway seems to promote DPC tolerance independently of all the established DPC repair mechanisms. Further studies will be crucial to identify the factors and mechanisms that allow the transcription-coupled removal of the DPC.

4.1.2 The fate of stalled RNAPII in transcription-coupled DPC repair

RNAPII stalling caused by a bulky lesion on the transcribed DNA strand is crucial to activate TCR and allow DNA repair. However, in order to allow TC-NER progression, it is essential that stalled elongation complexes get eventually released from the lesion site.
In response to UV irradiation, RPB1 is ubiquitylated and degraded by the proteasome (Bregman et al., 1996; Ratner et al., 1998). $CRL4^{CSA}$ and several other E3 ubiquitin ligases have been implicated in RPB1 turnover, however how this process is coordinated is not fully understood (Bregman et al., 1996; Kleiman et al., 2005; Starita et al., 2005; Anindya et al., 2007; Yasukawa et al., 2008; Nakazawa et al., 2020).
The results of this thesis revealed that FA treatment also induces RPB1 degradation. We observed that RPB1 turnover was partially affected by CSA and CSB loss, conversely it was completely blocked by NEDDylation inhibition (Figures 14, 15). This indicates the involvement of another Cullin-RING E3 ligase targeting RNAPII to regulate its turnover in response to DPC formation. Loss of UVSSA did not impact RPB1 degradation upon FA treatment, but it still had substantial effects on recovery of transcription. Since UVSSA has been shown to protect CSB from proteasomal degradation, one possibility is that the delay in transcription restart in UVSSA-deficient cells is caused by increased CSB turnover and subsequent impairment of DPC repair (Higa et al., 2016). Alternatively, loss of UVSSA may affect the correct positioning of CSA, thus impairing DPC ubiquitylation and degradation, rather than RNAPII removal. Loss of ELOF1 affects transcription restart upon FA treatment to a similar extent than UVSSA deficiency. Because ELOF1 has been shown to promote UVSSA recruitment, it is plausible that the delay of transcription recovery in *ELOF1 KO* is caused by impairment of UVSSA function (Geijer et al., 2021; van der Weegen et al., 2021).
Intriguingly, we observed that proteasome inhibition did not completely compromise RPB1 degradation, suggesting that additional proteolytic mechanisms may be involved. In yeast, upon UV and hydroxyurea exposure, Rpb1 is degraded by the aspartic protease Ddi1 in a

proteasomal-independent process (Serbyn et al., 2020). Therefore, it is reasonable to speculate that the Ddi1 homologs DDI1 or DDI2 contribute in a similar way to RPB1 degradation in humans. In addition, Ddi1 has been shown to have affinity *in vitro* for NEDD8 yeast homolog Rub1, suggesting the possibility that a NEDDylation event regulates this mechanism (Singh et al., 2012).

Another aspect to consider is the possibility that RNAPII gets itself crosslinked to DNA (RNAPII-DPC). Our DPC-seq data have established that FA-induced DPCs form preferentially around the transcription start site, suggesting that some of these adducts can effectively consist of covalently trapped RNAPIIs. Moreover, it is possible that elongating RNAPII can encounter and stall at crosslinked RNAPII, thus initiating – like in the presence of any other DPC – its transcription-coupled repair.

Finally, in CSB/CSA-deficient cells, the persistence of UV-lesion stalled RNAPIIs hampers the passage of further elongating complexes, thus progressively depleting phosphorylated RNAPII pool and causing transcription shut down (Rockx et al., 2000). Following UV irradiation, this phenotype is exacerbated by stress-induced expression and subsequent promoter binding of ATF3 repressor, whose degradation is impaired in CS-deficient cells (Epanchintsev et al., 2017). Our RPB1 degradation and RRS data suggest that the presence of RNAPII-blocking DPCs causes similar responses. However, conversely to UV irradiation, upon FA treatment TC-NER-deficient cells restart transcription following 16h of recovery (Figures 18, 20, 22, 23, 24). Therefore, we speculate that transcriptional responses to UV and FA only partially overlap, however, further experiments will be required to clarify these aspects.

4.2 Transcription-coupled DPC repair and implications for human health

Mutations in GG-NER and TC-NER genes are causative for Xeroderma pigmentosum (XP) and Cockayne syndrome (CS), respectively. XP and CS patients suffer from divergent symptoms: while XP patients show overall photosensitivity and increased skin cancer predisposition, CS patients exhibit a more complex pathological spectrum, ranging from neurological manifestation and premature aging to cachexia and renal disorders (Rapin et al., 2000). In addition, mutations in UVSSA have been shown to cause UV-sensitive syndrome ($UV^{S}S$), a milder form of TCR deficiency, whose patients suffer from UV hypersensitivity but completely lack neurological alterations and progeroid symptoms (Spivak, 2005).

At present, the pathological mechanisms underlying the phenotypical disparities between CS and XP patients have not been fully elucidated. Indeed, while UV light sensitivity of XP patients can be easily explained by a defect in repairing “classical” UV-induced NER substrates, CS aetiology is currently poorly understood. Surprisingly, TC-NER deficiency preferentially affects metabolically active tissues and non-proliferating cells, rather than UV light exposed tissues (Lans et al., 2010; Stern-Delfils et al., 2020). It is reasonable to hypothesise that the upstream TC-NER factors CSB and CSA are important for repairing DNA lesions generated by reactive metabolic products. In agreement, a recent study showed that FA accumulation is sufficient to precipitate the principal features of CS syndrome in mice, indicating that CSB plays a crucial protective role towards this endogenous metabolite (Mulderrig et al., 2021). More in detail, inactivation of *Csb* gene ($Csb^{m/m}$) in mice that lack the FA detoxifying enzyme *Adh5* caused cachexia, kidney failure and neurological alterations, thereby severely affecting life span (Mulderrig et al., 2021). Using single-cell RNA-sequencing, the authors uncovered that the aberrant phenotypes of $Adh5^{-/-}Csb^{m/m}$ mice are caused by transcriptional stress driven by FA-induced damage, however the nature of the involved DNA lesion(s) remained elusive (Mulderrig et al., 2021). In our study, we observed – in line with the above-mentioned work – that CSB and CSA functions are critical for transcription recovery following FA treatment. In addition, we demonstrated for the first time that CSB is required for the repair of DPCs in actively transcribed genes, thus ensuring cellular tolerance to these lesions. The evidence that FA-induced DPCs contributes to CS aetiology may clarify why CSB and CSA mutations impair the function of metabolically active tissues and contribute to the unique pathological features of CS patients.

Moreover, our finding that CSB and CSA function is independent of downstream TC-NER factors to repair FA-induced lesions is striking, because it might help explain pathological

disparities between CS and XP. The important separation of functions between Xpa and Csb is further strengthened by the observation that, although Xpa contributes to FA cellular tolerance, loss of *Csb* yields a more severe phenotype than loss of *Xpa* in *Adh5*$^{-/-}$ mice (Mulderrig et al., 2021). This is in line and may be explained by our finding that XP cells are fully proficient in the repair of FA-induced DPCs, while CS cells are not.

In conclusion, our study not only revealed the importance of CSB and CSA in protecting cells towards FA, but it also provided the first evidence that DPC-driven transcriptional toxicity significantly contributes to CS aetiology. Further dissecting transcription-coupled DPC repair mechanisms and their regulation will potentially enable the development of new therapies and improve CS patients' health.

5 MATERIALS AND METHODS

5.1 Cell lines

5.1.1 Cell lines used in this study and their maintenance

RPE1-TetOn-Cas9-PuroS-TP53$^{-/-}$ (RPE1-iCas9) cells were kindly provided by the Luijsterburg lab (Leiden University); details about these cell lines are outlined in Table 1. RPE1-iCas9 cells were cultivated in Dulbecco's Modified Eagle Medium (DMEM) GluTAMAX (Thermo Fisher Scientific-Gibco) supplemented with 10% (v/v) fetal bovine serum (FBS) (Thermo Fisher Scientific).

HAP1 WT (Product ID: C631) and *ERCC6 KO* (*CSB KO*) (Product ID: HZGHC000422c011) were acquired from Horizon Discovery and grown in IMDM (Thermo Fisher Scientific-Gibco) supplemented with 10% (v/v) FBS, 1% Penicillin-Streptomycin-Glutamine (10378016, Thermo Fisher Scientific). *ERCC6 KO* genotype was confirmed by Sanger sequencing. All cell lines were cultured at 37°C in an atmosphere of 5% CO_2.

RPE1-TetOn-Cas9-PuroS-TP53-/-	**Source**
WT	(van der Weegen et al., 2021)
CSB$^{-/-}$ (*CSB KO*)	(van der Weegen et al., 2021)
XPC$^{-/-}$ (*XPC KO*)	(van der Weegen et al., 2021)
XPC$^{-/-}$*CSB*$^{-/-}$ (*XPC/CSB dKO*)	(van Den Heuvel et al., 2023)
XPC$^{-/-}$*XPA*$^{-/-}$ (*XPC/XPA dKO*)	(van Den Heuvel et al., 2023)
SPRTN-ΔC clone 2 (*SPRTN-ΔC#2*)	This study
SPRTN-ΔC clone 4 (*SPRTN-ΔC#4*)	This study
SPRTN-ΔC clone 5 (*SPRTN-ΔC#5*)	This study
CSB$^{-/-}$*SPRTN-ΔC* clone 2 (*CSB KO/SPRTN-ΔC#2*)	This study
CSB$^{-/-}$*SPRTN-ΔC* clone 10 (*CSB KO/SPRTN-ΔC#10*)	This study
CSB$^{-/-}$*SPRTN-ΔC* clone 23 (*CSB KO/SPRTN-ΔC#23*)	This study
CSA$^{-/-}$ (*CSA KO*)	(van der Weegen et al., 2021)
UVSSA$^{-/-}$ (*UVSSA KO*)	(van der Weegen et al., 2021)
ERCC1$^{-/-}$ (*ERCC1 KO*)	Unpublished, Luijsterburg lab
XPG$^{-/-}$ (*XPG KO*)	(Apelt et al., 2021)
ELOF1$^{-/-}$ (*ELOF1 KO*)	(van der Weegen et al., 2021)
CSB$^{-/-}$*ELOF1*$^{-/-}$ (*CSB/ELOF1 dKO*)	(van der Weegen et al., 2021)

Table 1. List of RPE1-TetOn-Cas9-PuroS-TP53$^{-/-}$ cells.

5.1.2 Generation of cell lines

RPE1 *SPRTN-ΔC* and RPE1 *CSB KO/SPRTN-ΔC* double mutants genome-edited cell lines were generated from RPE1-TetOn-Cas9-PuroS-TP53$^{-/-}$ WT and *CSB KO*, respectively by co-transfection in 6-well plates with Lenti-multi-Guide plasmid containing gRNA_SPRTN-ΔC#1 TTGGCAGATAAACCCAACAG (exon 5) and gRNA_SPRTN-ΔC#2 ATTAACCAGAACTTCCTGAC (3'-UTR) and px330 plasmid containing gRNA_SPRTN-ΔC#2 (1µg+1µg DNA). 48 hours after transfection of plasmids using Lipofectamine 2000 (11668030, Thermo Fisher Scientific) (DNA:LIPO=1:1 ratio), cells were expanded to 10cm dishes. After 96h, puromycin (1µg/ml) was added and increased to 2µg/ml the following day. 48h later, puromycin-containing media was removed, cells washed twice with PBS and allowed to recover for 4 days. To generate single clones, cells were then seeded in 96-well plates at a concentration of 0.5 cells/well. When they reached confluency, single colonies were transferred progressively to 24- and 12-well plates. Editing efficiency was assessed by western blotting.

5.1.3 Genotyping of single clones

Genomic DNA of single clones was extracted by lysing cells in DirectPCR®-Cell lysis reagent (31-302-C, Viagen) in the presence of 0.2mg/ml proteinase K (25530049, Invitrogen). Samples were incubated at 55°C for 3h, before proteinase K was heat-inactivated for 45min at 85°C. Genomic DNA was used as substrate to amplify the edited region while adding overhangs homologous to the pDONR221 vector with primers: 5'-CGACGGCCAGTCattctgaagattgccctc-3' (oMG_69: oJC30 + overhangs) and 5'-CAGGAAACAGCTATGACgcaccctgagacacaaaacatc-3' (oMG_70: oJC31 + overhangs using Platinum II Hot-Start Green PCR Master Mix (14001012, Thermo Fisher Scientific). Next, PCR products were gel-purified and cloned by TEDA-based cloning (Xia et al., 2019) into a pDONR221 backbone amplified with 5'-GTCATAGCTGTTTCCTGGC-3' (pJS_86 Forward) and GACTGGCCGTCGTTTTAC-3' (pJS_86 Reverse) using Q5® Hot Start High-Fidelity 2X Master Mix (M0494S, NEB). Plasmid DNA was isolated from at least five single colonies and analysed by Sanger sequencing. Genotypes are listed in Table 2.

Cell line	Genotype allele 1	Genotype allele 2
SPRTN-ΔC#2	Full deletion of exon 5	2 bp insertion at exon 5 gRNA_SPRTN-ΔC#1 cutting site
SPRTN-ΔC#4	28 bp deletion at exon 5 gRNA_SPRTN-ΔC#1 cutting site	Full deletion of exon 5
SPRTN-ΔC#5	41 bp deletion at gRNA_SPRTN-ΔC#1 cutting site	Full deletion of exon 5
CSB KO/SPRTN-ΔC#2	1 bp deletion at gRNA_SPRTN-ΔC#1 cutting site	Full deletion of exon 5
CSB KO/SPRTN-ΔC#10	29 bp deletion at gRNA_SPRTN-ΔC#1 cutting site	11 bp deletion at gRNA_SPRTN-ΔC#1 cutting site
CSB KO/SPRTN-ΔC#23	34 bp deletion at gRNA_SPRTN-ΔC#1 cutting site	13 bp deletion at gRNA_SPRTN-ΔC#1 cutting site

Table 2. Genotypes of RPE1 *SPRTN-ΔC* and RPE1 *CSB KO/SPRTN-ΔC* cell lines.

5.2 Cell viability assays

5.2.1 AlamarBlue cell viability assay

To measure FA, 5-azadC, illudin S, CPT or etoposide sensitivity, 1000 RPE1-iCas9 or HAP1 cells/well were seeded in triplicates in 24-well plates. The following day, cells were treated with the indicated doses of compounds (methanol-free FA, 28906, Thermo Fisher Scientific; 5-azadC, A3656, Sigma-Aldrich; illudin S, sc-391575, Santa Cruz; CPT, 208925, Sigma-Aldrich; etoposide, 341205, Sigma-Aldrich). After 5 (RPE1) or 4 (HAP1) days of incubation the medium was replaced with 500µl AlamarBlue cell viability reagent (36 µg/ml resazurin in PBS) (R7017, Sigma-Aldrich) and cells were incubated for 1h at 37°C. Cell viability was then assessed by measuring fluorescence (560nm excitation/590nm emission).

5.2.1.1 AlamarBlue cell viability assay upon siRNA transfection

RPE1-iCas9 cells were seeded in 6-well plate and the following day transfected with respective siRNA. 4µl siRNA (20µM) and 5µl Lipofectamine RNAiMAX Transfection Reagent (13778075, Thermo Fisher Scientific) were each diluted in 100µl Opti-MEM Medium (31985062, Thermo Fisher Scientific-Gibco). Following a 5min incubation, siRNA and Lipofectamine RNAiMAX Transfection Reagent dilutions were mixed. After an additional 15min, the transfection mix was added to cells. After 24h, transfection media was removed and, following one PBS wash, replaced with fresh media. The following day, cells were re-seeded into 24-well plates at 2500 cells/well confluency and next morning treated

with FA, 5-azadC or illudin S (72h after transfection). After 4 days of incubation the medium was replaced with AlamarBlue cell viability reagent 500µl (36µg/ml resazurin in PBS) and plates were incubated for 1h at 37°C. Cell viability was then assessed by measuring fluorescence (560nm excitation/590nm emission). In parallel, 72h after transfection, protein samples were collected to assess knockdown efficiency by western blotting. siRNAs used in this study are listed in Table 3.

siRNA	Sequence	Manufacturer	Catalogue ID
siCTRL	Control pool	Horizon Discovery	D-001810-10-20
siCSB	SMARTpool	Horizon Discovery	L-004888-00-0005
siRNF4	SMARTpool	Horizon Discovery	L-006557-00-0005
siSPRTN#1	CAAGGAACCAGAGAAUUA	N/A	N/A

Table 3. List of siRNAs used in this study.

5.2.2 Colony formation assay

To measure UVC sensitivity, 4000 cells/plate were seeded in triplicates in 6cm dishes. The next day, media was removed and cells were irradiated in PBS with UVC 1 or 5J/m^2. After 7 days, cells were stained with crystal violet. To measure cell growth, RPE1-iCas9 WT, *CSB KO*, *SPRTN-ΔC*, *CSB KO/SPRTN-ΔC* cells were seeded in triplicate in 6-well plate at 2000 cells/well and let grow for 8 days, before crystal violet staining.

5.3 Protein analysis

5.3.1 Western blotting

Protein samples were boiled in 1x NuPAGE LDS sample buffer (NP0007, Thermo Fisher Scientific) containing NuPAGE Sample Reducing Agent (NP0009, Thermo Fisher Scientific). SDS-PAGE was run using NuPAGE 4-12% 20-well gels. Following electrophoresis, proteins were transferred on 0.45µm PVDF membranes (IPVH00010, Merck Millipore) using a wet transfer system (1704070, Bio-Rad) for 80min at 100V. PxP protein samples were run in 4-12%, 1.5mm Bolt gels (Thermo Fisher Scientific) and transferred using the dry Trans-Blot Turbo System (Bio-Rad) with the Bio-Rad standard 30min transfer protocol. Membranes were blocked in 5% milk in TBS-Tween20 for 1h before addition of primary antibody. Primary antibodies used in this study are listed in Table 4. Following overnight 4°C incubation with primary antibody, membranes were washed and incubated for 1h with corresponding secondary antibody (Table 5). Western blotting images

were acquired using ChemiDoc Imaging System (Bio-Rad) and in order to help visualization, brightness was adjusted using FIJI (ImageJ).

Primary antibody	Application	Manufacturer	Catalogue ID
Anti-Tubulin (Mouse)	WB (1:2000)	Sigma-Aldrich	T6074
Anti-Histone H3 (D1H2) (Rabbit)	WB (1:1000)	Cell Signaling	4499S
Anti-RNAPII-CTDpSer2 (3E10) (Rat)	WB (1:2000)	Millipore	04-1571
Anti-RNAPII-CTDpSer2 (Rabbit)	IP	Abcam	ab5095
Anti-CSB (Rabbit)	WB (1:1000)	Abcam	ab96089
Anti-CSA (Rabbit)	WB (1:500)	Abcam	ab137033
Anti-p89 (TFIIH) (Mouse)	WB (1:500)	Santa Cruz Biotechnology	sc-271500
Anti-p62 (TFIIH) (Mouse)	WB (1:500)	Santa Cruz Biotechnology	sc-25329
Anti-GAPDH antibody (14C10) (Rabbit)	WB (1:2000)	Cell Signaling	2118
Anti-RNAPII-CTDpSer5 (4H8) (Mouse)	WB (1:2000)	Abcam	ab5408
Anti-XPC (Mouse)	WB (1:1000)	Santa Cruz Biotechnology	sc-74410
Anti-SPRTN (6F2) (Rat)	WB (1:500)	Custum (Zhao et al., 2021)	N/A
Anti-RNF4 (Goat)	WB (1:500)	R&D systems	AF7964

Table 4: List of primary antibodies used in this study.

Secondary antibody	Application	Manufacturer	Catalogue ID
Goat Anti-Mouse Immunoglobulins/HRP	WB (1:5000)	Dako	P0447
Swine Anti-Rabbit Immunoglobulins/HRP	WB (1:5000)	Dako	P0399
Goat Anti-Rat Immunoglobulins/HRP	WB (1:3000)	Sigma-Aldrich	A9037
Rabbit Anti-Goat Immunoglobulins/HRP	WB (1:3000)	Sigma-Aldrich	A8919
Mouse Anti-Rabbit Immunoglobulin (Light-Chain Specific) (D4W3E)/HRP	WB (1:2000)	Cell Signaling	93702

Table 5: List of secondary antibodies used in this study.

5.3.2 Immunoprecipitation for Co-IP

Endogenous RNAPIIo immunoprecipitation for Co-IP was performed as described in van der Weegen et al., 2020. Cells were mock-treated, treated with methanol-free FA (1 or 1.75mM) or irradiated with UVC light (20J/m^2) and harvested after 1h. Where mentioned, cells were pre-treated with MG-132 (M7449, Sigma-Aldrich) 5μM for 1h prior to FA treatment or UVC irradiation and MG-132 has been kept during the whole recovery timeframe. Chromatin-enriched fractions were prepared by incubating the cells for 30min on ice in IP-130 buffer (30mM Tris-HCl pH7.5, 130mM NaCl, 2mM $MgCl_2$, 0.5% Triton X-100) supplemented with cOmplete EDTA-free protease inhibitor cocktail (4693132001, Merck Millipore). This step was followed by centrifugation at 10000g for 10min, and removal of the supernatant. Cell pellets (chromatin fractions) were lysed in IP-130 buffer in the presence of protease inhibitor cocktail, 500U/ml benzonase nuclease (70746, Merck Millipore) and 2μg RNAPII-S2 antibody (ab5095, Abcam) for 3h at 4°C. Protein complexes were pulled down by 1.5h incubation with Protein A Agarose Beads (16-157, Sigma-Aldrich). Beads were washed 6 times with IP-130 buffer and samples for western blotting were prepared by boiling in 2x NuPAGE LDS sample buffer.

5.3.3 RPB1 degradation assay (Cycloheximide chase)

Cells were seeded in 6-well tissue culture plates, grown to 80% confluency and then pre-treated with cycloheximide (CHX) 100μg/ml (C4859, Sigma-Aldrich) for 1h. When indicated, cells were pre-treated with MG-132 5μM or NEDDi (MLN-4924, ab216470, Abcam) 2μM for 1h prior to UVC 20J/m^2 irradiation or FA 1.75mM treatment. Finally, cells were lysed in 250μl 1x NuPAGE LDS sample buffer, followed by SDS-PAGE and western blotting with the indicated antibodies.

5.4 Microscopy-based assays

5.4.1 EU and EdU incorporation

For EU and EdU incorporation RPE1-iCas9 cells were seeded in 24-well plate in 10% FBS-containing media and 48h later cells were treated with different concentration of methanol-free FA (indicated in the figure legend). After 1h, FA-containing media was removed and cells were washed twice with PBS. Then, cells were pulse-labelled with 400μM 5-Ethynyl-uridine (EU, CLK-N002-10, Jena Bioscience) or with 100μM 5-Ethynyl-2'-deoxyuridine (5-EdU, CLK-N001-25, Jena Bioscience) for 1h, followed by a 15min medium chase with DMEM without supplements. Cells were fixed with 4% FA (methanol-free FA, 28908,

Thermo Fisher Scientific) in PBS for 20min and Click-iT labelling and analysis was performed as described below.

For EU incorporation upon 5-azadC treatments, RPE1 cells were seeded on coverslips and synchronized using a double thymidine block, based on two cycles of overnight incubation with 2mM thymidine (T9250, Sigma-Aldrich) and 9h release. Then, cells were released in thymidine-free media and treated with 5-azadC for the indicated time periods. In the final 30min of 5-azadC treatment, 400μM EU was added to monitor transcription. EU incorporation was followed by a 15min medium chase with DMEM without supplements. Cells were fixed with 4% methanol-free FA in PBS for 20min prior to Click-iT labelling.

5.4.2 Click-iT labelling

For Click-iT labelling cells previously fixed in 4% FA were permeabilized with 0.5% Triton X-100 in PBS for 10min at room temperature and blocked in 1.5% bovine serum albumin (BSA, Thermo Fisher Scientific) in PBS for 15min. Nascent RNA/DNA was visualized by Click-iT chemistry, incubating the cells in the dark for 1h with a mix of 60μM AF488-Azide (CLK-1275-1, Jena Bioscience), 4mM $CuSO_4$ (451657-10G, Sigma-Aldrich), 10mM ascorbic acid (A7631-100G, Sigma-Aldrich) and 0.5μg/ml DAPI (62248, Thermo Fisher Scientific) in a 50mM Tris-HCl pH8 buffer. Coverslips were washed 5 times with PBS and mounted in Prolong Gold Antifade Mountant (P10144, Thermo Fisher Scientific). Images were acquired using a ZEISS LSM710 microscope and ZEN 2009 software version 5.5.0.443 (Carl Zeiss). Signal intensity quantification was performed using Cell Profiler. For representative images, brightness was adjusted using FIJI (ImageJ) software.

5.4.3 Recovery of RNA synthesis (RRS) assay

For Recovery of RNA synthesis (RRS) assay, RPE1-iCas9 and HAP1 cells were seeded in 24-well plate (FA treatment) or 12-well plate (UVC irradiation) in 10% FBS-containing media. The following day media was removed, cells were washed once with PBS, and 1% FBS-containing media was added. 24h later cells were treated with methanol-free FA 1.75mM (RPE1) or 0.75mM (HAP1) or irradiated with UVC 20J/m^2. After 1h, FA-containing media was removed and cells were washed twice with PBS. Then, cells were allowed to recover for the indicated time periods and pulse-labelled with 400μM EU for 1h, followed by a 15min medium chase with DMEM without supplements. Cells were fixed with 4% methanol-free FA in PBS for 20min. Click-iT labelling and analysis was performed as described in the previous section.

5.5 DPCs isolation and analysis

5.5.1 KCl/SDS DPC-sequencing (DPC-seq)

To prepare DNA samples for KCl/SDS-DPC-seq, RPE1-iCas9 WT vs *CSB KO* were seeded in 6-well plate at 160000 cells/well in 10% FBS-containing media, 3 wells/condition (3 technical replicates). The following day, media was removed, cells were washed once with PBS and 1% FBS-containing media was added. 24h hours later, cells were treated with FA 1.75mM to induce DPCs. After 1h, FA-containing media was removed and cells were washed twice with PBS. Cells were either harvested immediately (T0) or allowed to recover for 6h (T6). Cells were harvested by scraping in 150µl 2%SDS, 20mM Tris-HCl pH7.5 (KCl/SDS lysis buffer), transferred to 1.5ml tubes, immediately frozen in liquid nitrogen and stored at -80°C.

For KCl/SDS precipitation, samples were thawed from -80°C at 55°C for 5min (1200rpm shaking) and sonicated using Covaris® Focused ultrasonicator E220evo in 130µl tubes (microTUBE AFA Fiber Pre-Slit Snap-Cap 6x16mm; 1x cycle, 120sec). Next, samples were transferred to 1.5ml tubes and 270µl 2% SDS, 20mM Tris-HCl pH7.5 was added to each sample up to a final volume of 400µl. DNA extraction was performed on 10% of the total lysate (40µl) using GeneJET Genomic DNA Purification Kit (10410450, Thermo Fisher Scientific) and considered as input. For KCl/SDS precipitation of the remaining lysate, 400µl of 200mM KCl, 20mM Tris-HCl pH7.5 (KCl/SDS precipitation buffer) was added to each sample, followed by incubation on ice for 5min and full speed centrifugation at 4°C (5min). Supernatants (soluble DNA) (~600µl) were transferred to a new tube for DNA quantification. Pellets (containing proteins and protein + crosslinked DNA) were washed three times according to the following steps: addition 400µl 200mM KCl, 20mM Tris-HCl pH7.5, incubation at 55°C for 5min (1200rpm shaking), incubation on ice (5min), full speed centrifugation 4°C (5min). Next, pellets were resuspended in 400µl of 200mM KCl, 20mM Tris-HCl pH7.5 containing 0.2mg/ml proteinase K and incubated at 55°C for 45min (800rpm shaking) for protein digestion. 10µl UltraPure BSA (AM2616, Thermo Fisher Scientific, stock 50mg/ml) was added to the solution followed by cooling down on ice for 5min and full speed centrifugation at 4°C for 5min. Next, supernatants containing crosslinked DNA were collected. Soluble DNA and crosslinked DNA samples were treated with 0.2mg/ml DNAse-free RNAse A solution (Sigma-Aldrich) for 30min at 37°C. DNA concentrations were determined using Qubit™ dsDNA HS Assay Kit (Q32851, Thermo Fisher Scientific) according to the manufacturer's instructions. Relative DPC amounts among conditions were calculated as the ratio between crosslinked DNA and total DNA (crosslinked + soluble DNA) as a surrogate for DPCs persistence.

At this stage, DNA samples have been shipped to Cancer Research UK Cambridge Institute and the following steps have been performed by our collaborator Dr. Aldo Bader.
50ng of DNA was concentrated via ethanol precipitation with 300mM sodium acetate, 1µl glycogen and 2.5x ethanol and resuspending in 20µl of nuclease-free water. DNA was run on 1% agarose gels cast in 1.5mm Mini-PROTEAN cassettes (Bio-Rad), stained with SYBR-Gold and the DNA fragment smear of 400-1000bp was dissected from the gel. Gel slices were immersed in 500µl gel-extraction buffer (10mM Tris pH8.0, 1mM EDTA, 0.02% SDS) and rotated at 4°C overnight. The gel slices and buffer were loaded into Spin-X columns (CLS8160, Corning Costar) and centrifuged at 14000g for 10min at 4°C. The eluted DNA containing buffer was ethanol precipitated as before and resuspended in 50µl nuclease free water. DNA was then subjected to library preparation via the NEB Next Ultra-II DNA library prep kit (E7645L, NEB) using a 1 in 10 adapter dilution and 7 PCR cycles. Libraries were analysed via Qubit and Tapestation, pooled at equimolar concentrations and sequenced on an Illumina NovaSeq with PE50 cycles.

5.5.1.1 DPC-seq analysis

DPC-seq analysis has been performed by Dr. Aldo Bader (Cancer Research UK Cambridge Institute). Fastq files were generated using bcl2fastq2 (v2.20), low quality reads were filtered out using fastp (Chen et al., 2018) (v0.23.2) and aligned to the hg38 human genome via Bowtie2 Bowtie2 (Langmead and Salzberg, 2012) (v2.4.5). Alignments were then sorted and indexed using Samtools (Li et al., 2009) (v1.16.1). Read coverages were calculated from alignments using either Deeptools (Ramírez et al., 2014) (v3.5.0) bamCoverage or bedtools (Quinlan and Hall, 2010) (v2.30.0) coverage using the GRCh38 annotations as a reference. Per gene coverage was normalised to number of reads per sample and also to the length of each gene. Further analysis was conducted in R (v4.1.2) using custom scripts. WT and *CSB*$^{-/-}$ read coverage was compared via log2 fold change and via t-tests with Bonferroni correction. All box-plots, dot plots and genome track plots were generated using ggplot2 (v3.4.0) whereas metagene line plots and heatmaps were generated using Deeptools. Comparisons to other datasets from ATAC-seq (GSE209659) and RNAPII ChIP-seq (GSE141798) was completed by analysing the read coverage of these datasets in the same way as for the DPC-seq data. All analytical code for both upstream processing and downstream analysis and plot generation are publicly available at https://github.com/aldob/DPC-Seq.

5.5.2 Purification of x-linked Proteins (PxP)

PxP was performed as described in Weickert et al., 2023. DPCs were induced by addition of methanol-free FA 1mM (RPE1) or 0.5-1mM (HAP1) to asynchronous or G1-arrested cells. To arrest RPE1 cells in G1, cells were seeded in 10cm dishes at 100% confluency 48h prior the FA treatment. The same number of cells was seeded in 15cm dishes, as asynchronous control. Cells were treated for 1h with 1mM (RPE1) and 0.5-1mM FA (HAP1), then FA-containing media was removed and cells were washed twice with PBS. Fresh media was added and cells were allowed to recover for the indicated time. At the indicated timepoint, cells were harvested by trypsinization, washed with PBS, pelleted and immediately froze at -80°C for short-term storage. To isolate DPCs, cell pellets were thawed and resuspended in ice-cold PBS at 25000 cells/µl (HAP1) or 35000 cells/µl (RPE1); 10µl of the cell suspension were directly lysed in 1x NuPAGE LDS sample buffer to serve as input samples. The remaining cell suspension was prewarmed for 45sec at 45°C, mixed with an equal volume of low melt agarose (2% in PBS, 1613111, Bio-Rad) and immediate casted into plug molds (1703713, Bio-Rad) with a total volume of ~90µl. Plugs were placed at 4°C for 5min, prior to transfer into 1ml ice-cold PxP lysis buffer (1x PBS, 0.5mM EDTA, 2% sarkosyl (L7414, Sigma-Aldrich), cOmplete EDTA-free protease inhibitor cocktail). Lysis was carried out on a rotating wheel at 4°C for 4h. Following lysis, for electro-elution, plugs were transferred to the wells of 10-well SDS-PAGE gels (12%, 1.5mm Bolt gels, Thermo Fisher Scientific). Electrophoresis was carried out in 300ml MOPS buffer at 20mA per gel for 60min in a Mini Gel Tank (Thermo Fisher Scientific). Following electro-elution, plugs were retrieved and transferred to tubes containing 1ml PxP wash buffer (50mM Tris-HCl pH8, 0.5mM $MgCl_2$, 0.01% sarkosyl), while the gel was stained using InstantBlue (ISB1L, Sigma-Aldrich) to confirm successful extraction of non-crosslinked cellular proteins. Plugs were incubated on a rotating wheel at 4°C for 10min. Plugs of the same conditions were pooled at this stage of the purification; for western blotting analysis of FA-induced DPCs, 3 plugs per condition were used. The supernatant was aspirated and plugs were melted at 99°C for 5min, followed by addition of 20µl PxP wash buffer containing 50U of benzonase nuclease and incubation at 37°C for 30min. Samples were then frozen at -80°C. For analysis by western blotting, NuPAGE LDS sample buffer was added and samples were subjected to western blotting using the indicated primary antibodies (listed in Table 4).

6 LIST OF ABBREVIATIONS

5-azadC	5-aza-2'-deoxycytidine
ACRC	Acid repeat-containing protein
ADH	Alcohol dehydrogenase
ALDH	Aldehyde dehydrogenase
ALKBH	AlkB homolog
AP	Apurinic/apyrimidinic
APE	AP endonuclease
APTX	Aprataxin
Arg	Arginine
Asn	Asparagine
Asp	Aspartic acid
ATF3	Activating transcription factor 3
BARD1	BRCA1 Associated RING Domain 1
BER	Base excision repair
BLM	Bloom syndrome protein
bp	Base pair
BR	Basic region
BSA	Bovine serum albumin
C. elegans	*Caenorhabditis elegans*
CAK	CDK-activating kinase subcomplex
CHO	Chinese hamster ovary
CHX	Cycloheximide
CIM	CSA-interaction motif
Co-IP	Co-immunoprecipitation
CPD	Cyclobutane pyrimidine dimer
CPT	Camptothecin
CS	Cockayne syndrome
CSA/B	Cockayne syndrome group A/B
CTD	Carboxy-Terminal Domain

CtIP	CtBP-interacting protein
CUL4	Cullin 4
Cys	Cysteine
DBD	DNA-binding domain
DDR	DNA damage response
DEB	Diepoxybutane
DNA	Deoxyribonucleic acid
DNA-PKcs	DNA-dependent protein kinase catalytic subunit
DNMT1	DNA methyltransferase 1
DPC	DNA-protein crosslink
DPC-seq	DPC-sequencing
DSB	Double-strand break
dsDNA	Double-stranded DNA
DUB	Deubiquitylating enzyme
DDI1/2	DNA damage inducible 1/2
EdU	5-Ethynyl-2'-deoxyuridine
ELOF1	Elongation factor 1
EXO1	Exonuclease 1
EU	5-Ethynyl-uridine
FAM111A	Family with sequence similarity 111 member A
FAN1	Fanconi-associated nuclease 1
FBS	Fetal bovine serum
FEN1	Flap structure-specific endonuclease 1
GCNA	Germ cell nuclear antigen
GG-NER	Global genome NER
GSH	Glutathione
h	Hour
His	Histidine
HMCES	5-hydroxymethylcytosine binding, ES cell specific
HNPCC	Hereditary nonpolyposis colorectal cancer

ICL	Inter-strand crosslink
IDR	Intrinsically disordered region
IEG	Immediate early gene
IR	Ionizing radiation
K	Lysine
kb	Kilobase
kD	Kilodalton
LIG1/3	DNA ligase 1/3
M	Molar
MEF	Mouse embryonic fibroblast
MGMT	O^6-methylguanine-DNA methyltransferase
Min	Minute
NAD	Nicotinamide adenine dinucleotide
NEDDi	NEDDylation inhibitor
NER	Nucleotide excision repair
NGS	Next generation sequencing
NHEJ	Non-homologous end joining
NLS	Nuclear localization signal
OGG1	8-oxoguanine DNA glycosylase 1
8-oxoG	8-oxoguanine
PARP	Poly (ADP-ribose) polymerase
PARPi	PARPi
PCNA	Proliferating cell nuclear antigen
PIP	PCNA-interacting protein
PIP-box	PCNA-interacting protein box
PNKP	Polynucleotide kinase/phosphatase
Pol	Polymerase
6-4PP	Pyrimidine-pyrimidone photoproduct
PTM	Post-translational modification
PxP	Purification of x-linked proteins

RBX1	RING box protein 1
RFC	Replication factor C
RJALS	Ruijs-Aalfs syndrome
RNAPII	RNA polymerase II
RNF4	RING finger protein 4
RPA	Replication protein A
RPM	Reads per million
ROS	Reactive oxygen species
RTEL1	Regulator of telomere elongation helicase 1
RTF2	Replication termination factor 2
RVP	Retroviral-like protease domain
S. cerevisiae	*Saccharomyces cerevisiae*
SAM	S-adenosylmethionine
SCAN1	Spinocerebellar ataxia with axonal neuropathy
Ser	Serine
SIM	SUMO interacting motif
SNM1A/B	Sensitive to nitrogen mustard 1A/B
SPRTN	SprT-like N-terminal domain
SRAP	SOS response-associated peptidase
SSB	Single-strand break
SSBR	SSB repair
ssDNA	Single-stranded DNA
STUbL	SUMO-targeted ubiquitin ligase
TC	Transcription-coupled
TC-NER	Transcription-coupled NER
TCR	Transcription-coupled repair
TDG	Thymine DNA glycosylase
TDP1/2	Tyrosyl-DNA phosphodiesterase 1/2
TEX264	Testis expressed 264
TIR	TFIIH-interacting region

TLS	Translesion synthesis
TOP1/2	Topoisomerase 1/2
TOP1/2-cc	TOP1/2-cleavage complex
TRAIP	TRAF-interacting protein
TSS	Transcription start site
TTD	Trichothiodystrophy
Tyr	Tyrosine
UBA	Ubiquitin-associated domain
UBE2T	Ubiquitin-conjugating enzyme E2 T
UBL	Ubiquitin binding-like domain
UBZ	Ubiquitin-binding zinc finger
UDG	Uracil DNA glycosylase
USP1/7	Ubiquitin specific peptidase 1/7
UV	Ultraviolet
UV-DDB	UV-damaged DNA-binding protein
UV^{S}S	UV-sensitive syndrome
UVSSA	UV-stimulated scaffold protein A
VCP	Valosin-containing protein
VCPIP1	Valosin-containing protein interacting protein 1
XLF	XRCC4-like factor
XP	Xeroderma pigmentosum
XRCC	X-ray repair cross-complementing protein
ZBD	Zinc-binding domain

7 REFERENCES

Abbotts, R., and Wilson, D.M. 3rd (2017). Coordination of DNA Single Strand Break Repair. *Free Radical Biology and Medicine* 107, 228–44.

Akkari, Y.M., Bateman, R.L., Reifsteck, C.A., Olson, S.B., and Grompe, M. (2000). DNA Replication Is Required To Elicit Cellular Responses to Psoralen-Induced DNA Interstrand Cross-Links. *Molecular and Cellular Biology* 20(21), 8283–89.

Alabert, C., Bukowski-Wills, J.C., Lee, S.B., Kustatscher, G., Nakamura, K., de Lima Alves, F., Menard, P., Mejlvang, J., Rappsilber, and J., Groth, A. (2014). Nascent Chromatin Capture Proteomics Determines Chromatin Dynamics during DNA Replication and Identifies Unknown Fork Components. *Nature Cell Biology* 16(3), 281–91.

Ali, K., Mahjabeen, I., Sabir, M., Mehmood, H., and Kayani, M.A. (2015). OGG1 Mutations and Risk of Female Breast Cancer: Meta-Analysis and Experimental Data. *Disease Markers* 2015, 1–16.

Almeida, K.H., and Sobol, R.W. (2007). A Unified View of Base Excision Repair: Lesion-Dependent Protein Complexes Regulated by Post-Translational Modification. *DNA Repair* 6(6), 695–711.

Anindya, R., Aygün O., and Svejstrup, J.Q. (2007). Damage-Induced Ubiquitylation of Human RNA Polymerase II by the Ubiquitin Ligase Nedd4, but Not Cockayne Syndrome Proteins or BRCA1. *Molecular Cell* 28(3), 386–97.

Aparicio, T., Baer, R., Gottesman, M., and Gautier, J. (2016). MRN, CtIP, and BRCA1 Mediate Repair of Topoisomerase II–DNA Adducts. *Journal of Cell Biology* 212(4), 399–408.

Apelt K., White, S.M., Kim, H.S., Yeo, J.E., Kragten, A., Wondergem, A.P., Rooimans, M.A., González-Prieto, R., Wiegant, W.W., Lunke, S., Flanagan, D., Pantaleo, S., Quinlan, C., Hardikar, W., van Attikum, H., Vertegaal, A.C.O., Wilson, B.T., Wolthuis, R.M.F., Schärer, O.D., and Luijsterburg, M.S. (2021). *ERCC1* Mutations Impede DNA Damage Repair and Cause Liver and Kidney Dysfunction in Patients. *Journal of Experimental Medicine* 218(3), e20200622.

Araki, M., Masutani, C., Takemura, M., Uchida, A., Sugasawa, K., Kondoh, J., Ohkuma, Y., and Hanaoka, F. (2001). Centrosome Protein Centrin 2/Caltractin 1 Is Part of the Xeroderma Pigmentosum Group C Complex That Initiates Global Genome Nucleotide Excision Repair. *Journal of Biological Chemistry* 276(22), 18665–72.

Avery, O.T., MacLeod, C.M., and McCarty, M. (1944). STUDIES ON THE CHEMICAL NATURE OF THE SUBSTANCE INDUCING TRANSFORMATION OF PNEUMOCOCCAL TYPES. *Journal of Experimental Medicine* 79(2), 137–58.

Bahrami, S., and Drabløs, F. (2016). Gene Regulation in the Immediate-Early Response Process. *Advances in Biological Regulation* 62, 37–49.

Baker, D.J., Wuenschell, G., Xia, L., Termini, J., Bates, S.E., Riggs, A.D., and O'Connor, T.R. (2007). Nucleotide Excision Repair Eliminates Unique DNA-Protein Cross-Links from Mammalian Cells. *Journal of Biological Chemistry* 282(31), 22592–604.

Balajee, A.S., May, A., Dianov, G.L., Friedberg, E.C., and Bohr, V.A. (1997). Reduced RNA Polymerase II Transcription in Intact and Permeabilized Cockayne Syndrome Group B Cells. *Proceedings of the National Academy of Sciences* 94(9), 4306–11.

Barker., S., Weinfeld, M., and Murray, D. (2005). DNA-Protein Crosslinks: Their Induction, Repair, and Biological Consequences. *Mutation Research/Reviews in Mutation Research* 589(2), 111–35.

References

Barnes, D.E., and Lindahl, T. (2004). Repair and Genetic Consequences of Endogenous DNA Base Damage in Mammalian Cells. *Annual Review of Genetics* 38(1), 445–76.

Bashtrykov, P., Jankevicius, G., Smarandache, A., Jurkowska, R.Z., Ragozin, S., and Jeltsch, A. (2012). Specificity of Dnmt1 for Methylation of Hemimethylated CpG Sites Resides in Its Catalytic Domain. *Chemistry & Biology* 19(5), 572–78.

Beaudenon, S.L., Huacani, M.R., Wang, G., McDonnell, D.P., and Huibregtse, J.M. (1999). Rsp5 Ubiquitin-Protein Ligase Mediates DNA Damage-Induced Degradation of the Large Subunit of RNA Polymerase II in *Saccharomyces Cerevisiae*. *Molecular and Cellular Biology* 19(10), 6972–79.

Bebenek, K., and Kunkel, T.A. (2004). Functions of DNA Polymerases. In *Advances in Protein Chemistry* 69, 37–65.

Bhargava, V., Goldstein, C.D., Russell, L., Xu, L., Ahmed, M., Li, W., Casey, A., Servage, K., Kollipara, R., Picciarelli, Z., Kittler, R., Yatsenko, A., Carmell, M., Orth, K., Amatruda J.F., Yanowitz, J.L., and Buszczak, M. (2020). GCNA Preserves Genome Integrity and Fertility Across Species. *Developmental Cell* 52(1), 38-52.e10.

Bohr, V. (1985). DNA Repair in an Active Gene: Removal of Pyrimidine Dimers from the DHFR Gene of CHO Cells Is Much More Efficient than in the Genome Overall. *Cell* 40(2), 359–69.

Borgermann, N., Ackermann, L., Schwertman, P., Hendriks, I.A., Thijssen, K., Liu, J.C., Lans, H., Nielsen, M.L., and Mailand, N. (2019). SUMOylation Promotes Protective Responses to DNA -protein Crosslinks. *The EMBO Journal* 38(8), e101496.

Bradford, P.T., Goldstein, A.M., Tamura, D., Khan, S.G., Ueda, T., Boyle, J., Oh, K.S., Imoto, K., Inui, H., Moriwaki, S., Emmert, S., Pike, K.M., Raziuddin, A., Plona, T.M., DiGiovanna, J.J., Tucker, M.A., and Kraemer, K.H. (2011). Cancer and Neurologic Degeneration in Xeroderma Pigmentosum: Long Term Follow-up Characterises the Role of DNA Repair. *Journal of Medical Genetics* 48(3), 168–76.

Bregman, D.B., Halaban, R., van Gool, A.J., Henning, K.A., Friedberg, E.C., and Warren, S.L. (1996). UV-Induced Ubiquitination of RNA Polymerase II: A Novel Modification Deficient in Cockayne Syndrome Cells. *Proceedings of the National Academy of Sciences* 93(21), 11586–90.

Breiling, A., and Lyko, F. (2015). Epigenetic Regulatory Functions of DNA Modifications: 5-Methylcytosine and Beyond. *Epigenetics & Chromatin* 8(1), 24.

Brem, R., Guven, M., and Karran, P. (2017). Oxidatively-Generated Damage to DNA and Proteins Mediated by Photosensitized UVA. *Free Radical Biology and Medicine* 107, 101–9.

Brooks, P.J., and Zakhari, S. (2014). Acetaldehyde and the Genome: Beyond Nuclear DNA Adducts and Carcinogenesis: Acetaldehyde and the Genome. *Environmental and Molecular Mutagenesis* 55(2), 77–91.

Caldecott, K.W. (2008). Single-Strand Break Repair and Genetic Disease. *Nature Reviews Genetics* 9(8), 619–31.

Carmell, M.A., Dokshin, G.A., Skaletsky, H., Hu, Y.C., van Wolfswinkel, J.C., Igarashi, K.J., Bellott, D.W., Nefedov, M., Reddien, P.W., Enders, G.C., Uversky, V.N., Mello, C.C., and Page, D.C. (2016). A Widely Employed Germ Cell Marker Is an Ancient Disordered Protein with Reproductive Functions in Diverse Eukaryotes. *eLife* 5, e19993.

Ceccaldi, R., Sarangi, P., and D'Andrea, A.D. (2016). The Fanconi Anaemia Pathway: New Players and New Functions. *Nature Reviews Molecular Cell Biology* 17(6), 337–49.

Centore, R.C., Yazinski, S.A., Tse, A., and Zou, L. (2012). Spartan/C1orf124, a Reader of PCNA Ubiquitylation and a Regulator of UV-Induced DNA Damage Response. *Molecular Cell* 46(5), 625–35.

Champoux, J.J. (2001). DNA Topoisomerases: Structure, Function, and Mechanism. *Annual Review of Biochemistry* 70(1), 369–413.

Chapman, J.R., Taylor, M.R.G., and Boulton, S.J. (2012). Playing the End Game: DNA Double-Strand Break Repair Pathway Choice. *Molecular Cell* 47(4), 497–510.

Chatterjee, N., and Walker, G.C. (2017). Mechanisms of DNA Damage, Repair, and Mutagenesis: DNA Damage and Repair. *Environmental and Molecular Mutagenesis* 58(5), 235–63.

Chen, H., Yao, L., Brown, C., Rizzo, C.J., and Turesky, R.J. (2019). Quantitation of Apurinic/Apyrimidinic Sites in Isolated DNA and in Mammalian Tissue with a Reduced Level of Artifacts. *Analytical Chemistry* 91(11), 7403–10.

Chen, S., Zhou, Y., Chen, Y., and Gu, J. (2018). fastp: an ultra-fast all-in-one FASTQ preprocessor. Bioinformatics 34(17), i884–i890.0.

Chesner, L.N., and Campbell, C. (2018). A Quantitative PCR-Based Assay Reveals That Nucleotide Excision Repair Plays a Predominant Role in the Removal of DNA-Protein Crosslinks from Plasmids Transfected into Mammalian Cells. *DNA Repair* 62, 18–27.

Chiang, S.C., Carroll, J., and El-Khamisy, S.F. (2010). TDP1 Serine 81 Promotes Interaction with DNA Ligase IIIα and Facilitates Cell Survival Following DNA Damage. *Cell Cycle* 9(3), 588–95.

Chiou, Y.Y., Hu, J., Sancar, A., and Selby, C.P. (2018). RNA polymerase II is released from the DNA template during transcription-coupled repair in mammalian cells. *Journal of Biological Chemistry* 293(7), 2476–86.

Chválová, K., Brabec, V., and Kašpárková, J. (2007). Mechanism of the Formation of DNA–Protein Cross-Links by Antitumor Cisplatin. *Nucleic Acids Research* 35(6), 1812–21.

Cockayne, E.A. (1936). Dwarfism with Retinal Atrophy and Deafness. *Archives of Disease in Childhood* 11(61), 1–8.

Cohen, S.M., and Lippard, S.J. (2001). Cisplatin: From DNA Damage to Cancer Chemotherapy. In *Progress in Nucleic Acid Research and Molecular Biology* 67, 93–130.

Coin, F., Oksenych, V., and Egly, J.M. (2007). Distinct Roles for the XPB/P52 and XPD/P44 Subcomplexes of TFIIH in Damaged DNA Opening during Nucleotide Excision Repair. *Molecular Cell* 26(2), 245–56.

Coin, F., Oksenych, V., Mocquet, V., Groh. S., Blattner, C., and Egly, J.M. (2008). Nucleotide Excision Repair Driven by the Dissociation of CAK from TFIIH. *Molecular Cell* 31(1), 9–20.

Connelly, J.C., de Leau, E.S., and Leach, D.R.F. (2003). Nucleolytic Processing of a Protein-Bound DNA End by the E. Coli SbcCD (MR) Complex. *DNA Repair* 2(7), 795–807.

Cooke, M.S., Evans M.D., Dizdaroglu, M., and Lunec, J. (2003). Oxidative DNA Damage: Mechanisms, Mutation, and Disease. *The FASEB Journal* 17(10), 1195–1214.

Cui, H., Li, X., Han, C., Wang, Q.E., Wang, H., Ding, H.F., Zhang, J., and Yan, C. (2016). The Stress-Responsive Gene ATF3 Mediates Dichotomous UV Responses by Regulating the Tip60 and P53 Proteins. *Journal of Biological Chemistry* 291(20), 10847–57.

Dantzer, F., Schreiber, V., Niedergang, C., Trucco, C., Flatter, E., De La Rubia, G., Oliver, J., Rolli, V., Ménissier-de Murcia, J., and de Murcia, G. (1999). Involvement of Poly(ADP-Ribose) Polymerase in Base Excision Repair. *Biochimie* 81(1–2), 69–75.

Das, B.B., Huang, S.Y., Murai, J., Rehman, I., Amé, J.C., Sengupta, S., Das, S.K., Majumdar, P., Zhang, H., Biard, D., Majumder, H.K., Schreiber, V., and Pommier, Y. (2014) PARP1–TDP1 Coupling for the Repair of Topoisomerase I-Induced DNA Damage. *Nucleic Acids Research* 42(7), 4435–49.

Dasari, S., and Tchounwou, P.B. (2014). Cisplatin in Cancer Therapy: Molecular Mechanisms of Action. *European Journal of Pharmacology* 740, 364–78.

Davies, R.J.H. (1995). Ultraviolet Radiation Damage in DNA. *Biochemical Society Transactions* 23(2), 407–18.

Davis, E.J., Lachaud, C., Appleton, P., Macartney, T.J., Näthke, I., and Rouse, J. (2012). DVC1 (C1orf124) Recruits the P97 Protein Segregase to Sites of DNA Damage. *Nature Structural & Molecular Biology* 19(11), 1093–1100.

DeMott, M.S., Beyret, E., Wong, D., Bales, B.C., Hwang, J.T., Greenberg, M.M., and Demple, B. (2002). Covalent Trapping of Human DNA Polymerase β by the Oxidative DNA Lesion 2-Deoxyribonolactone. *Journal of Biological Chemistry* 277(10), 7637–40.

Derbyshire, V., Pinsonneault, J.K., and Joyce, C.M. (1995). Structure-Function Analysis of 3′ → 5′-Exonuclease of DNA Polymerases. In *Methods in Enzymology* 262, 363-85.

Deshpande, R.A., Lee, J.H., Arora S., and Paull T.T. (2016). Nbs1 Converts the Human Mre11/Rad50 Nuclease Complex into an Endo/Exonuclease Machine Specific for Protein-DNA Adducts. *Molecular Cell* 64(3), 593–606.

Desouky, O., Ding, N., and Zhou, G. (2015). Targeted and Non-Targeted Effects of Ionizing Radiation. *Journal of Radiation Research and Applied Sciences* 8(2), 247–54.

Dianov, G.L., Houle, J.F., Iyer, N., Bohr, V.A., and Friedberg, E.C. (1997). Reduced RNA Polymerase II Transcription in Extracts of Cockayne Syndrome and Xeroderma Pigmentosum/Cockayne Syndrome Cells. *Nucleic Acids Research* 25(18), 3636–42.

DiGiovanna, J.J., and Kraemer, K.H. (2012). Shining a Light on Xeroderma Pigmentosum. *Journal of Investigative Dermatology* 132(3), 785–96.

Dingler, F.A., Wang, M., Mu, A., Millington, C.L., Oberbeck, N., Watcham, S., Pontel, L.B., Kamimae-Lanning, A.N., Langevin, F., Nadler, C., Cordell, R.L., Monks, P.S., Yu, R., Wilson, N.K., Hira, A., Yoshida, K., Mori, M., Okamoto, Y., Okuno, Y., Muramatsu, H., Shiraishi, Y., Kobayashi, M., Moriguchi, T., Osumi, T., Kato, M., Miyano, S., Ito, E., Kojima, S., Yabe, H., Yabe, M., Matsuo, K., Ogawa, S., Göttgens, B., Hodskinson, M.R.G., Takata, M., and Patel, K.J. (2020). Two Aldehyde Clearance Systems Are Essential to Prevent Lethal Formaldehyde Accumulation in Mice and Humans. *Molecular Cell* 80(6), 996-1012.e9.

Dirac-Svejstrup, A.B., Walker, J., Faull, P., Encheva ,V., Akimov, V., Puglia, M., Perkins, D., Kümper, S., Hunjan, S.S., Blagoev, B., Snijders, A.P., Powell, D.J., and Svejstrup, J.Q. (2020). DDI2 Is a Ubiquitin-Directed Endoprotease Responsible for Cleavage of Transcription Factor NRF1. *Molecular Cell* 79(2), 332-341.e7.

Dizdaroglu, M., Jaruga, P., Birincioglu, M., and Rodriguez, H. (2002). Free Radical-Induced Damage to DNA: Mechanisms and Measurement. *Free Radical Biology and Medicine* 32(11), 1102–15.

Dokshin, G.A., Davis, G.M., Sawle, A.D., Eldridge, M.D., Nicholls, P.K., Gourley, T.E., Romer, K.A., Molesworth, L.W., Tatnell, H.R., Ozturk, A.R., de Rooij, D.G., Hannon, G.J.,

Page, D.C., Mello, C.C., and Carmell, M.A. (2020). GCNA Interacts with Spartan and Topoisomerase II to Regulate Genome Stability. *Developmental Cell* 52(1), 53-68.e6.

Duncan, T., Trewick, S.C., Koivisto, P., Bates, P.A., Lindahl. T., and Sedgwick, B. (2002). Reversal of DNA Alkylation Damage by Two Human Dioxygenases. *Proceedings of the National Academy of Sciences* 99(26), 16660–65.

Duxin, J.P., Dewar, J.M., Yardimci, H., and Walter. J.C. (2014). Repair of a DNA-Protein Crosslink by Replication-Coupled Proteolysis. *Cell* 159(2), 346–57.

Eastman, A. (1987). The Formation, Isolation and Characterization of DNA Adducts Produced by Anticancer Platinum Complexes. *Pharmacology & Therapeutics* 34(2), 155–66.

Ehara, H., Yokoyama, T., Shigematsu, H., Yokoyama, S., Shirouzu, M., Sekine, S.I. (2017). Structure of the Complete Elongation Complex of RNA Polymerase II with Basal Factors. *Science* 357(6354), 921–24.

Emadi, A., Jones, R.J., and Brodsky, R.A. (2009). Cyclophosphamide and Cancer: Golden Anniversary. *Nature Reviews Clinical Oncology* 6(11), 638–47.

Enoiu, M., Jiricny, J., and Schärer, O.D. (2012). Repair of Cisplatin-Induced DNA Interstrand Crosslinks by a Replication-Independent Pathway Involving Transcription-Coupled Repair and Translesion Synthesis. *Nucleic Acids Research* 40(18), 8953–64.

Epanchintsev, A., Costanzo, F., Rauschendorf, M.A., Caputo, M., Ye, T., Donnio, L.M., Proietti-de-Santis, L., Coin, F., Laugel, V., and Egly, J.M. (2017). Cockayne's Syndrome A and B Proteins Regulate Transcription Arrest after Genotoxic Stress by Promoting ATF3 Degradation. *Molecular Cell* 68(6), 1054-1066.e6.

Epanchintsev, A., Rauschendorf, M.A., Costanzo, F., Calmels, N., Obringer, C., Sarasin, A., Coin, F., Laugel, V., and Egly, J.M. (2020). Defective Transcription of ATF3 Responsive Genes, a Marker for Cockayne Syndrome. *Scientific Reports* 10(1), 1105.

Eren, E., Unlu, H.T., Ceylaner, S., and Tarim, O. (2021). Compound Heterozygous Variants in *FAM111A* Cause Autosomal Recessive Kenny-Caffey Syndrome Type 2. *Journal of Clinical Research in Pediatric Endocrinology* 15(1), 97–102.

Evans, E. (1997). Mechanism of Open Complex and Dual Incision Formation by Human Nucleotide Excision Repair Factors. *The EMBO Journal* 16(21), 6559–73.

Ewig, R.A.G., and Kohn K.W. (1977). DNA Damage and Repair in Mouse Leukemia L1210 Cells Treated with Nitrogen Mustard, 1,3-Bis(2-Chloroethyl)-1-Nitrosourea, and Other Nitrosoureas. *Cancer Research* 37(7 Pt 1), 2114–22.

Fei, J., Kaczmarek, N., Luch, A., Glas, A., Carell, T., and Naegeli, H. (2011). Regulation of Nucleotide Excision Repair by UV-DDB: Prioritization of Damage Recognition to Internucleosomal DNA. *PLoS Biology* 9(10), e1001183.

Fei, J., and Chen, J. (2012). KIAA1530 Protein Is Recruited by Cockayne Syndrome Complementation Group Protein A (CSA) to Participate in Transcription-Coupled Repair (TCR). *Journal of Biological Chemistry* 287(42), 35118–26.

Fenaux, P., Mufti, G.J., Hellstrom-Lindberg, E., Santini, V., Finelli, C., Giagounidis, A., Schoch, R., Gattermann, N., Sanz, G., List, A., Gore, S.D., Seymour, J.F., Bennett, J.M., Byrd, J., Backstrom, J., Zimmerman, L., McKenzie, D., Beach, C., Silverman, L.R.; International Vidaza High-Risk MDS Survival Study Group (2009). Efficacy of Azacitidine Compared with That of Conventional Care Regimens in the Treatment of Higher-Risk Myelodysplastic Syndromes: A Randomised, Open-Label, Phase III Study. *The Lancet Oncology* 10(3), 223–32.

Fielden, J., Wiseman, K., Torrecilla, I., Li, S., Hume, S., Chiang, S.C., Ruggiano, A., Narayan Singh, A., Freire, R., Hassanieh, S., Domingo, E., Vendrell, I., Fischer, R., Kessler, B.M., Maughan, T.S., El-Khamisy, S.F., and Ramadan K. (2020). TEX264 Coordinates p97- and SPRTN-Mediated Resolution of Topoisomerase 1-DNA Adducts. *Nature Communications* 11(1), 1274.

Finley, D. (2009). Recognition and Processing of Ubiquitin-Protein Conjugates by the Proteasome. *Annual Review of Biochemistry* 78(1), 477–513.

Fishel, R., and Kolodner, R.D. (1995). Identification of Mismatch Repair Genes and Their Role in the Development of Cancer. *Current Opinion in Genetics & Development* 5(3), 382–95.

Fisher, A.E.O., Hochegger, H., Takeda, S., and Caldecott, K.W. (2007). Poly(ADP-Ribose) Polymerase 1 Accelerates Single-Strand Break Repair in Concert with Poly(ADP-Ribose) Glycohydrolase. *Molecular and Cellular Biology* 27(15), 5597–5605.

Flohr, C. (2003). Poly(ADP-Ribosyl)Ation Accelerates DNA Repair in a Pathway Dependent on Cockayne Syndrome B Protein. *Nucleic Acids Research* 31(18), 5332–37.

Fornace, A.J., and Little, J.B. (1977). DNA Crosslinking Induced by X-Rays and Chemical Agents. *Biochimica et Biophysica Acta (BBA) - Nucleic Acids and Protein Synthesis* 477(4), 343–55.

Fu, D., Calvo J.A., and Samson, L.D. (2012). Balancing Repair and Tolerance of DNA Damage Caused by Alkylating Agents. *Nature Reviews Cancer* 12(2), 104–20.

Fujiwara, Y., Masutani, C., Mizukoshi, T., Kondo, J., Hanaoka, F., and Iwai, S. (1999). Characterization of DNA Recognition by the Human UV-Damaged DNA-Binding Protein. *Journal of Biological Chemistry* 274(28), 20027–33.

Furuta, T., Ueda, T., Aune, G., Sarasin, A., Kraemer, K.H., and Pommier, Y. (2002). Transcription-Coupled Nucleotide Excision Repair as a Determinant of Cisplatin Sensitivity of Human Cells. *Cancer Research* 62(17), 4899–4902.

Gallina, I., Hendriks, I.A., Hoffmann, S., Larsen, N.B., Johansen, J., Colding-Christensen, C.S., Schubert, L., Sellés-Baiget, S., Fábián, Z., Kühbacher, U., Gao, A.O., Räschle, M., Rasmussen, S., Nielsen, M.L., Mailand, N., and Duxin, J.P. (2021). The Ubiquitin Ligase RFWD3 Is Required for Translesion DNA Synthesis. *Molecular Cell* 81(3), 442-458.e9.

Gao, R., Huang, S.N., Marchand C., and Pommier Y. (2012). Biochemical Characterization of Human Tyrosyl-DNA Phosphodiesterase 2 (TDP2/TTRAP). *Journal of Biological Chemistry* 287(36), 30842–52.

Geijer, M.E., and Marteijn J.A. (2018). What Happens at the Lesion Does Not Stay at the Lesion: Transcription-Coupled Nucleotide Excision Repair and the Effects of DNA Damage on Transcription in Cis and Trans. *DNA Repair* 71, 56–68.

Geijer, M.E., Zhou, D., Selvam, K., Steurer, B., Mukherjee, C., Evers, B., Cugusi, S., van Toorn, M., van der Woude, M., Janssens, R.C., Kok, Y.P., Gong, W., Raams, A., Lo, C.S.Y., Lebbink, J.H.G., Geverts, B., Plummer. D.A., Bezstarosti. K., Theil, A.F., Mitter, R., Houtsmuller, A.B., Vermeulen, W., Demmers, J.A.A., Li, S., van Vugt, M.A.T.M., Lans, H., Bernards, R., Svejstrup, J.Q., Ray Chaudhuri, A., Wyrick, J.J., and Marteijn, J.A. (2021). Elongation Factor ELOF1 Drives Transcription-Coupled Repair and Prevents Genome Instability. *Nature Cell Biology* 23(6), 608–19.

Genschel, J., and Modrich, P. (2003). Mechanism of 5'-Directed Excision in Human Mismatch Repair. *Molecular Cell* 12(5), 1077–86.

Gentil, A., Cabral-Neto, J.B., Mariage-Samson, R., Margot, A., Imbach, J.L., Rayner, B., and Sarasin, A. (1992). Mutagenicity of a Unique Apurinic/Apyrimidinic Site in Mammalian Cells. *Journal of Molecular Biology* 227(4), 981–84.

Gherezghiher, T.B., Ming, X., Villalta, P.W., Campbell, C., and Tretyakova, N.Y. (2013). 1,2,3,4-Diepoxybutane-Induced DNA–Protein Cross-Linking in Human Fibrosarcoma (HT1080) Cells. *Journal of Proteome Research* 12(5), 2151–64.

Ghosal, G., Leung, J.W., Nair, B.C., Fong, K.W., and Chen J. (2012). Proliferating Cell Nuclear Antigen (PCNA)-Binding Protein C1orf124 Is a Regulator of Translesion Synthesis. *Journal of Biological Chemistry* 287(41), 34225–33.

Gillet, L.C.J., and Schärer, O.D. (2006). Molecular Mechanisms of Mammalian Global Genome Nucleotide Excision Repair. *Chemical Reviews* 106(2), 253–76.

Gillette, T.G., Gonzalez, F., Delahodde, A., Johnston, S.A., and Kodadek, T. (2004). Physical and Functional Association of RNA Polymerase II and the Proteasome. *Proceedings of the National Academy of Sciences* 101(16), 5904–9.

Gómez-Herreros, F., Romero-Granados, R., Zeng, Z., Alvarez-Quilón, A., Quintero, C., Ju, L., Umans, L., Vermeire, L., Huylebroeck, D., Caldecott, K.W., and Cortés-Ledesma, F. (2013). TDP2–Dependent Non-Homologous End-Joining Protects against Topoisomerase II–Induced DNA Breaks and Genome Instability in Cells and In Vivo. *PLoS Genetics* 9(3), e1003226.

de Graaf, B., Clore A., and McCullough, A.K. (2009). Cellular Pathways for DNA Repair and Damage Tolerance of Formaldehyde-Induced DNA-Protein Crosslinks. *DNA Repair* 8(10), 1207–14.

Graham, T.G.W., Walter, J.C., and Loparo, J.J. (2016). Two-Stage Synapsis of DNA Ends during Non-Homologous End Joining. *Molecular Cell* 61(6), 850–58.

Gregersen, L.H., and Svejstrup, J.Q. (2018). The Cellular Response to Transcription-Blocking DNA Damage. *Trends in Biochemical Sciences* 43(5), 327–41.

Groehler, A., Villalta, P.W., Campbell, C., and Tretyakova, N. (2016). Covalent DNA–Protein Cross-Linking by Phosphoramide Mustard and Nornitrogen Mustard in Human Cells. *Chemical Research in Toxicology* 29(2), 190–202.

Groisman, R., Polanowska, J., Kuraoka, I., Sawada, J., Saijo, M., Drapkin, R., Kisselev, A.F., Tanaka, K., and Nakatani Y. (2003). The Ubiquitin Ligase Activity in the DDB2 and CSA Complexes Is Differentially Regulated by the COP9 Signalosome in Response to DNA Damage. *Cell* 113(3), 357–67.

Groisman, R., Kuraoka, I., Chevallier, O., Gaye, N., Magnaldo, T., Tanaka, K., Kisselev, A.F., Harel-Bellan, A., and Nakatani, Y. (2006). CSA-Dependent Degradation of CSB by the Ubiquitin–Proteasome Pathway Establishes a Link between Complementation Factors of the Cockayne Syndrome. *Genes & Development* 20(11), 1429–34.

Gueranger, Q., Kia, A., Frith, D., and Karran, P. (2011). Crosslinking of DNA Repair and Replication Proteins to DNA in Cells Treated with 6-Thioguanine and UVA. *Nucleic Acids Research* 39(12), 5057–66.

Gujar, H., Weisenberger, D., and Liang, G. (2019). The Roles of Human DNA Methyltransferases and Their Isoforms in Shaping the Epigenome. *Genes* 10(2), 172.

Halder, S., Torrecilla, I., Burkhalter, M.D., Popović, M., Fielden, J., Vaz, B., Oehler, J., Pilger, D., Lessel, D., Wiseman, K., Singh, A.N., Vendrell, I., Fischer, R., Philipp, M., and Ramadan, K. (2019). SPRTN protease and checkpoint kinase 1 cross-activation loop safeguards DNA replication. *Nature Communications* 10(1), 3142.

Harada, S., Agarwal, D.P., and Goedde, H.W. (1981). ALDEHYDE DEHYDROGENASE DEFICIENCY AS CAUSE OF FACIAL FLUSHING REACTION TO ALCOHOL IN JAPANESE. *The Lancet* 318(8253), 982.

Harreman, M., Taschner, M., Sigurdsson, S., Anindya, R., Reid, J., Somesh, B., Kong, S.E., Banks, C.A., Conaway, R.C., Conaway, J.W., and Svejstrup, J.Q. (2009). Distinct Ubiquitin Ligases Act Sequentially for RNA Polymerase II Polyubiquitylation. *Proceedings of the National Academy of Sciences* 106(49), 20705–10.

Hartsuiker, E., Mizuno, K., Molnar, M., Kohli, J., Ohta, K., and Carr, A.M. (2009a). Ctp1 ^{CtIP} and Rad32 ^{Mre11} Nuclease Activity Are Required for Rec12 ^{Spo11} Removal, but Rec12 ^{Spo11} Removal Is Dispensable for Other MRN-Dependent Meiotic Functions. *Molecular and Cellular Biology* 29(7), 1671–81.

Hartsuiker, E., Neale, M.J., and Carr, A.M. (2009b). Distinct Requirements for the Rad32Mre11 Nuclease and Ctp1CtIP in the Removal of Covalently Bound Topoisomerase I and II from DNA. *Molecular Cell* 33(1), 117–23.

He, J., Zhu, Q., Wani, G., Sharma, and N., Wani, A.A. (2016). Valosin-Containing Protein (VCP)/P97 Segregase Mediates Proteolytic Processing of Cockayne Syndrome Group B (CSB) in Damaged Chromatin. *Journal of Biological Chemistry* 291(14), 7396–7408.

He, J., Zhu, Q., Wani, G., and Wani, A.A. (2017). UV-Induced Proteolysis of RNA Polymerase II Is Mediated by VCP/P97 Segregase and Timely Orchestration by Cockayne Syndrome B Protein. *Oncotarget* 8(7), 11004–19.

Heck, H.D., Casanova-Schmitz, M., Dodd, P.B., Schachter, E.N., Witek, T.J., and Tosu, T. (1985). Formaldehyde (CH_2O) Concentrations in the Blood of Humans and Fischer-344 Rats Exposed to CH_2O Under Controlled Conditions. *American Industrial Hygiene Association Journal* 46(1), 1–3.

Heck, H.D., Casanova, M., and Starr, T.B. (1990). Formaldehyde Toxicity—New Understanding. *Critical Reviews in Toxicology* 20(6), 397–426.

Herrero-Ruiz, A., Martínez-García, P.M., Terrón-Bautista, J., Millán-Zambrano, G., Lieberman, J.A., Jimeno-González, S., Cortés-Ledesma, F. (2021). Topoisomerase IIα Represses Transcription by Enforcing Promoter-Proximal Pausing. *Cell Reports* 35(2), 108977.

Heyer, W.D., Ehmsen, K.T., and Liu, J. (2010). Regulation of Homologous Recombination in Eukaryotes. *Annual Review of Genetics* 44(1), 113–39.

Higa, M., Zhang, X., Tanaka, K., and Saijo, M. (2016). Stabilization of Ultraviolet (UV)-Stimulated Scaffold Protein A by Interaction with Ubiquitin-Specific Peptidase 7 Is Essential for Transcription-Coupled Nucleotide Excision Repair. *Journal of Biological Chemistry* 291(26), 13771–79.

Ho, H.N., and West, S.C. (2022). Generation of Double Holliday Junction DNAs and Their Dissolution/Resolution within a Chromatin Context. *Proceedings of the National Academy of Sciences* 119(18), e2123420119.

Hoa, N.N., Shimizu, T., Zhou, Z.W., Wang, Z.Q., Deshpande, R.A., Paull, T.T., Akter, S., Tsuda, M., Furuta, R., Tsutsui, K., Takeda, S., and Sasanuma, H. (2016). Mre11 Is Essential for the Removal of Lethal Topoisomerase 2 Covalent Cleavage Complexes. *Molecular Cell* 64(3), 580–92.

Hoffmann, S., Pentakota, S., Mund, A., Haahr, P., Coscia, F., Gallo, M., Mann, M., Taylor, N.M., and Mailand, N. (2020). FAM111 Protease Activity Undermines Cellular Fitness and Is Amplified by Gain-of-function Mutations in Human Disease. *EMBO reports* 21(10), e50662.

Hong, G., and Kreuzer, K.N. (2000). An Antitumor Drug-Induced Topoisomerase Cleavage Complex Blocks a Bacteriophage T4 Replication Fork In Vivo. *Molecular and Cellular Biology* 20(2), 594–603.

Hsieh, P., and Yamane, K. (2008). DNA Mismatch Repair: Molecular Mechanism, Cancer, and Ageing. *Mechanisms of Ageing and Development* 129(7–8), 391–407.

Hu, W., Wang, Y., Yang, B., Lin, C., Yu, H., Liu, G., Deng, Z., Ou, H.Y., and He, X. (2021). Bacterial YedK Represses Plasmid DNA Replication and Transformation through Its DNA Single-Strand Binding Activity. *Microbiological Research* 252, 126852.

Huang, H., and Hopkins, P.B. (1993). DNA Interstrand Cross-Linking by Formaldehyde: Nucleotide Sequence Preference and Covalent Structure of the Predominant Cross-Link Formed in Synthetic Oligonucleotides. *Journal of the American Chemical Society* 115(21), 9402–8.

Huang, J., Zhou, Q., Gao, M., Nowsheen, S., Zhao, F., Kim, W., Zhu, Q., Kojima, Y., Yin, P., Zhang, Y., Guo, G., Tu, X., Deng, M., Luo, K., Qin, B., Machida, Y., and Lou, Z. (2020). Tandem Deubiquitination and Acetylation of SPRTN Promotes DNA-Protein Crosslink Repair and Protects against Aging. *Molecular Cell* 79(5), 824-835.e5.

Hudson, J.J., Chiang, S.C., Wells, O.S., Rookyard, C., and El-Khamisy, S.F. (2012). SUMO Modification of the Neuroprotective Protein TDP1 Facilitates Chromosomal Single-Strand Break Repair. *Nature Communications* 3(1), 733.

Huffman, J.L., Sundheim, O., and Tainer, J.A. (2005). DNA Base Damage Recognition and Removal: New Twists and Grooves. *Mutation Research/Fundamental and Molecular Mechanisms of Mutagenesis* 577(1–2), 55–76.

Huibregtse, J.M., Yang, J.C., and Beaudenon, S.L. (1997). The Large Subunit of RNA Polymerase II Is a Substrate of the Rsp5 Ubiquitin-Protein Ligase. *Proceedings of the National Academy of Sciences* 94(8), 3656–61.

Hutchinson, F. 1985. Chemical Changes Induced in DNA by Ionizing Radiation. In *Progress in Nucleic Acid Research and Molecular Biology* 32,115-54.

Ide, H., Yagi, R., Yamaoka, T., and Kimura, Y. (1993). Misincorporation of Ribonucleotides by DNA Polymerase during in Vitro DNA Replication. *Nucleic Acids Symposium Series* (29), 133–34.

Ide, H., and Kotera, M. (2004). Human DNA Glycosylases Involved in the Repair of Oxidatively Damaged DNA. *Biological and Pharmaceutical Bulletin* 27(4), 480–85.

Interthal, H., Chen, H.J., and Champoux, J.J. (2005). Human Tdp1 Cleaves a Broad Spectrum of Substrates, Including Phosphoamide Linkages. *Journal of Biological Chemistry* 280(43), 36518–28.

Interthal, H., and Champoux, J.J. (2011). Effects of DNA and Protein Size on Substrate Cleavage by Human Tyrosyl-DNA Phosphodiesterase 1. *Biochemical Journal* 436(3), 559–66.

Islas, A.L., Vos, J.M., and Hanawalt, P.C. (1991). Differential Introduction and Repair of Psoralen Photoadducts to DNA in Specific Human Genes. *Cancer Research* 51(11), 2867–73.

Iyama, T., Lee, S.Y., Berquist, B.R., Gileadi, O., Bohr, V.A., Seidman, M.M., McHugh, P.J., and Wilson, D.M. 3rd (2015). CSB Interacts with SNM1A and Promotes DNA Interstrand Crosslink Processing. *Nucleic Acids Research* 43(1), 247–58.

Jackson, S.P., and Bartek, J. (2009). The DNA-Damage Response in Human Biology and Disease. *Nature* 461(7267), 1071–78.

Jacob, K.D., Noren Hooten, N., Tadokoro, T., Lohani, A., Barnes, J., and Evans, M.K. (2013). Alzheimer's Disease-Associated Polymorphisms in Human OGG1 Alter Catalytic Activity and Sensitize Cells to DNA Damage. *Free Radical Biology and Medicine* 63, 115–25.

Jacobson, M.K., and Bernofsky, C. (1974). Mitochondrial Acetaldehyde Dehydrogenase from Saccharomyces Cerevisiae. *Biochimica et Biophysica Acta (BBA) - Enzymology* 350(2), 277–91.

Jaspers, N.G., Raams, A., Kelner, M.J., Ng, J.M., Yamashita, Y.M., Takeda, S., McMorris, T.C., and Hoeijmakers, J.H. (2002). Anti-Tumour Compounds Illudin S and Irofulven Induce DNA Lesions Ignored by Global Repair and Exclusively Processed by Transcription- and Replication-Coupled Repair Pathways. *DNA Repair* 1(12), 1027–38.

Ji, S., Thomforde, J., Rogers, C., Fu, I., Broyde, S., and Tretyakova, N.Y. (2019). Transcriptional Bypass of DNA–Protein and DNA–Peptide Conjugates by T7 RNA Polymerase. *ACS Chemical Biology* 14(12), 2564–75.

Jia, N., Nakazawa, Y., Guo, C., Shimada, M., Sethi, M., Takahashi, Y., Ueda, H., Nagayama, Y., and Ogi, T. (2015). A Rapid, Comprehensive System for Assaying DNA Repair Activity and Cytotoxic Effects of DNA-Damaging Reagents. *Nature Protocols* 10(1), 12–24.

Johnson, R.E., Yu, S.L., Prakash, S., and Prakash, L. (2007). A Role for Yeast and Human Translesion Synthesis DNA Polymerases in Promoting Replication through 3-Methyl Adenine. *Molecular and Cellular Biology* 27(20), 7198–7205.

Juhasz, S., Balogh, D., Hajdu, I., Burkovics, P., Villamil, M.A., Zhuang, Z., and Haracska, L. (2012). Characterization of Human Spartan/C1orf124, an Ubiquitin-PCNA Interacting Regulator of DNA Damage Tolerance. *Nucleic Acids Research* 40(21), 10795–808.

Kadyrova, L.Y., and Kadyrov, F.A. (2016). Endonuclease Activities of MutLα and Its Homologs in DNA Mismatch Repair. *DNA repair* 38, 42–49.

Karikkineth, A.C., Scheibye-Knudsen, M., Fivenson, E., Croteau, D.L., and Bohr, V.A. (2017). Cockayne Syndrome: Clinical Features, Model Systems and Pathways. *Ageing Research Reviews* 33, 3–17.

Kashiyama, K., Nakazawa, Y., Pilz, D.T., Guo, C., Shimada, M., Sasaki, K., Fawcett, H., Wing, J.F., Lewin, S.O., Carr, L., Li, T.S., Yoshiura, K., Utani, A., Hirano, A., Yamashita, S., Greenblatt, D., Nardo, T., Stefanini, M., McGibbon, D., Sarkany, R., Fassihi, H., Takahashi, Y., Nagayama, Y., Mitsutake, N., Lehmann, A.R., and Ogi, T. (2013). Malfunction of Nuclease ERCC1-XPF Results in Diverse Clinical Manifestations and Causes Cockayne Syndrome, Xeroderma Pigmentosum, and Fanconi Anemia. *The American Journal of Human Genetics* 92(5), 807–19.

Kato, N., Kawasoe, Y., Williams, H., Coates, E., Roy, U., Shi, Y., Beese, L.S., Schärer, O.D., Yan, H., Gottesman, M.E., Takahashi, T.S., and Gautier, J. (2017) Sensing and Processing of DNA Interstrand Crosslinks by the Mismatch Repair Pathway. *Cell Reports* 21(5), 1375–85.

Kawanishi, M., Matsuda, T., and Takashi Y. (2014). Genotoxicity of Formaldehyde: Molecular Basis of DNA Damage and Mutation. *Frontiers in Environmental Science* 2.

Kee, Y., and D'Andrea, A.D. (2012). Molecular Pathogenesis and Clinical Management of Fanconi Anemia. *The Journal of Clinical Investigation* 122(11), 3799–3806.

Keeney, S., Giroux, C.N., and Kleckner, N. (1997). Meiosis-Specific DNA Double-Strand Breaks Are Catalyzed by Spo11, a Member of a Widely Conserved Protein Family. *Cell* 88(3), 375–84.

Kemp, M.G., Reardon, J.T., Lindsey-Boltz, L.A., and Sancar, A. (2012). Mechanism of Release and Fate of Excised Oligonucleotides during Nucleotide Excision Repair. *Journal of Biological Chemistry* 287(27), 22889–99.

Khan, F.A., and Ali, S.O. (2017). Physiological Roles of DNA Double-Strand Breaks. *Journal of Nucleic Acids* 2017, 1–20.

Kiefer, J. (2007). Effects of Ultraviolet Radiation on DNA. *Chromosomal Alterations* 39–53.

Klages-Mundt, N.L., and Li, L. (2017). Formation and Repair of DNA-Protein Crosslink Damage. *Science China Life Sciences* 60(10), 1065–76.

Kleiman, F.E., Wu-Baer, F., Fonseca, D., Kaneko, S., Baer, R., and Manley, J.L. (2005). BRCA1/BARD1 Inhibition of MRNA 3′ Processing Involves Targeted Degradation of RNA Polymerase II. *Genes & Development* 19(10), 1227–37.

Kojima, Y., Machida, Y., Palani, S., Caulfield, T.R., Radisky, E.S., Kaufmann, S.H., and Machida, Y.J. (2020). FAM111A Protects Replication Forks from Protein Obstacles via Its Trypsin-like Domain. *Nature Communications* 11(1), 1318.

Kokic, G., Wagner, F.R., Chernev, A., Urlaub, H., and Cramer, P. (2021). Structural Basis of Human Transcription–DNA Repair Coupling. *Nature* 598(7880), 368–72.

Kottemann, M.C., Conti, B.A., Lach, F.P., and Smogorzewska, A. (2018). Removal of RTF2 from Stalled Replisomes Promotes Maintenance of Genome Integrity. *Molecular Cell* 69(1), 24-35.e5.

Kristensen, U., Epanchintsev, A., Rauschendorf, M.A., Laugel, V., Stevnsner, T., Bohr, V.A., Coin, F., and Egly, J.M. (2013). Regulatory Interplay of Cockayne Syndrome B ATPase and Stress-Response Gene *ATF3* Following Genotoxic Stress. *Proceedings of the National Academy of Sciences* 110(25), E2261-70.

Krokan, H.E., and Bjoras, M. (2013). Base Excision Repair. *Cold Spring Harbor Perspectives in Biology* 5(4), a012583–a012583.

Kühbacher, U., and Duxin, J.P. (2020). How to Fix DNA-Protein Crosslinks. *DNA Repair* 94, 102924.

Kuo, H.K., Griffith, J.D., and Kreuzer, K.N. (2007). 5-Azacytidine–Induced Methyltransferase-DNA Adducts Block DNA Replication *In Vivo*. *Cancer Research* 67(17), 8248–54.

Kusakabe, M., Onishi, Y., Tada, H., Kurihara, F., Kusao, K., Furukawa, M., Iwai, S., Yokoi, M., Sakai, W., and Sugasawa, K. (2019). Mechanism and Regulation of DNA Damage Recognition in Nucleotide Excision Repair. *Genes and Environment* 41(1), 2.

Lange, S.S., Takata, K., and Wood, R.D. (2011). DNA Polymerases and Cancer. *Nature Reviews Cancer* 11(2), 96–110.

Langmead, B., and Salzberg, S.L. (2012). Fast gapped-read alignment with Bowtie 2. Nature Methods 9(4), 357–9.

Lans, H., Marteijn, J.A., Schumacher, B., Hoeijmakers, J.H., Jansen, G., and Vermeulen, W. (2010). Involvement of Global Genome Repair, Transcription Coupled Repair, and Chromatin Remodeling in UV DNA Damage Response Changes during Development. *PLoS Genetics* 6(5), e1000941.

Lans, H., Hoeijmakers, J.H.J., Vermeulen, W., and Marteijn, J.A. (2019). The DNA Damage Response to Transcription Stress. *Nature Reviews Molecular Cell Biology* 20(12), 766–84.

Larminat, F., Zhen, W., and Bohr, V.A. (1993). Gene-Specific DNA Repair of Interstrand Cross-Links Induced by Chemotherapeutic Agents Can Be Preferential. *Journal of Biological Chemistry* 268(4), 2649–54.

Larsen, N.B., Gao, A.O., Sparks, J.L., Gallina, I., Wu, R.A., Mann, M., Räschle, M., Walter, J.C., and Duxin, J.P. (2019). Replication-Coupled DNA-Protein Crosslink Repair by SPRTN and the Proteasome in Xenopus Egg Extracts. *Molecular Cell* 73(3), 574-588.e7.

Lee, K.C., Padget, K., Curtis, H., Cowell, I.G., Moiani, D., Sondka, Z., Morris, N.J., Jackson, G.H., Cockell, S.J., Tainer, J.A., and Austin, C.A. (2012). MRE11 Facilitates the Removal of Human Topoisomerase II Complexes from Genomic DNA. *Biology Open* 1(9), 863–73.

Leng, X., and Duxin, J.P. (2022). Targeting DNA-Protein Crosslinks via Post-Translational Modifications. *Frontiers in Molecular Biosciences* 9, 944775.

Lessel, D., Vaz, B., Halder, S., Lockhart, P.J., Marinovic-Terzic, I., Lopez-Mosqueda, J., Philipp, M., Sim, J.C., Smith, K.R., Oehler, J., Cabrera, E., Freire, R., Pope, K., Nahid, A., Norris, F., Leventer, R.J., Delatycki, M.B., Barbi, G., von Ameln, S., Högel, J., Degoricija, M., Fertig, R., Burkhalter, M.D., Hofmann, K., Thiele, H., Altmüller, J., Nürnberg, G., Nürnberg, P., Bahlo, M., Martin, G.M., Aalfs, C.M., Oshima, J., Terzic, J., Amor, D.J., Dikic, I., Ramadan, K., and Kubisch, C. (2014). Mutations in SPRTN Cause Early Onset Hepatocellular Carcinoma, Genomic Instability and Progeroid Features. *Nature Genetics* 46(11), 1239–44.

Li, C.L., Golebiowski, F.M., Onishi, Y., Samara, N.L., Sugasawa, K., and Yang, W. (2015). Tripartite DNA Lesion Recognition and Verification by XPC, TFIIH, and XPA in Nucleotide Excision Repair. *Molecular Cell* 59(6),1025–34.

Li, F., Raczynska, J.E., Chen, Z., and Yu, H. (2019). Structural Insight into DNA-Dependent Activation of Human Metalloprotease Spartan. *Cell Reports* 26(12), 3336-3346.e4.

Li, F., Mao, G., Tong, D., Huang, J., Gu, L., Yang, W., and Li, G.M. (2013). The Histone Mark H3K36me3 Regulates Human DNA Mismatch Repair through Its Interaction with MutSα. *Cell* 153(3), 590–600.

Li, H., Handsaker, B., Wysoker, A., Fennell, T., Ruan, J., Homer, N., Marth, G., Abecasis, G., and Durbin, R.; 1000 Genome Project Data Processing Subgroup (2009). The Sequence Alignment/Map format and SAMtools. Bioinformatics 25(16), 2078–9.

Liang, C.C., Zhan, B., Yoshikawa, Y., Haas, W., Gygi, S.P., and Cohn, M.A. (2015). UHRF1 Is a Sensor for DNA Interstrand Crosslinks and Recruits FANCD2 to Initiate the Fanconi Anemia Pathway. *Cell Reports* 10(12), 1947–56.

Liebelt, F., Schimmel, J., Verlaan-de Vries, M., Klemann, E., van Royen, M.E., van der Weegen, Y., Luijsterburg, M.S., Mullenders, L.H., Pines, A., Vermeulen, W., and Vertegaal A.C.O. (2019). Transcription-Coupled Nucleotide Excision Repair Is Coordinated by Ubiquitin and SUMO in Response to Ultraviolet Irradiation. *Nucleic Acids Research* 48(1), 231-248.

Lieber, M.R. (2010). The Mechanism of Double-Strand DNA Break Repair by the Nonhomologous DNA End-Joining Pathway. *Annual Review of Biochemistry* 79(1), 181–211.

Lin, C.P., Ban, Y., Lyu, Y.L., Desai, S.D., and Liu, L.F. (2008). A Ubiquitin-Proteasome Pathway for the Repair of Topoisomerase I-DNA Covalent Complexes. *Journal of Biological Chemistry* 283(30), 21074–83.

Lindahl, T. (1979). DNA Glycosylases, Endonucleases for Apurinic/Apyrimidinic Sites, and Base Excision-Repair. In *Progress in Nucleic Acid Research and Molecular Biology* 22,135-92.

Lindahl, T. (1993). Instability and Decay of the Primary Structure of DNA. *Nature* 362(6422), 709–15.

Liu, J.C.Y., Kühbacher, U., Larsen, N.B., Borgermann, N., Garvanska, D.H., Hendriks, I.A., Ackermann, L., Haahr, P., Gallina, I., Guérillon, C., Branigan, E., Hay, R.T., Azuma, Y., Nielsen, M.L., Duxin, J.P., and Mailand, N. (2021). Mechanism and Function of DNA Replication-independent DNA-protein Crosslink Repair via the SUMO-RNF4 Pathway. *The EMBO Journal* 40(18), e107413.

Liu, X., Gao, Q., Li, P., Zhao, Q., Zhang, J., Li, J., Koseki, H., and Wong, J. (2013). UHRF1 Targets DNMT1 for DNA Methylation through Cooperative Binding of Hemi-Methylated DNA and Methylated H3K9. *Nature Communications* 4(1), 1563.

Lliakis, G. (1991). The Role of DNA Double Strand Breaks in Lonizing Radiation-Induced Killing of Eukaryotic Cells. *BioEssays* 13(12), 641–48.

Loeb, L.A., and Preston, B.D. (1986). MUTAGENESIS BY APURINIC/APYRIMIDINIC SITES. *Annual Review of Genetics* 20(1), 201–30.

Loeber, R., Michaelson, E., Fang, Q., Campbell, C., Pegg, A.E., and Tretyakova, N. (2008). Cross-Linking of the DNA Repair Protein O^6-Alkylguanine DNA Alkyltransferase to DNA in the Presence of Antitumor Nitrogen Mustards. *Chemical Research in Toxicology* 21(4), 787–95.

Lopez-Mosqueda, J., Maddi, K., Prgomet, S., Kalayil, S., Marinovic-Terzic, I., Terzic, J., and Dikic, I. (2016). SPRTN Is a Mammalian DNA-Binding Metalloprotease That Resolves DNA-Protein Crosslinks. *eLife* 5, e21491.

Ma, X., Tang, T.S., and Guo, C. (2020). Regulation of Translesion DNA Synthesis in Mammalian Cells. *Environmental and Molecular Mutagenesis* 61(7), 680–92.

Machida, Y., Kim, M.S., and Machida, Y.J. (2012). Spartan/C1orf124 Is Important to Prevent UV-Induced Mutagenesis. *Cell Cycle* 11(18), 3395–3402.

Mao, Y., Desai, S.D., Ting, C.Y, Hwang, J., and Liu, L.F. (2001). 26 S Proteasome-Mediated Degradation of Topoisomerase II Cleavable Complexes. *Journal of Biological Chemistry* 276(44), 40652–58.

Marteijn, J.A., Lans, H., Vermeulen, W., and Hoeijmakers, J.H.J. (2014). Understanding Nucleotide Excision Repair and Its Roles in Cancer and Ageing. *Nature Reviews Molecular Cell Biology* 15(7), 465–81.

Maskey, R.S., Kim, M.S., Baker, D.J., Childs, B., Malureanu, L.A., Jeganathan, K.B., Machida, Y., van Deursen, J.M., and Machida, Y.J. (2014). Spartan Deficiency Causes Genomic Instability and Progeroid Phenotypes. *Nature Communications* 5(1), 5744.

Maskey, R.S., Flatten, K.S., Sieben, C.J., Peterson, K.L., Baker, D.J., Nam, H.J., Kim, M.S., Smyrk, T.C., Kojima, Y., Machida, Y., Santiago, A., van Deursen, J.M., Kaufmann, S.H., and Machida, Y.J. (2017). Spartan Deficiency Causes Accumulation of Topoisomerase 1 Cleavage Complexes and Tumorigenesis. *Nucleic Acids Research* 45(8), 4564–76.

Maslov, A.Y., Lee, M., Gundry, M., Gravina, S., Strogonova, N., Tazearslan, C., Bendebury, A., Suh, Y., and Vijg, J. (2012). 5-Aza-2'-Deoxycytidine-Induced Genome Rearrangements Are Mediated by DNMT1. *Oncogene* 31(50), 5172–79.

Masutani, C., Sugasawa, K., Yanagisawa, J., Sonoyama, T., Ui, M., Enomoto, T., Takio, K., Tanaka, K., van der Spek, P.J., and Bootsma, D. (1994). Purification and Cloning of a Nucleotide Excision Repair Complex Involving the Xeroderma Pigmentosum Group C Protein and a Human Homologue of Yeast RAD23. *The EMBO Journal* 13(8), 1831–43.

Masutani, C., Araki, M., Yamada, A., Kusumoto, R., Nogimori, T., Maekawa, T., Iwai, S., and Hanaoka, F. (1999). Xeroderma Pigmentosum Variant (XP-V) Correcting Protein from HeLa Cells Has a Thymine Dimer Bypass DNA Polymerase Activity. *The EMBO Journal* 18(12), 3491–3501.

Meetei, A.R., de Winter, J.P., Medhurst, A.L., Wallisch, M., Waisfisz, Q., van de Vrugt, H.J., Oostra, A.B., Yan, Z., Ling, C., Bishop, C.E., Hoatlin, M.E., Joenje, H., and Wang, W. (2003). A Novel Ubiquitin Ligase Is Deficient in Fanconi Anemia. *Nature Genetics* 35(2), 165–70.

Mellon, I. (1987). Selective Removal of Transcription-Blocking DNA Damage from the Transcribed Strand of the Mammalian DHFR Gene. *Cell* 51(2), 241–49.

Mellon, I., and Hanawalt, P.C. (1989). Induction of the Escherichia Coli Lactose Operon Selectively Increases Repair of Its Transcribed DNA Strand. *Nature* 342(6245), 95–98.

Menoni, H., Hoeijmakers, J.H.J., and Vermeulen, W. (2012). Nucleotide Excision Repair–Initiating Proteins Bind to Oxidative DNA Lesions in Vivo. *Journal of Cell Biology* 199(7), 1037–46.

Milletti, G., Strocchio, L., Pagliara, D., Girardi, K., Carta, R., Mastronuzzi, A., Locatelli, F., and Nazio, F. (2020). Canonical and Noncanonical Roles of Fanconi Anemia Proteins: Implications in Cancer Predisposition. *Cancers* 12(9), 2684.

Min, J.H., and Pavletich, N.P. (2007). Recognition of DNA Damage by the Rad4 Nucleotide Excision Repair Protein. *Nature* 449(7162), 570–75.

Ming, X., Groehler, A. 4th, Michaelson-Richie, E.D., Villalta, P.W., Campbell, C., and Tretyakova, N.Y. (2017). Mass Spectrometry Based Proteomics Study of Cisplatin-Induced DNA–Protein Cross-Linking in Human Fibrosarcoma (HT1080) Cells. *Chemical Research in Toxicology* 30(4), 980–95.

Minko, I.G., Zou, Y., and Lloyd, R.S. (2002). Incision of DNA–Protein Crosslinks by UvrABC Nuclease Suggests a Potential Repair Pathway Involving Nucleotide Excision Repair. *Proceedings of the National Academy of Sciences* 99(4), 1905–9.

Minko, I.G., Kurtz, A.J., Croteau, D.L., Van Houten, B., Harris, T.M., and Lloyd, R.S. (2005). Initiation of Repair of DNA−Polypeptide Cross-Links by the UvrABC Nuclease. *Biochemistry* 44(8), 3000–3009.

Mitchell, D.L., Jen, J., and Cleaver, J.E. (1991). RELATIVE INDUCTION OF CYCLOBUTANE DIMERS and CYTOSINE PHOTOHYDRATES IN DNA IRRADIATED in Vitro and in Vivo WITH ULTRAVIOLET-C and ULTRAVIOLET-B LIGHT. *Photochemistry and Photobiology* 54(5), 741–46.

Mohni, K.N., Wessel, S.R., Zhao, R., Wojciechowski, A.C., Luzwick, J.W., Layden, H., Eichman, B.F., Thompson, P.S., Mehta, K.P.M., Cortez, D. (2019). HMCES Maintains Genome Integrity by Shielding Abasic Sites in Single-Strand DNA. *Cell* 176(1–2), 144-153.e13.

Moldovan, G.L., Pfander, B., and Jentsch, S. (2007). PCNA, the Maestro of the Replication Fork. *Cell* 129(4), 665–79.

Mórocz, M., Zsigmond, E., Tóth, R., Enyedi, M.Z., Pintér, L., Haracska, L. (2017). DNA-Dependent Protease Activity of Human Spartan Facilitates Replication of DNA–Protein Crosslink-Containing DNA. *Nucleic Acids Research* 45(6), 3172-3188.

Mosbech, A., Gibbs-Seymour, I., Kagias, K., Thorslund, T., Beli, P., Povlsen, L., Nielsen, S,V., Smedegaard, S., Sedgwick, G., Lukas, C., Hartmann-Petersen, R., Lukas, J., Choudhary, C., Pocock, R., Bekker-Jensen, S., and Mailand, N. (2012). DVC1 (C1orf124)

Is a DNA Damage–Targeting P97 Adaptor That Promotes Ubiquitin-Dependent Responses to Replication Blocks. *Nature Structural & Molecular Biology* 19(11), 1084–92.

Moss, T., Dimitrov, S.I. and Houde, D. (1997). UV-Laser Crosslinking of Proteins to DNA. *Methods* 11(2), 225–34.

Mulderrig, L., Garaycoechea, J.I., Tuong, Z.K., Millington, C.L., Dingler, F.A., Ferdinand, J.R., Gaul, L., Tadross, J.A., Arends, M.J., O'Rahilly, S., Crossan, G.P., Clatworthy, M.R., and Patel, K.J. (2021). Aldehyde-Driven Transcriptional Stress Triggers an Anorexic DNA Damage Response. *Nature* 600(7887), 158–63.

Murai, J., Huang, S.Y., Das, B.B., Dexheimer, T.S., Takeda, S., and Pommier, Y. (2012a). Tyrosyl-DNA Phosphodiesterase 1 (TDP1) Repairs DNA Damage Induced by Topoisomerases I and II and Base Alkylation in Vertebrate Cells. *Journal of Biological Chemistry* 287(16), 12848–57.

Murai, J., Huang, S.Y., Das, B.B., Renaud, A., Zhang, Y., Doroshow, J.H., Ji, J., Takeda, S., and Pommier, Y. (2012b). Trapping of PARP1 and PARP2 by Clinical PARP Inhibitors. *Cancer Research* 72(21), 5588–99.

Nakamura, J., and Nakamura, M. (2020). DNA-Protein Crosslink Formation by Endogenous Aldehydes and AP Sites. *DNA Repair* 88, 102806.

Nakano, T., Morishita, S., Katafuchi, A., Matsubara, M., Horikawa, Y., Terato, H., Salem, A.M., Izumi, S., Pack, S.P., Makino, K., and Ide, H. (2007). Nucleotide Excision Repair and Homologous Recombination Systems Commit Differentially to the Repair of DNA-Protein Crosslinks. *Molecular Cell* 28(1), 147–58.

Nakano, T., Katafuchi, A., Matsubara, M., Terato, H., Tsuboi, T., Masuda, T., Tatsumoto, T., Pack, S.P., Makino, K., Croteau, D.L., Van Houten, B., Iijima, K., Tauchi, H., and Ide, H. (2009). Homologous Recombination but not Nucleotide Excision Repair Plays a Pivotal Role in Tolerance of DNA-Protein Cross-Links in Mammalian Cells. *Journal of Biological Chemistry* 284(40), 27065–76.

Nakano, T., Ouchi, R., Kawazoe, J., Pack, S.P., Makino, K., and Ide, H. (2012). T7 RNA Polymerases Backed up by Covalently Trapped Proteins Catalyze Highly Error Prone Transcription. *Journal of Biological Chemistry* 287(9), 6562–72.

Nakano, T., Mitsusada, Y., Salem, A.M., Shoulkamy, M.I., Sugimoto, T., Hirayama, R., Uzawa, A., Furusawa, Y., and Ide, H. (2015). Induction of DNA–Protein Cross-Links by Ionizing Radiation and Their Elimination from the Genome. *Mutation Research/Fundamental and Molecular Mechanisms of Mutagenesis* 771, 45–50.

Nakano, T., Xu, X., Salem, A.M.H., Shoulkamy, M.I., and Ide, H. (2017). Radiation-Induced DNA–Protein Cross-Links: Mechanisms and Biological Significance. *Free Radical Biology and Medicine* 107, 136–45.

Nakazawa, Y., Sasaki, K., Mitsutake, N., Matsuse, M., Shimada, M., Nardo, T., Takahashi, Y., Ohyama, K., Ito, K., Mishima, H., Nomura, M., Kinoshita, A., Ono, S., Takenaka, K., Masuyama, R., Kudo, T., Slor, H., Utani, A., Tateishi, S., Yamashita, S., Stefanini, M., Lehmann, A.R., Yoshiura, K., and Ogi, T. (2012). Mutations in UVSSA Cause UV-Sensitive Syndrome and Impair RNA Polymerase IIo Processing in Transcription-Coupled Nucleotide-Excision Repair. *Nature Genetics* 44(5), 586–92.

Nakazawa, Y., Hara, Y., Oka, Y., Komine, O., van den Heuvel, D., Guo, C., Daigaku, Y., Isono, M., He, Y., Shimada, M., Kato, K., Jia, N., Hashimoto, S., Kotani, Y., Miyoshi, Y., Tanaka, M., Sobue, A., Mitsutake, N., Suganami, T., Masuda, A., Ohno, K., Nakada, S., Mashimo, T., Yamanaka, K., Luijsterburg, M.S., and Ogi, T. (2020). Ubiquitination of DNA Damage-Stalled RNAPII Promotes Transcription-Coupled Repair. *Cell* 180(6), 1228-1244.e24.

Natale, V., and Raquer, H. (2017). Xeroderma Pigmentosum-Cockayne Syndrome Complex. *Orphanet Journal of Rare Diseases* 12(1), 65.

Ng, J.M., Vermeulen, W., van der Horst, G.T., Bergink, S., Sugasawa, K., Vrieling, H., and Hoeijmakers, J.H. (2003). A Novel Regulation Mechanism of DNA Repair by Damage-Induced and RAD23-Dependent Stabilization of Xeroderma Pigmentosum Group C Protein. *Genes & Development* 17(13), 1630–45.

Nie, M., Oravcová, M., Jami-Alahmadi, Y., Wohlschlegel, J.A., Lazzerini-Denchi, E., and Boddy, M.N. (2021). FAM111A Induces Nuclear Dysfunction in Disease and Viral Restriction. *EMBO reports* 22(2), e50803.

Nimonkar, A.V., Genschel, J., Kinoshita, E., Polaczek, P., Campbell, J.L., Wyman, C., Modrich, P., and Kowalczykowski, S.C. (2011). BLM–DNA2–RPA–MRN and EXO1–BLM–RPA–MRN Constitute Two DNA End Resection Machineries for Human DNA Break Repair. *Genes & Development* 25(4), 350–62.

Nishi, R., Okuda, Y., Watanabe, E., Mori, T., Iwai, S., Masutani, C., Sugasawa, K., and Hanaoka, F. (2005). Centrin 2 Stimulates Nucleotide Excision Repair by Interacting with Xeroderma Pigmentosum Group C Protein. *Molecular and Cellular Biology* 25(13), 5664–74.

Nishi, R., Sakai, W., Tone, D., Hanaoka, F., and Sugasawa, K. (2013). Structure-Function Analysis of the EF-Hand Protein Centrin-2 for Its Intracellular Localization and Nucleotide Excision Repair. *Nucleic Acids Research* 41(14), 6917–29.

Nitiss, J.L. (2009). Targeting DNA Topoisomerase II in Cancer Chemotherapy. *Nature Reviews Cancer* 9(5), 338–50.

Nowicka, U., Zhang, D., Walker, O., Krutauz, D., Castañeda, C.A., Chaturvedi, A., Chen, T.Y., Reis, N., Glickman, M.H., and Fushman, D. (2015). DNA-Damage-Inducible 1 Protein (Ddi1) Contains an Uncharacteristic Ubiquitin-like Domain That Binds Ubiquitin. *Structure* 23(3), 542–57.

Ogi, T., Limsirichaikul, S., Overmeer, R.M., Volker, M., Takenaka, K., Cloney, R., Nakazawa, Y., Niimi, A., Miki, Y., Jaspers, N.G., Mullenders, L.H., Yamashita, S., Fousteri, M.I., and Lehmann, A.R. (2010). Three DNA Polymerases, Recruited by Different Mechanisms, Carry Out NER Repair Synthesis in Human Cells. *Molecular Cell* 37(5), 714–27.

Okafuji, A., Biskup, T., Hitomi, K., Getzoff, E.D., Kaiser, G., Batschauer, A., Bacher, A., Hidema, J., Teranishi, M., Yamamoto, K., Schleicher, E., Weber, S. (2010). Light-Induced Activation of Class II Cyclobutane Pyrimidine Dimer Photolyases. *DNA Repair* 9(5), 495–505.

Oksenych, V., Bernardes de Jesus, B., Zhovmer, A., Egly, J.M., and Coin, F. (2009). Molecular Insights into the Recruitment of TFIIH to Sites of DNA Damage. *The EMBO Journal* 28(19), 2971–80.

Okuda, M., Nakazawa, Y., Guo, C., Ogi, T., and Nishimura, Y. (2017). Common TFIIH Recruitment Mechanism in Global Genome and Transcription-Coupled Repair Subpathways. *Nucleic Acids Research* 45(22), 13043–55.

Orelli, B., McClendon, T.B., Tsodikov, O.V., Ellenberger, T., Niedernhofer, L.J., and Schärer, O.D. (2010). The XPA-Binding Domain of ERCC1 Is Required for Nucleotide Excision Repair but Not Other DNA Repair Pathways. *Journal of Biological Chemistry* 285(6), 3705–12.

Overmeer, R.M., Moser, J., Volker, M., Kool, H., Tomkinson, A.E., van Zeeland, A.A., Mullenders, L.H., and Fousteri, M. (2011). Replication Protein A Safeguards Genome Integrity by Controlling NER Incision Events. *Journal of Cell Biology* 192(3), 401–15.

Payne, A., and Chu, G. (1994). Xeroderma Pigmentosum Group E Binding Factor Recognizes a Broad Spectrum of DNA Damage. *Mutation Research/Fundamental and Molecular Mechanisms of Mutagenesis* 310(1), 89–102.

Peak, M.J., and Peak, J.G. (1986). DNA-to-Protein Crosslinks and Backbone Breaks Caused by Far- and Near-Ultraviolet, and Visible Light Radiations in Mammalian Cells. In *Mechanisms of DNA Damage and Repair*, eds. 38,193-202.

Pećina-Šlaus, N., Kafka, A., Salamon, I., and Bukovac, A. (2020). Mismatch Repair Pathway, Genome Stability and Cancer. *Frontiers in Molecular Biosciences* 7,122.

Perry, M., Biegert, M., Kollala, S.S., Mallard, H., Su, G., Kodavati, M., Kreiling, N., Holbrook, A., and Ghosal, G. (2021). USP11 Mediates Repair of DNA–Protein Cross-Links by Deubiquitinating SPRTN Metalloprotease. *Journal of Biological Chemistry* 296, 100396.

Perry, M., and Ghosal, G. (2022). Mechanisms and Regulation of DNA-Protein Crosslink Repair During DNA Replication by SPRTN Protease. *Frontiers in Molecular Biosciences* 9, 916697.

Pleschke, J.M., Kleczkowska, H.E., Strohm, M., and Althaus, F.R. (2000). Poly(ADP-Ribose) Binds to Specific Domains in DNA Damage Checkpoint Proteins. *Journal of Biological Chemistry* 275(52), 40974–80.

Pohlhaus, J.R., and Kreuzer, K.N. (2005). Norfloxacin-Induced DNA Gyrase Cleavage Complexes Block *Escherichia Coli* Replication Forks, Causing Double-Stranded Breaks *in Vivo*: Cleavage Complexes Block Replication Forks *in Vivo*. *Molecular Microbiology* 56(6), 1416–29.

Pommier, Y. (2006). Topoisomerase I Inhibitors: Camptothecins and Beyond. *Nature Reviews Cancer* 6(10), 789–802.

Pommier, Y., and Marchand, C. (2012). Interfacial Inhibitors: Targeting Macromolecular Complexes. *Nature Reviews Drug Discovery* 11(1), 25–36.

Pommier, Y., Huang, S.Y., Gao, R., Das, B.B., Murai, J., and Marchand, C. (2014). Tyrosyl-DNA-Phosphodiesterases (TDP1 and TDP2). *DNA Repair* 19, 114–29.

Pommier, Y., O'Connor, M.J., and de Bono, J. (2016). Laying a Trap to Kill Cancer Cells: PARP Inhibitors and Their Mechanisms of Action. *Science Translational Medicine* 8 (362).

Pontel, L.B., Rosado, I.V., Burgos-Barragan, G., Garaycoechea, J.I., Yu, R., Arends, M.J., Chandrasekaran, G., Broecker, V., Wei, W., Liu, L., Swenberg, J.A., Crossan, G.P., and Patel, K.J. (2015). Endogenous Formaldehyde Is a Hematopoietic Stem Cell Genotoxin and Metabolic Carcinogen. *Molecular Cell* 60(1), 177–88.

Pouliot, J.J., Yao, K.C., Robertson, C.A., and Nash, H.A. (1999). Yeast Gene for a Tyr-DNA Phosphodiesterase That Repairs Topoisomerase I Complexes. *Science* 286(5439), 552–55.

Prasad, R., Horton, J.K., Chastain, P.D. 2nd, Gassman, N.R., Freudenthal, B.D., Hou, E.W., and Wilson, S.H. (2014). Suicidal Cross-Linking of PARP-1 to AP Site Intermediates in Cells Undergoing Base Excision Repair. *Nucleic Acids Research* 42(10), 6337–51.

Prasad, R., Horton, J.K., Dai, D.P., and Wilson, S.H. (2019). Repair Pathway for PARP-1 DNA-Protein Crosslinks. *DNA Repair* 73, 71–77.

Prasad, R., Horton, J.K., and Wilson, S.H. (2020). Requirements for PARP-1 Covalent Crosslinking to DNA (PARP-1 DPC). *DNA Repair* 90, 102850.

Prindle, M.J., and Loeb, L.A. (2012). DNA Polymerase Delta in DNA Replication and Genome Maintenance. *Environmental and Molecular Mutagenesis* 53(9), 666–82.

Proietti-De-Santis, L., Drané, P., and Egly, J.M. (2006). Cockayne Syndrome B Protein Regulates the Transcriptional Program after UV Irradiation. *The EMBO Journal* 25(9), 1915–23.

Quennet, V., Beucher, A., Barton, O., Takeda, S., and Löbrich, M. (2011). CtIP and MRN Promote Non-Homologous End-Joining of Etoposide-Induced DNA Double-Strand Breaks in G1. *Nucleic Acids Research* 39(6), 2144–52.

Quievryn, G., and Zhitkovich, A. (2000). Loss of DNA–Protein Crosslinks from Formaldehyde-Exposed Cells Occurs through Spontaneous Hydrolysis and an Active Repair Process Linked to Proteosome Function. *Carcinogenesis* 21(8), 1573–80.

Quinlan, A.R., and Hall, I.M. (2010). BEDTools: a flexible suite of utilities for comparing genomic features. Bioinformatics 26(6), 841–2.

Quiñones, J.L., Thapar, U., Yu, K., Fang, Q., Sobol, R.W., and Demple, B. (2015). Enzyme Mechanism-Based, Oxidative DNA–Protein Cross-Links Formed with DNA Polymerase β in Vivo. *Proceedings of the National Academy of Sciences* 112(28), 8602–7.

Quiñones, J.L., Thapar, U., Wilson, S.H., Ramsden, D.A., and Demple, B. (2020). Oxidative DNA-Protein Crosslinks Formed in Mammalian Cells by Abasic Site Lyases Involved in DNA Repair. *DNA Repair* 87, 102773.

Ramírez, F., Dündar, F., Diehl, S., Grüning, B.A., and Manke, T. (2014) deepTools: a flexible platform for exploring deep-sequencing data. Nucleic Acids Research 42, W187–91.

Rapin, I., Lindenbaum, Y., Dickson, D.W., Kraemer, K.H., and Robbins, J.H. (2000). Cockayne Syndrome and Xeroderma Pigmentosum: DNA Repair Disorders with Overlaps and Paradoxes. *Neurology* 55(10), 1442–49.

Räschle, M., Knipscheer, P., Enoiu, M., Angelov, T., Sun, J., Griffith, J.D., Ellenberger, T.E., Schärer, O.D., and Walter, J.C. (2008). Mechanism of Replication-Coupled DNA Interstrand Crosslink Repair. *Cell* 134(6), 969–80.

Ratner, J.N., Balasubramanian, B., Corden, J., Warren, S.L., and Bregman, D.B. (1998). Ultraviolet Radiation-Induced Ubiquitination and Proteasomal Degradation of the Large Subunit of RNA Polymerase II. *Journal of Biological Chemistry* 273(9), 5184–89.

Raymond, A.C., Staker, B.L., and Burgin, A.B. Jr. (2005). Substrate Specificity of Tyrosyl-DNA Phosphodiesterase I (Tdp1). *Journal of Biological Chemistry* 280(23), 22029–35.

Reardon, J.T., and Sancar, A. (2006). Repair of DNA–Polypeptide Crosslinks by Human Excision Nuclease. *Proceedings of the National Academy of Sciences* 103(11), 4056–61.

Reardon, J.T., Cheng, Y., and Sancar, A. (2006). Repair of DNA–Protein Cross-Links in Mammalian Cells. *Cell Cycle* 5(13), 1366–70.

Reha-Krantz, L.J. (2010). DNA Polymerase Proofreading: Multiple Roles Maintain Genome Stability. *Biochimica et Biophysica Acta (BBA) - Proteins and Proteomics* 1804(5), 1049–63.

Reinking, H.K., Kang, H.S., Götz, M.J., Li, H.Y., Kieser, A., Zhao, S., Acampora, A.C., Weickert, P., Fessler, E., Jae, L.T., Sattler, M., and Stingele, J. (2020). DNA Structure-

Specific Cleavage of DNA-Protein Crosslinks by the SPRTN Protease. *Molecular Cell* 80(1), 102-113.e6.

Renkawitz, J., Lademann, C.A., and Jentsch, S. (2014). Mechanisms and Principles of Homology Search during Recombination. *Nature Reviews Molecular Cell Biology* 15(6), 369–83.

Robert, M.F., Morin, S., Beaulieu, N., Gauthier, F., Chute, I.C., Barsalou, A., and MacLeod, A.R. (2003). DNMT1 Is Required to Maintain CpG Methylation and Aberrant Gene Silencing in Human Cancer Cells. *Nature Genetics* 33(1), 61–65.

Rochette, P.J., Therrien, J.P., Drouin, R., Perdiz, D., Bastien, N., Drobetsky, E.A., and Sage, E. (2003). UVA-Induced Cyclobutane Pyrimidine Dimers Form Predominantly at Thymine-Thymine Dipyrimidines and Correlate with the Mutation Spectrum in Rodent Cells. *Nucleic Acids Research* 31(11), 2786–94.

Rockx,D.A., Mason, R., van Hoffen, A., Barton, M.C., Citterio, E., Bregman, D.B., van Zeeland, A.A., Vrieling, H., and Mullenders, L.H. (2000). UV-Induced Inhibition of Transcription Involves Repression of Transcription Initiation and Phosphorylation of RNA Polymerase II. *Proceedings of the National Academy of Sciences* 97(19), 10503–8.

Rose, M., Burgess, J.T., O'Byrne, K., Richard, D.J., and Bolderson, E. (2020). PARP Inhibitors: Clinical Relevance, Mechanisms of Action and Tumor Resistance. *Frontiers in Cell and Developmental Biology* 8, 564601.

Rothwell, P.J., and Waksman, G. (2005). Structure and Mechanism of DNA Polymerases. In *Advances in Protein Chemistry*, 71,401-40.

Ruggiano, A., Vaz, B., Kilgas, S., Popović, M., Rodriguez-Berriguete, G., Singh, A.N., Higgins, G.S., Kiltie, A.E., and Ramadan, K. (2021). The Protease SPRTN and SUMOylation Coordinate DNA-Protein Crosslink Repair to Prevent Genome Instability. *Cell Reports* 37(10), 110080.

Ruggiano, A., and Ramadan, K. (2021). DNA–Protein Crosslink Proteases in Genome Stability. *Communications Biology* 4(1), 11.

Ruijs, M.W., van Andel, R.N., Oshima, J., Madan, K., Nieuwint, A.W., and Aalfs, C.M. (2003). Atypical Progeroid Syndrome: An Unknown Helicase Gene Defect? *American Journal of Medical Genetics* 116A(3), 295–99.

Rüthemann, P., Balbo Pogliano, C., and Naegeli, H. (2016). Global-Genome Nucleotide Excision Repair Controlled by Ubiquitin/Sumo Modifiers. *Frontiers in Genetics* 7, 68.

Saeki, H., and Svejstrup, J.Q. (2009). Stability, Flexibility, and Dynamic Interactions of Colliding RNA Polymerase II Elongation Complexes. *Molecular Cell* 35(2), 191–205.

Sale, J. (2013). Translesion DNA Synthesis and Mutagenesis in Eukaryotes. *Cold Spring Harbor Perspectives in Biology* 5(3), a012708.

Sampath, H., Vartanian, V., Rollins, M.R., Sakumi, K., Nakabeppu, Y., and Lloyd, R.S. (2012). 8-Oxoguanine DNA Glycosylase (OGG1) Deficiency Increases Susceptibility to Obesity and Metabolic Dysfunction ed. Ferenc Gallyas. *PLoS ONE* 7(12), e51697.

San Filippo, J., Sung, P., and Klein, H. (2008). Mechanism of Eukaryotic Homologous Recombination. *Annual Review of Biochemistry* 77(1), 229–57.

Santi, D.V., Norment, A., and Garrett, C.E. (1984). Covalent Bond Formation between a DNA-Cytosine Methyltransferase and DNA Containing 5-Azacytosine. *Proceedings of the National Academy of Sciences* 81(22), 6993–97.

Sarker, A.H., Tsutakawa, S.E., Kostek, S., Ng, C., Shin, D.S., Peris, M., Campeau, E., Tainer, J.A., Nogales, E., and Cooper, P.K. (2005). Recognition of RNA Polymerase II and Transcription Bubbles by XPG, CSB, and TFIIH: Insights for Transcription-Coupled Repair and Cockayne Syndrome. *Molecular Cell* 20(2), 187–98.

Scharer, O.D. (2013). Nucleotide Excision Repair in Eukaryotes. *Cold Spring Harbor Perspectives in Biology* 5(10), a012609–a012609.

Schellenberg, M.J., Lieberman, J.A., Herrero-Ruiz, A., Butler, L.R., Williams, J.G., Muñoz-Cabello, A.M., Mueller, G.A., London, R.E., Cortés-Ledesma, F., and Williams, R.S. (2017). ZATT (ZNF451)–Mediated Resolution of Topoisomerase 2 DNA-Protein Cross-Links. *Science* 357(6358), 1412–16.

Schieber, M., and Chandel, N.S. (2014). ROS Function in Redox Signaling and Oxidative Stress. *Current Biology* 24(10), R453–62.

Schwertman, P., Vermeulen, W., and Marteijn, J.A. (2013). UVSSA and USP7, a New Couple in Transcription-Coupled DNA Repair. *Chromosoma* 122(4), 275–84.

Schwertman, P., Lagarou, A., Dekkers, D.H., Raams, A., van der Hoek, A.C., Laffeber, C., Hoeijmakers, J.H., Demmers, J.A., Fousteri, M., Vermeulen, W., and Marteijn, J.A. (2012). UV-Sensitive Syndrome Protein UVSSA Recruits USP7 to Regulate Transcription-Coupled Repair. *Nature Genetics* 44(5), 598–602.

Scully, R., Panday, A., Elango, R., and Willis, N.A. (2019). DNA Double-Strand Break Repair-Pathway Choice in Somatic Mammalian Cells. *Nature Reviews Molecular Cell Biology* 20(11), 698–714.

Sedgwick, B., Bates, P.A., Paik, J., Jacobs, S.C., and Lindahl, T. (2007). Repair of Alkylated DNA: Recent Advances. *DNA Repair* 6(4), 429–42.

Selby, C.P., and Sancar, A. (1997). Human Transcription-Repair Coupling Factor CSB/ERCC6 Is a DNA-Stimulated ATPase but Is Not a Helicase and Does Not Disrupt the Ternary Transcription Complex of Stalled RNA Polymerase II. *Journal of Biological Chemistry* 272(3), 1885–90.

Semlow, D.R., and Walter, J.C. (2021). Mechanisms of Vertebrate DNA Interstrand Cross-Link Repair. *Annual Review of Biochemistry* 90(1), 107–35.

Serbyn, N., Noireterre, A., Bagdiul, I., Plank, M., Michel, A.H., Loewith, R., Kornmann, B., and Stutz, F. (2020). The Aspartic Protease Ddi1 Contributes to DNA-Protein Crosslink Repair in Yeast. *Molecular Cell* 77(5), 1066-1079.e9.

Sethi, M., Lehmann, A.R., Fawcett, H., Stefanini, M., Jaspers, N., Mullard, K., Turner, S., Robson, A., McGibbon, D., Sarkany, R., and Fassihi, H. (2013). Patients with Xeroderma Pigmentosum Complementation Groups C, E and V Do Not Have Abnormal Sunburn Reactions. *British Journal of Dermatology* 169(6), 1279–87.

Sharma, V., Collins, L.B., Chen, T.H., Herr, N., Takeda, S., Sun, W., Swenberg, J.A., and Nakamura, J. (2016). Oxidative Stress at Low Levels Can Induce Clustered DNA Lesions Leading to NHEJ Mediated Mutations. *Oncotarget* 7(18), 25377–90.

Shen, L., Song, C.X., He, C., and Zhang, Y. (2014). Mechanism and Function of Oxidative Reversal of DNA and RNA Methylation. *Annual Review of Biochemistry* 83(1), 585–614.

Shi, Y., Lan, F., Matson, C., Mulligan, P., Whetstine, J.R., Cole, P.A., Casero, R.A., and Shi, Y. (2004). Histone Demethylation Mediated by the Nuclear Amine Oxidase Homolog LSD1. *Cell* 119(7), 941–53.

Shoulkamy, M.I., Nakano, T., Ohshima, M., Hirayama, R., Uzawa, A., Furusawa, Y.,and Ide, H. (2012). Detection of DNA–Protein Crosslinks (DPCs) by Novel Direct Fluorescence

Labeling Methods: Distinct Stabilities of Aldehyde and Radiation-Induced DPCs. *Nucleic Acids Research* 40(18), e143–e143.

Sin, Y., Tanaka, K., and Saijo, M. (2016). The C-Terminal Region and SUMOylation of Cockayne Syndrome Group B Protein Play Critical Roles in Transcription-Coupled Nucleotide Excision Repair. *Journal of Biological Chemistry* 291(3), 1387–97.

Singh, R.K., Zerath, S., Kleifeld, O., Scheffner, M., Glickman, M.H., and Fushman, D. (2012). Recognition and Cleavage of Related to Ubiquitin 1 (Rub1) and Rub1-Ubiquitin Chains by Components of the Ubiquitin-Proteasome System. *Molecular & Cellular Proteomics* 11(12), 1595–1611.

Sirkis, R., Gerst, J.E., and Fass, D. (2006). Ddi1, a Eukaryotic Protein With the Retroviral Protease Fold. Journal of Molecular Biology 364(3), 376–87.

Smeaton, M.B., Hlavin, E.M., McGregor Mason, T., Noronha, A.M., Wilds, C.J., and Miller, P.S. (2008). Distortion-Dependent Unhooking of Interstrand Cross-Links in Mammalian Cell Extracts. *Biochemistry* 47(37), 9920–30.
Smerdon, M.J., and Thoma, F. (1990). Site-Specific DNA Repair at the Nucleosome Level in a Yeast Minichromosome. *Cell* 61(4), 675–84.

Smogorzewska, A., Matsuoka, S., Vinciguerra, P., McDonald, E.R. 3rd, Hurov, K.E., Luo, J., Ballif, B.A., Gygi, S.P., Hofmann, K., D'Andrea, A.D., and Elledge, S.J. (2007). Identification of the FANCI Protein, a Monoubiquitinated FANCD2 Paralog Required for DNA Repair. *Cell* 129(2), 289–301.

Soll, J.M., Sobol, R.W., and Mosammaparast, N. (2017). Regulation of DNA Alkylation Damage Repair: Lessons and Therapeutic Opportunities. *Trends in Biochemical Sciences* 42(3), 206–18.

Sparks, J.L., Chistol, G., Gao, A.O., Räschle, M., Larsen, N.B., Mann, M., Duxin, J.P., and Walter, J.C. (2019). The CMG Helicase Bypasses DNA-Protein Cross-Links to Facilitate Their Repair. *Cell* 176(1–2), 167-181.e21.

Spivak, G. (2005). UV-Sensitive Syndrome. *Mutation Research/Fundamental and Molecular Mechanisms of Mutagenesis* 577(1–2), 162–69.

Staresincic, L., Fagbemi, A.F., Enzlin, J.H., Gourdin, A.M., Wijgers, N., Dunand-Sauthier, I., Giglia-Mari, G., Clarkson, S.G., Vermeulen, W., and Schärer, O.D. (2009). Coordination of Dual Incision and Repair Synthesis in Human Nucleotide Excision Repair. *The EMBO Journal* 28(8), 1111–20.

Starita, L.M., Horwitz, A.A., Keogh, M.C., Ishioka, C., Parvin, J.D., and Chiba, N. (2005). BRCA1/BARD1 Ubiquitinate Phosphorylated RNA Polymerase II. *Journal of Biological Chemistry* 280(26), 24498–505.

Stern-Delfils, A., Spitz, M.A., Durand, M., Obringer, C., Calmels, N., Olagne, J., Pillay, K., Fieggen, K., Laugel, V., and Zaloszyc, A. (2020). Renal Disease in Cockayne Syndrome. *European Journal of Medical Genetics* 63(1), 103612.

Stingele, J., Schwarz, M.S., Bloemeke, N., Wolf, P.G., and Jentsch, S. (2014). A DNA-Dependent Protease Involved in DNA-Protein Crosslink Repair. *Cell* 158(2), 327–38.

Stingele, J., and Stefan, J. (2015). DNA–Protein Crosslink Repair. *Nature Reviews Molecular Cell Biology* 16(8), 455–60.

Stingele, J., Bellelli, R., Alte, F., Hewitt, G., Sarek, G., Maslen, S.L., Tsutakawa, S.E., Borg, A., Kjær, S., Tainer, J.A., Skehel, J.M., Groll, M., and Boulton, S.J. (2016). Mechanism and Regulation of DNA-Protein Crosslink Repair by the DNA-Dependent Metalloprotease SPRTN. *Molecular Cell* 64(4), 688–703.

Stingele, J., Bellelli, R., and Boulton, S.J. (2017). Mechanisms of DNA–Protein Crosslink Repair. *Nature Reviews Molecular Cell Biology* 18(9), 563–73.

Sugasawa, K., Okamoto, T., Shimizu, Y., Masutani, C., Iwai, S., and Hanaoka, F. (2001). A Multistep Damage Recognition Mechanism for Global Genomic Nucleotide Excision Repair. *Genes & Development* 15(5), 507–21.

Sugasawa, K., Akagi, J., Nishi, R., Iwai, S., and Hanaoka, F. (2009). Two-Step Recognition of DNA Damage for Mammalian Nucleotide Excision Repair: Directional Binding of the XPC Complex and DNA Strand Scanning. *Molecular Cell* 36(4), 642–53.

Sun, Y., Miller Jenkins, L.M., Su, Y.P., Nitiss, K.C., Nitiss, J.L., and Pommier, Y. (2020). A Conserved SUMO Pathway Repairs Topoisomerase DNA-Protein Cross-Links by Engaging Ubiquitin-Mediated Proteasomal Degradation. *Science Advances* 6(46), eaba6290.

Sung, P., and Klein, H. (2006). Mechanism of Homologous Recombination: Mediators and Helicases Take on Regulatory Functions. *Nature Reviews Molecular Cell Biology* 7(10), 739–50.

Svilar, D., Goellner, E.M., Almeida, K.H., and Sobol, R.W. (2011). Base Excision Repair and Lesion-Dependent Subpathways for Repair of Oxidative DNA Damage. *Antioxidants & Redox Signaling* 14(12), 2491–2507.

Svoboda, M., Konvalinka, J., Trempe, J.F., and Grantz Saskova, K. (2019). The Yeast Proteases Ddi1 and Wss1 Are Both Involved in the DNA Replication Stress Response. *DNA Repair* 80, 45–51.

Swenberg, J.A., Moeller, B.C., Lu, K., Rager, J.E., Fry, R.C., and Starr, T.B. (2013). Formaldehyde Carcinogenicity Research: 30 Years and Counting for Mode of Action, Epidemiology, and Cancer Risk Assessment. *Toxicologic Pathology* 41(2), 181–89.

Takashima, H., Boerkoel, C.F., John, J., Saifi, G.M., Salih, M.A., Armstrong, D., Mao, Y., Quiocho, F.A., Roa, B.B., Nakagawa, M., Stockton, D.W., and Lupski, J.R. (2002). Mutation of TDP1, Encoding a Topoisomerase I–Dependent DNA Damage Repair Enzyme, in Spinocerebellar Ataxia with Axonal Neuropathy. *Nature Genetics* 32(2), 267–72.

Tang, J.Y., Hwang, B.J., Ford, J.M., Hanawalt, P.C., and Chu, G. (2000). Xeroderma Pigmentosum P48 Gene Enhances Global Genomic Repair and Suppresses UV-Induced Mutagenesis. *Molecular Cell* 5(4), 737–44.

Tapias, A., Auriol, J., Forget, D., Enzlin, J.H., Schärer, O.D., Coin, F., Coulombe, B., and Egly, J.M. (2004). Ordered Conformational Changes in Damaged DNA Induced by Nucleotide Excision Repair Factors. *Journal of Biological Chemistry* 279(18), 19074–83.

Thomas, C., and Tulin, A.V. (2013). Poly-ADP-Ribose Polymerase: Machinery for Nuclear Processes. *Molecular Aspects of Medicine* 34(6), 1124–37.

Thompson, P.S., Amidon, K.M., Mohni, K.N., Cortez, D., and Eichman, B.F. (2019). Protection of Abasic Sites during DNA Replication by a Stable Thiazolidine Protein-DNA Cross-Link. *Nature Structural & Molecular Biology* 26(7), 613–18.

Tiwari, V., Baptiste, B.A., Okur, M.N., and Bohr, V.A. (2021). Current and Emerging Roles of Cockayne Syndrome Group B (CSB) Protein. *Nucleic Acids Research* 49(5), 2418–34.

Trempe, J.F., Šašková, K.G., Sivá, M., Ratcliffe, C.D., Veverka, V., Hoegl, A., Ménade, M., Feng, X., Shenker, S., Svoboda, M., Kožíšek, M., Konvalinka, J., and Gehring, K. (2016). Structural Studies of the Yeast DNA Damage-Inducible Protein Ddi1 Reveal Domain Architecture of This Eukaryotic Protein Family. *Scientific Reports* 6(1), 33671.

Tretyakova, N.Y., Groehler, A. 4th, and Ji, S. (2015). DNA–Protein Cross-Links: Formation, Structural Identities, and Biological Outcomes. *Accounts of Chemical Research* 48(6), 1631–44.

Tsodikov, O.V., Ivanov, D., Orelli, B., Staresincic, L., Shoshani, I., Oberman, R., Schärer, O.D., Wagner, G., and Ellenberger, T. (2007). Structural Basis for the Recruitment of ERCC1-XPF to Nucleotide Excision Repair Complexes by XPA. *The EMBO Journal* 26(22), 4768–76.

Tufegdžić Vidaković, A., Mitter, R., Kelly, G.P., Neumann, M., Harreman, M., Rodríguez-Martínez, M., Herlihy, A., Weems, J.C., Boeing, S., Encheva, V., Gaul, L., Milligan, L., Tollervey, D., Conaway, R.C., Conaway, J.W., Snijders, A.P., Stewart, A., and Svejstrup, J.Q. (2020). Regulation of the RNAPII Pool Is Integral to the DNA Damage Response. *Cell* 180(6), 1245-1261.e21.

Unger, S., Górna, M.W., Le Béchec, A., Do Vale-Pereira, S., Bedeschi, M.F., Geiberger, S., Grigelioniene, G., Horemuzova, E., Lalatta, F., Lausch, E., Magnani, C., Nampoothiri, S., Nishimura, G., Petrella, D., Rojas-Ringeling, F., Utsunomiya, A., Zabel, B., Pradervand, S., Harshman, K., Campos-Xavier, B., Bonafé, L., Superti-Furga, G., Stevenson, B., and Superti-Furga, A. (2013). FAM111A Mutations Result in Hypoparathyroidism and Impaired Skeletal Development. *The American Journal of Human Genetics* 92(6), 990–95.

Valles, G.J., Bezsonova, I., Woodgate, R., and Ashton, N.W. (2020). USP7 Is a Master Regulator of Genome Stability. *Frontiers in Cell and Developmental Biology* 8, 717.

van den Boom, V., Citterio, E., Hoogstraten, D., Zotter, A., Egly, J.M., van Cappellen, W.A., Hoeijmakers, J.H., Houtsmuller, A.B., and Vermeulen, W. (2004). DNA Damage Stabilizes Interaction of CSB with the Transcription Elongation Machinery. *Journal of Cell Biology* 166(1), 27–36.

van den Heuvel, D., van der Weegen, Y., Boer, D.E.C., Ogi, T., and Luijsterburg, M.S. (2021). Transcription-Coupled DNA Repair: From Mechanism to Human Disorder. *Trends in Cell Biology* 31(5), 359–71.

van den Heuvel, D., Kim, M., Wondergem, A.P., van der Meer, P.J., Witkamp, M., Lambregtse, F., Kim, H.S., Kan, F., Apelt, K., Kragten, A., González-Prieto, R., Vertegaal, A.C.O., Yeo, J.E., Kim, B.G., van Doorn, R., Schärer, O.D., and Luijsterburg, M.S. (2023). A Disease-Associated XPA Allele Interferes with TFIIH Binding and Primarily Affects Transcription-Coupled Nucleotide Excision Repair. *Proceedings of the National Academy of Sciences* 120(11), e2208860120.

van der Weegen, Y., Golan-Berman, H., Mevissen, T.E.T., Apelt, K., González-Prieto, R., Goedhart, J., Heilbrun, E.E., Vertegaal, A.C.O., van den Heuvel, D., Walter, J.C., Adar, S., and Luijsterburg, M.S. (2020). The Cooperative Action of CSB, CSA, and UVSSA Target TFIIH to DNA Damage-Stalled RNA Polymerase II. *Nature Communications* 11(1), 2104.

van der Weegen, Y., de Lint, K., van den Heuvel, D., Nakazawa, Y., Mevissen, T.E.T., van Schie, J.J.M., San Martin Alonso, M., Boer, D.E.C., González-Prieto, R., Narayanan, I.V., Klaassen, N.H.M., Wondergem, A.P., Roohollahi, K., Dorsman, J.C., Hara, Y., Vertegaal, A.C.O., de Lange, J., Walter, J.C., Noordermeer, S.M., Ljungman, M., Ogi, T., Wolthuis, R.M.F., and Luijsterburg, M.S. (2021). ELOF1 Is a Transcription-Coupled DNA Repair Factor That Directs RNA Polymerase II Ubiquitylation. *Nature Cell Biology* 23(6), 595–607.

Vannier, J.B., Sarek, G., and Boulton, S.J. (2014). RTEL1: Functions of a Disease-Associated Helicase. *Trends in Cell Biology* 24(7), 416–25.

Vaz, B., Popovic, M., Newman, J.A., Fielden, J., Aitkenhead, H., Halder, S., Singh, A.N., Vendrell, I., Fischer, R., Torrecilla, I., Drobnitzky, N., Freire, R., Amor, D.J., Lockhart, P.J., Kessler, B.M., McKenna, G.W., Gileadi, O., and Ramadan, K. (2016). Metalloprotease

SPRTN/DVC1 Orchestrates Replication-Coupled DNA-Protein Crosslink Repair. *Molecular Cell* 64(4), 704–19.

Vaz, B., Popovic, M., and Ramadan, K. (2017). DNA–Protein Crosslink Proteolysis Repair. *Trends in Biochemical Sciences* 42(6), 483–95.

Velmurugu, Y., Chen, X., Slogoff Sevilla, P., Min, J.H., and Ansari, A. (2016). Twist-Open Mechanism of DNA Damage Recognition by the Rad4/XPC Nucleotide Excision Repair Complex. *Proceedings of the National Academy of Sciences* 113(16), E2296-305.

Verma, R., Oania, R., Fang, R., Smith, G.T., and Deshaies, R.J. (2011). Cdc48/P97 Mediates UV-Dependent Turnover of RNA Pol II. *Molecular Cell* 41(1), 82–92.

Vijayraghavan, S., and Saini, N. (2023). Aldehyde-Associated Mutagenesis─Current State of Knowledge. *Chemical Research in Toxicology* 36(7), 983–1001.

Wallace, S.S. (1998). Enzymatic Processing of Radiation-Induced Free Radical Damage in DNA. *Radiation Research* 150(5 Suppl), S60-79.

Walport, L.J., Hopkinson, R.J., and Schofield, C.J. (2012). Mechanisms of Human Histone and Nucleic Acid Demethylases. *Current Opinion in Chemical Biology* 16(5–6), 525–34.

Wang, A.T., Sengerová, B., Cattell, E., Inagawa, T., Hartley, J.M., Kiakos, K., Burgess-Brown, N.A., Swift, L.P., Enzlin, J.H., Schofield, C.J., Gileadi, O., Hartley, J.A., and McHugh P.J. (2011). Human SNM1A and XPF–ERCC1 Collaborate to Initiate DNA Interstrand Cross-Link Repair. *Genes & Development* 25(17), 1859–70.

Wang, J.C. (2002). Cellular Roles of DNA Topoisomerases: A Molecular Perspective. *Nature Reviews Molecular Cell Biology* 3(6), 430–40.

Wang, N., Bao, H., Chen, L., Liu, Y., Li, Y., Wu, B., and Huang, H. (2019). Molecular Basis of Abasic Site Sensing in Single-Stranded DNA by the SRAP Domain of E. Coli YedK. *Nucleic Acids Research* 47(19), 10388–99.

Wang, Y., Chakravarty, P., Ranes, M., Kelly, G., Brooks, P.J., Neilan, E., Stewart, A., Schiavo, G., and Svejstrup, J.Q. (2014). Dysregulation of Gene Expression as a Cause of Cockayne Syndrome Neurological Disease. *Proceedings of the National Academy of Sciences* 111(40), 14454–59.

Ward, J.F. (1988). DNA Damage Produced by Ionizing Radiation in Mammalian Cells: Identities, Mechanisms of Formation, and Reparability. In *Progress in Nucleic Acid Research and Molecular Biology*, 35,95-125.

Ward, J.F. (1994). The Complexity of DNA Damage: Relevance to Biological Consequences. *International Journal of Radiation Biology* 66(5), 427–32.

Warren, J.J., Forsberg, L.J., and Beese, L.S. (2006). The Structural Basis for the Mutagenicity of O^6-Methyl-Guanine Lesions. *Proceedings of the National Academy of Sciences* 103(52), 19701–6.

Waters, L.S., Minesinger, B.K., Wiltrout, M.E., D'Souza, S., Woodruff, R.V., and Walker, G.C. (2009). Eukaryotic Translesion Polymerases and Their Roles and Regulation in DNA Damage Tolerance. *Microbiology and Molecular Biology Reviews* 73(1), 134–54.

Watson J.D., and Crick, F.H. (1953). Molecular Structure of Nucleic Acids: A Structure for Deoxyribose Nucleic Acid. *Nature* 171(4356), 737–38.

Weickert, P., Li, H.Y., Götz, M.J., Dürauer, S., Yaneva, D., Zhao, S., Cordes, J., Acampora, A.C., Forne, I., Imhof, A., and Stingele, J. (2023). SPRTN Patient Variants Cause Global-Genome DNA-Protein Crosslink Repair Defects. *Nature Communications* 14(1), 352.

Williams, H.L., Gottesman, M.E., and Gautier, J. (2013). The Differences between ICL Repair during and Outside of S Phase. *Trends in Biochemical Sciences* 38(8), 386–93.

Williamson, L., Saponaro, M., Boeing, S., East, P., Mitter, R., Kantidakis, T., Kelly, G.P., Lobley, A., Walker, J., Spencer-Dene, B., Howell, M., Stewart, A., and Svejstrup, J.Q. (2017). UV Irradiation Induces a Non-Coding RNA That Functionally Opposes the Protein Encoded by the Same Gene. *Cell* 168(5), 843-855.e13.

Wilson, M.D., Harreman, M., and Svejstrup, J.Q. (2013). Ubiquitylation and Degradation of Elongating RNA Polymerase II: The Last Resort. *Biochimica et Biophysica Acta (BBA) - Gene Regulatory Mechanisms* 1829(1), 151–57.

Wilson, V.L., Jones, P.A., and Momparler, R.L. (1983). Inhibition of DNA Methylation in L1210 Leukemic Cells by 5-Aza-2'-Deoxycytidine as a Possible Mechanism of Chemotherapeutic Action. *Cancer Research* 43(8), 3493–96.

Woźniak, K., and Walter, Z. (2000). Induction of DNA-Protein Cross-Links by Platinum Compounds. *Zeitschrift für Naturforschung C* 55(9–10), 731–36.

Wright, W.D., Shah, S.S., and Heyer, W.D. (2018). Homologous Recombination and the Repair of DNA Double-Strand Breaks. *Journal of Biological Chemistry* 293(27), 10524–35.

Xia, Y., Li, K., Li, J., Wang, T., Gu, L., and Xun, L. (2019). T5 Exonuclease-Dependent Assembly Offers a Low-Cost Method for Efficient Cloning and Site-Directed Mutagenesis. *Nucleic Acids Research* 47(3), e15–e15.

Xu, J., Lahiri, I., Wang, W., Wier, A., Cianfrocco, M.A., Chong, J., Hare, A.A., Dervan, P.B., DiMaio, F., Leschziner, A.E., and Wang, D. (2017). Structural Basis for the Initiation of Eukaryotic Transcription-Coupled DNA Repair. *Nature* 551(7682), 653–57.

Yaneva, D., Sparks, J.L., Donsbach, M., Zhao, S., Weickert, P., Bezalel-Buch, R., Stingele, J., and Walter, J.C. (2023). The FANCJ Helicase Unfolds DNA-Protein Crosslinks to Promote Their Repair. *Molecular Cell* 83(1), 43-56.e10.

Yang, S.W., Burgin, A.B. Jr., Huizenga, B.N., Robertson, C.A., Yao, K.C., and Nash, H.A. (1996). A Eukaryotic Enzyme That Can Disjoin Dead-End Covalent Complexes between DNA and Type I Topoisomerases. *Proceedings of the National Academy of Sciences* 93(21), 11534–39.

Yasukawa, T., Kamura, T., Kitajima, S., Conaway, R.C., Conaway, J.W., and Aso, T. (2008). Mammalian Elongin A Complex Mediates DNA-Damage-Induced Ubiquitylation and Degradation of Rpb1. *The EMBO Journal* 27(24), 3256–66.

Yi, C, and He, C. (2013). DNA Repair by Reversal of DNA Damage. *Cold Spring Harbor Perspectives in Biology* 5(1), a012575–a012575.

Yonekura, S., Nakamura, N., Yonei, S., and Zhang-Akiyama, Q.M. (2009). Generation, Biological Consequences and Repair Mechanisms of Cytosine Deamination in DNA. *Journal of Radiation Research* 50(1), 19–26.

Yu, SL., and Lee, SK. (2017). Ultraviolet Radiation: DNA Damage, Repair, and Human Disorders. *Molecular & Cellular Toxicology* 13(1), 21–28.

Zandarashvili, L., Langelier, M.F., Velagapudi, U.K., Hancock, M.A., Steffen, J.D., Billur, R., Hannan, Z.M., Wicks, A.J., Krastev, D.B., Pettitt, S.J., Lord, C.J., Talele, T.T., Pascal, J.M., and Black, B.E. (2020). Structural Basis for Allosteric PARP-1 Retention on DNA Breaks. *Science* 368(6486), eaax6367.

Zhang, H., and Wheeler, K.T (1993). Radiation-Induced DNA Damage in Tumors and Normal Tissues: I. Feasibility of Estimating the Hypoxic Fraction. *Radiation Research* 136(1), 77.

Zhang, H., Xiong, Y., and Chen, J. (2020). DNA–Protein Cross-Link Repair: What Do We Know Now? *Cell & Bioscience* 10(1), 3.

Zhang, L., Steinmaus, C., Eastmond, D.A., Xin, X.K., and Smith, M.T. (2009). Formaldehyde Exposure and Leukemia: A New Meta-Analysis and Potential Mechanisms. *Mutation Research/Reviews in Mutation Research* 681(2–3), 150–68.

Zhang, X., Horibata, K., Saijo, M., Ishigami, C., Ukai, A., Kanno, S., Tahara, H., Neilan, E.G., Honma, M., Nohmi, T., Yasui, A., and Tanaka, K. (2012). Mutations in UVSSA Cause UV-Sensitive Syndrome and Destabilize ERCC6 in Transcription-Coupled DNA Repair. *Nature Genetics* 44(5), 593–97.

Zhao, F., Zhu, J., Shi, L., and Wu, X. (2022). OGG1 in the Kidney: Beyond Base Excision Repair. *Oxidative Medicine and Cellular Longevity* 2022, 5774641.

Zhao, S., Kieser, A., Li, H.Y., Reinking, H.K., Weickert, P., Euteneuer, S., Yaneva, D., Acampora, A.C., Götz, M.J., Feederle, R., and Stingele, J. (2021). A Ubiquitin Switch Controls Autocatalytic Inactivation of the DNA–Protein Crosslink Repair Protease SPRTN. *Nucleic Acids Research* 49(2), 902–15.

Zheng, H., Wang, X., Warren, A.J., Legerski, R.J., Nairn, R.S., Hamilton, J.W., and Li, L. (2003). Nucleotide Excision Repair- and Polymerase η-Mediated Error-Prone Removal of Mitomycin C Interstrand Cross-Links. *Molecular and Cellular Biology* 23(2), 754–61.

8 ACKNOWLEDGEMENTS

Doing a PhD in a foreign country during of such a dramatic changing era like that of the COVID-19 pandemic has not been an easy task. However, despite the many unforeseen (scientific and not) obstacles that arose, in the end, the day of the last reading of the thesis has arrived. If I go back and recapitulate with my mind this whole challenging and uncertain, but also stimulating and exciting path, I feel deeply grateful to all the people that I met during the PhD journey and that contributed to its successful accomplishment.

First, I am extremely thankful to my supervisor Prof. Dr. Julian Stingele who, four yours ago, gave me the opportunity to start my PhD in his research group; I could not have asked for a more supportive and encouraging supervisor. Julian has been a real mentor, he guided me through this path literally every day from the initial stages of refining my research proposal to the final version of the thesis. His guidance, dedication and constant enthusiasm – even in front of a negative result – have been invaluable throughout the entire process. I thank you for always believing in me!

I would like to acknowledge the members of my PhD thesis committee, who agreed on evaluating my thesis. I particularly want to thank Prof. Dr. Boris Pfander and Prof. Dr. Lucas Jae that, as members of my thesis advisory committee, have given me precious feedback and ideas that have greatly enriched the quality of my work over the entire PhD time.

I want to deeply thank Prof. Sir Steve Jackson, Chris and Aldo in Cambridge for our fantastic collaboration. I thank Prof. Sir Jackson for the inspiring discussions and always enriching scientific input. Thank you, Chris for all the technical and scientific suggestions, for sharing with me the joy and pain of the CSB project, for being so patient to go through my sometimes confusing data…and of course, thanks for continuing our project! Thank you, Aldo, for setting up with me the DPC-seq assay, your expertise has been crucial to finally prove the existence of the transcription-coupled DPC repair pathway. You have been two fantastic “remote” labmates! Thank you all for your great contribution: without your effort our study would not have been so successful!

I would like to extend my thank to Prof. Dr. Martijn Luijsterburg who four years ago allowed us to start working on transcription-coupled repair of DPCs. I thank Martijn for the very valuable and helpful discussions, his deep knowledge of transcription-coupled NER field has been essential for the development of the project and my thesis.

Acknowledgements

I cannot forget to thank all the Stingele group members who have passed by the lab during my PhD. Special thanks go to Ricky for being an infinite source not only of protocols and reagents, but also – and most importantly – of advice, suggestions and continuous support. Thank you, Ricky! I want to say thank you to Max G. for all the times that I annoyed him with any kind of IT concerns, from scripts, setups, settings to whatever. Thanks for being so helpful all the time! I want to acknowledge Jackie for always being helpful and positive, I enjoyed working with you. I also want to acknowledge Anja and Katharina who, with their help, always facilitate our work and make our lab life much easier. I finally want to say thanks to Fernanda who contributed to setting up and finding the perfect conditions for the RRS assay. It was great to work with you in the lab!

I would also like to thank the IMPRS coordination office, particularly Dr. Hans-Joerg Schaeffer and Dr. Ingrid Wolf for always being very supportive and close to PhD students.

Finally, I am thankful to my friends and family. There are no words to express my gratitude to my mother for her support during these four years and my entire life, for giving me complete freedom and for being by my side in front of any difficulties, always and in any case. Without her unconditional love this would never have been possible.